Aleksander Veksler

Optimization-based control of diesel-electric ships in dynamic positioning

Thesis for the degree of philosophiae doctor
Trondheim, August 2014

Norwegian University of Science and Technology
Faculty of Information Technology, Mathematics and Electrical Engineering
Department of Engineering Cybernetics

NTNU
Norwegian University of Science and Technology

Thesis for the degree of philosophiae doctor

Faculty of Information Technology, Mathematics and Electrical Engineering
Department of Engineering Cybernetics

ISBN 978-82-326-0516-3 (printed version)
ISBN 978-82-326-0517-0 (electronic version)
ISSN 1503-8181
ITK Report 2014-4-W

Doctoral theses at NTNU, 2014:302

1st edition, August 2014

Printed by Xerox

Scientiae cedit mare

Summary

Recent advances in computer hardware and algorithms make it possible to consider more computationally demanding control methods, allowing more effective exploitation of the equipment under control.

This thesis explores new ways of controlling ships (or other marine vessels) that are designed to keep a pre-determined position and heading automatically exclusively by the means of their thrusters – a task called "Dynamic Positioning", or DP. Special attention is given to the interplay between the thruster system and the power plant that supplies it.

A DP control architecture typically consists of at least 1) a DP control algorithm that considers the current position and velocity of the vessel against the DP setpoint, and calculates the total forces and the moment that the thruster system should produce, and 2) a thrust allocation (TA) algorithm that calculates the forces to be produced by the individual thrusters to match the command from the DP control algorithm. Chapter 2 describes a TA algorithm that enables centralized control over the power consumption in the thruster system. It achieves that by allowing the TA to make short-term deviations from the command it receives from the DP control algorithm; the resulting deviations in position and velocity of the vessel are carefully monitored and constrained, and are usually small due to the large inertia of a typical marine vessel. This enables the thrusters to counter-act load variations from other consumers on the ship, reducing the total variations on the power plant. The TA algorithm is tested on a simulated marine vessel, which includes a realistic marine power plant.

In Chapter 3, a more efficient version of this algorithm is described. The improvement in efficiency is achieved by positioning the vessel against the slowly-varying component of the environmental forces in a way that increases the acceptable deviation margins in the likely drift-off direction. In Chapter 4, the capabilities of the thruster system to control its power consumption are examined from a theoretical perspective.

Much of the work above required a mathematical model of the power output from a diesel engine; a model that is well-suited for controller design and verification purposes was designed based on first-principle models in the literature. This model was then used to design an improved diesel engine governor (controller) algorithm, which is described in Chapter 5.

The TA algorithms that are described in the literature usually focus on solving one or a few aspects of the TA problem at a time. In Chapter 6, functionality from several earlier publications is gathered into a single TA algorithm. The singularity avoidance functionality is given additional theoretical treatment.

Implementing a DP control algorithm that is aware of thruster limitations such as saturations and rotation rate constraints involves largely heuristic adaptions. Chapter 7 introduces a DP control architecture that avoids having separate DP and TA algorithms, and is instead based on a single MPC-based controller. This allows better coordination between control of the thrusters and control of the ship.

Contents

Preface

This thesis is submitted in partial fulfillment of the requirements for the degree of philosophiae doctor (PhD) at the Norwegian University of Science and Technology (NTNU).

This doctoral work has been mainly performed at the Department of Engineering Cybernetics, with Professor Tor Arne Johansen as the main supervisor, and Professors Roger Skjetne and Asgeir Sørensen as a co-supervisors.

During my PhD studies I had the privilege of visiting Professor Francesco Borrelli at UC Berkeley.

The work has been funded by the Research Council of Norway through the Strategic University Program on Control, Information and Communication Systems for Environmental and Safety Critical Systems. It was performed in close association with the D2V project, which is financed by the Research Council of Norway in collaboration with DNV GL and Kongsberg Maritime.

Acknowledgments

First of all, I want to thank my supervisors, Professors Roger Skjetne, Asgeir Sørensen, and especially my main supervisor Professor Tor Arne Johansen for taking genuine interest in my research, and for continuously supporting me throughout my PhD work. I am grateful to Professor Francesco Borrelli for giving me an opportunity to visit the Model Predictive Control Laboratory at UC Berkeley in California. The research was performed in close collaboration with Kongsberg Maritime, and I would like to thank the Principal Engineers Eirik Mathiesen and Bjørnar Realfsen for the assistance in keeping the research project anchored in the reality and not allowing it to drift too close to the shores of pure academic speculations. I would also like to thank my supervisors during my master thesis, Alexey Pavlov and Miroslav Krstić, for motivating me to continue pursuing my academic interests.

I received less formal but nonetheless essential advise and assistance from my senior PhD student colleagues and postdoctoral fellows at the department, including Esten Ingar Grøtli, Milan Milovanovic, Anders Fougner, Giancarlo Marafiotti and Christian Holden.

I consider myself particularly fortunate in that both the institutions where I was working are permeated by the spirit of good will, friendship and collaboration, which allows a free flow of ideas and knowledge in a way that is essential in a working environment where knowledge is highly specialized. This is certainly not some-

thing that happens by itself. In addition to the people mentioned above, I would like to thank all of my colleagues and friends, including Christoph Backi, Bjarne Grimstad, Parsa Rahmanpour, Morten Pedersen, Torstein Bø, Anne Mai Ersdal, Serge Gale, Mansoureh Jesmani, Eleni Kelasidi, Joakim Haugen, Walter Caharija, Stepan Pchelkin, Magnus Bjerkeng, Espen Hauge, Øyvind Stamnes, Jonas Ingvaldsen, Sarah Koehler, Theresa Lin, Ashwin Carvalho, Sergey Vichik, Tony Kelman, Claudio Ruch, Stefan Bauer and many others, really too many to be named.

I would like to thank my good friends from outside academia for helping me to keep the perspective in both life and in research. First and foremost, I would like to thank a very special and most dear friend Cheau Ling Poon, who was with me though all ups and downs of life in the recent years, whom I learned to rely upon, confide to, and also ask for help when I had troubles with my English or LaTeX grammar. I would also like to specially mention Sigurd Larsen, Arnt Selnes, Øyvind Lorgen, Edvard Fielding, Morten Bakke and Amtall Khawaja. Last but not least I would like to thank my extended family – my parents Rosa and Vladimir, as well as my aunt Nina Davidsen and my stepdad Edgar Kristiansen.

Chapter 1

Introduction

This chapter introduces the reader to the topic of dynamic positioning of ships and other marine vessels. Special attention is given to the issues concerning the power supply of the thruster units.

1.1 Background

Dynamic positioning technology is an answer to the practical challenge of keeping the position of a ship steady in presence of non-stationary load from wind, waves and ocean currents. In that sense, this technology is an alternative, and sometimes an augment, to anchoring. While anchoring was achieved since at least 1900 BCE [44, p. 82], positioning the ship using its thrusters has been first introduced in 1961, when the drilling vessel CUSS I attempted to drill through the oceanic crust into the mantle [32, p. 548], [2, Appendix X], [35]. In that case, positioning the vessel had to be done by manually controlling the thrusters, a task which was both difficult and tedious. Vessels equipped with controllers that maintained position and heading automatically followed quickly [23]. The advantages of dynamic positioning include faster and more practical repositioning on greater depth, less danger to divers and subsea installations.

Unlike anchoring, dynamic positioning always requires an active energy source, and the thrusters in dynamic positioning are typically among the largest power consumers on the ship. To maximize the capability of the dynamic positioning system, the thrusters should be placed on distant locations on the ship, which makes mechanical transfer of power from the engines less practical compared to electrical distribution. This and other operational advantages [19, p. 6] result in electric power distribution being almost ubiquitous in vessels with dynamic positioning.

The type of prime mover predominantly in use with dynamic positioning is the diesel engine, although other sources such as LNG are also available. A power grid on a dynamic positioning vessel typically consists of several diesel generators connected to the thrusters and other consumers through a flexible distribution network with several separable segments and several voltage levels. The control architecture for the resulting system is highly distributed, with independent controllers for diesel engine fuel injection, generator rotor magnetization, circuit breakers, cen-

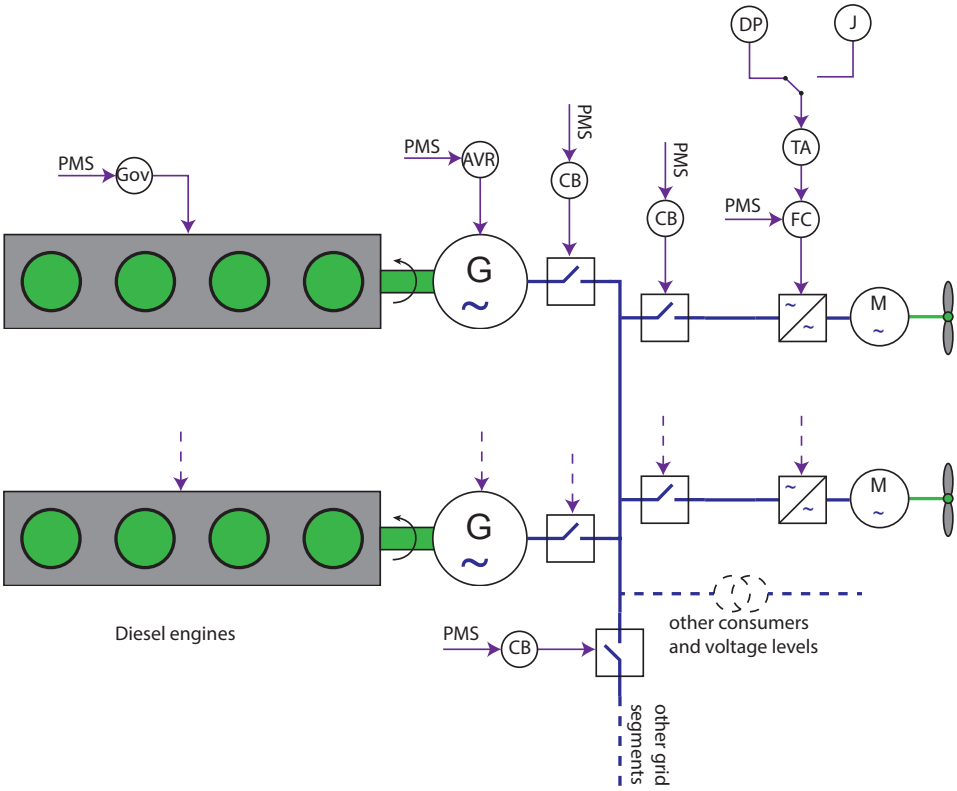

Figure 1.1: An illustration showing some of the controllers on the electric grid. A diesel engine controller, conventionally called governor (Gov) controls the amount of fuel injected into the engines; Automatic Voltage Regulator (AVR) controls the magnetization of the rotor coils; various circuit breakers (CB) connect and disconnect equipment and also isolate faults such as short circuits; the Frequency Converters (FC) are used for local control of the thrusters, and receive commands from both the Thrust Allocation (TA) and the Power Management System (PMS). Finally, the TA can receive the generalized force command from either the DP control system or from a Joystick (J).

Abbreviation	Description
$f \in \mathbb{R}^{Nthrusters}$	The thrust vector describing the forces produced by each thruster that is installed on the ship, with f_i being the force produced by thruster i.
$r_i = \begin{bmatrix} l_{i,x} & l_{i,y} \end{bmatrix}^T$	The location of the thruster device with index i
$\alpha \in \mathbb{R}^{Nthrusters}$	The directions in which the thrusters are pointing, with α_i being the direction of thrusters i.
$\tau \in \mathbb{R}^3$	The resultant generalized force produced by all thrusters on the vessel
$T(\alpha) \in \mathbb{R}^{3 \times Nthrusters}$	The thrust allocation matrix. The linear operation $T(\alpha)f$ calculates and sums up the general forces produced by the individual thrusters.

Table 1.1: Variables used for thruster force calculations.

tralized and local thruster controllers et cetera. An example of such network with controllers is shown on Figure 1.1.

In legacy implementations in the literature and the industry, many of the controllers do not directly communicate with each other, but instead gain information about the situation on the electric grid by monitoring voltage levels, current and frequency on the bus. This has changed in the recent years with increased communication between the individual controllers through a separate data network. The control algorithms that are presented in this dissertation has been enabled largely by the increased information availability and capability to process more information.

1.2 A DP ship model

As with many other physical phenomena, the most precise way to describe the observed motions of a marine vessel is by a mathematical model. Many different models for ships have been formulated and are in use by engineers. Several such models are presented in [24] and more recently in [25]. The models in [22] and [88] focus on high-speed vessels and in [12] the focus is on accurately representing the parametric roll resonance phenomenon. [31] provides a mathematically rigorous reference work. Different models focus on accurate representation of different aspects of the vessel in different conditions and in different operations. Usually, accuracy of the model has to be balanced against mathematical and computational complexity, and convenience of the parametrization. In general, the models that are used in design of marine vessels are more complex than the models that are used for control purposes. Sometimes, the simplified models that are specifically designed to be used for control purposes are called “Control Plant Models”, while the models that are used for simulation of the system are called “Process Plant Models”[30].

Abbreviation	Description
$\eta = \begin{bmatrix} N & E & \psi \end{bmatrix}^T \in \mathbb{R}^3$	Position and orientation of the vessel in an inertial frame of reference, in this case North-East-Down
$\nu = \begin{bmatrix} u & v & r \end{bmatrix}^T \in \mathbb{R}^3$	Velocity of the vessel in its own (body) frame of reference, expressed at the end point of the vector $\begin{bmatrix} N & E \end{bmatrix}^T$

Table 1.2: Abbreviations that are used to describe the position and velocity of the vessel, as per convention from [1] and [25, especially p. 19].

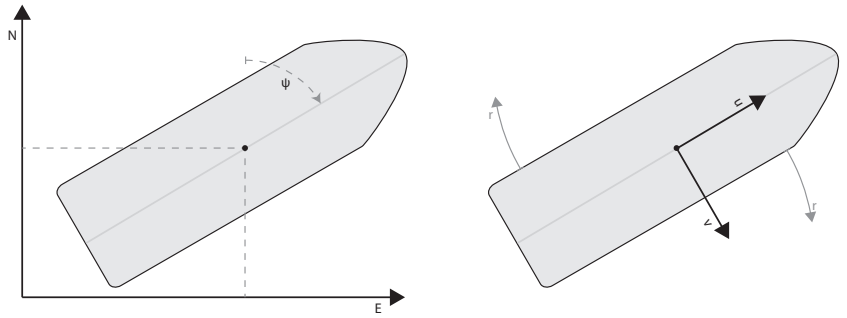

(a) The position of the vessel is defined in the NED coordinate system.

(b) The velocity is defined in the body coordinate system.

Figure 1.2: Coordinate systems.

Other published works focus on how a vessel interacts with the environment such as ice, ocean waves and wind.

The intention of this section is to provide a basic explanation of the ship model that is used in this work. A detailed discussion of mathematical modeling of marine vessels unfortunately falls outside the scope of this publication, and the reader is invited to consult the literature that is referenced in this section.

1.2.1 Geometry and kinematics

The investigation that is presented here deals with a ship that moves on the ocean surface at relatively low velocities, where the roll and pitch motions of the vessel are neither monitored nor compensated. The model that is used therefore only describes the planar position and orientation of the vessel. A coordinate system is selected with the origin at or near the the DP setpoint, x-axis pointing to North, y-axis pointing to East, and the (unused) z-axis pointing downwards per the right-hand rule. The orientation of the ship in the xy-plane is defined as clockwise rotation with the orientation in which the bow points to the North as the reference.

The velocity of the vessel is usually described in its own frame of reference, with the forward velocity u, sideways velocity v towards the starboard and the

clockwise yaw rotation rate r. The abbreviations that are used to describe the position and the velocity of the vessel are presented in Table 1.2 and in Figure 1.2. The relationship between them is purely geometric, and is described by

$$\dot{\eta} = \underbrace{\begin{bmatrix} \cos(\psi) & \sin(\psi) & 0 \\ -\sin(\psi) & \cos(\psi) & 0 \\ 0 & 0 & 1 \end{bmatrix}}_{P(\psi)} \nu \tag{1.1}$$

1.2.2 Dynamics

Forces and torques (taken together they are called "generalized force"[26]) from several physical sources act on the vessel. If the torques are expressed with the same pivot, their total effect is equivalent to their algebraic sum. The generalized force that is generated by the thrusters is perhaps the one that is the most important to the control systems engineer. Other forces that act on the ship include hydrodynamic drag, waves and currents. The velocity and angular rotation speed are expressed in a frame of reference that is bound to the ship, which may be rotating. A rotating frame of reference is not inertial, and the Newtonian equations of motion normally have to include corrective terms for Coriolis and centripetal pseudo forces [5]. If the rate of yaw rotation is modest however, these terms may reasonably be disregarded, as will be done in this treatment.

For slow speeds a linearization of the hydrodynamic drag is also reasonable. A significant component of the hydrodynamic drag on a rigid body in a fluid is proportional to acceleration of the rigid body, resisting the acceleration. Its effect is that the body behaves as if it had more mass [86]. Unlike the physical mass, this effect is not symmetric, and for ships it is typically larger in the lateral direction than in the longitudinal direction. It can be shown that the resulting equations of motions can be represented in vector form as

$$M\dot{\nu} + D\nu = \tau + \tau_{env} \tag{1.2}$$

where $M \in \mathbb{R}^{3\times3}$ is the generalized mass matrix and represents the physical mass and the hydrodynamic added mass. The drag approximation $D\nu$ is conventionally placed on the left side of this equation, changing the signs of the elements of D accordingly.

The environmental forces that are not included in $M\dot{\nu}$ or $D\nu$ are collected in τ_{env}. Those include the force due to current, high- and low-frequency components of the wave forces, and wind. The current force and the low-frequency components of the wave forces can be handled by e.g. the integral action in the DP control algorithm. Typically, it is not necessary to compensate for the high-frequency components of the wave forces, since they are essentially just rock the boat back and forth. Those motions are usually discarded by a wave filter before the position measurement is sent to the DP system. The wind forces are usually estimated with wind sensors. Theoretically, this can be done fairly accurately, but the practitioners often encounter complications due to the difficult geometry of the ships and local variations in the wind speed.

Modeling and predicting the force that is generated by various thruster devices is an active area of research. In this work, the actual force that is produced by the thrusters is assumed to be the controlled variable. This assumption implies that the local thruster controllers can accept a setpoint force as their input. The mapping from a force request to an RPM setpoint is non-trivial. For example, [59] proposes a feedback-based strategy that ensures the propeller torque can be set as needed, and in [54] the thruster-hull interactions are modeled, which could make it possible to create local thruster controllers that could compensate for those effects automatically.

Resultant thruster force calculations

A thruster that is located at r_i relative to the origin of a common coordinate system, generating force f_i at an angle α_i clockwise from the forward direction (ref Table 1.1) will generate a generalized force

$$\tau_i = \begin{bmatrix} \cos(\alpha_i) \\ \sin(\alpha_i) \\ -l_{yi}\cos(\alpha_i) + l_{xi}\sin(\alpha_i) \end{bmatrix} f_i \tag{1.3}$$

The resultant generalized force from all the thrusters can be represented as

$$\tau = T(\alpha) f \tag{1.4}$$

where the columns of $T(\alpha) \in \mathbb{R}^{3 \times Nthrusters}$ are of the form (1.3). A very simple thrust allocation algorithm can be implemented by Moore-Penrose pseudo-inverting $T(\alpha)$, calculating the force commands f per

$$f = \underbrace{\left(T(\alpha)T^T(\alpha)\right)^{-1} T^T(\alpha)}_{T^+(\alpha)} \tau \tag{1.5}$$

This algorithm does not consider thruster saturations or azimuth changes, so the algorithms in practical use are normally more advanced [39].

Relationship between generated force and power consumption of the thrusters

Dimensional analysis of a propeller in free water (i.e. far from a ship hull or other obstructions and disturbances) combined with a few other hydrodynamical assumptions lead to a model where both the thrust and the torque produced by a propeller which is stationary in the water are proportional to the square of the speed of rotation of the propeller [77, p. 145]. The power that is required to keep the propeller at a constant speed of rotation is the torque times the speed of rotation, which means that it is reasonable to assume that the power required to drive a propeller is proportional to the force it produces to the power of $3/2$. This approximation is used in many treatments, such as [39, 78, 79]. A second-order approximation is often used as well, that is that the power needed to drive the propeller is assumed to be proportional to the square of the delivered force. In either case, the coefficient of proportionality can variate greatly between propeller designs.

1.3 Diesel engine model

In this section, the main principles of modeling of a marine diesel engine are discussed.

A very accurate model for a turbocharged diesel engine can be constructed using a CFD simulation of the process fluids in the engine combined with a model of the dynamic behavior of the mechanical parts throughout the combustion cycles. Less accurate but more practical cycle-mean quasi-steady models, such as those examined in [74, 75, 89], are capable of making reasonable quantitative prediction of the diesel engine behavior on the time scales comparable to a drive shaft revolution.

A diesel engine deployed in a power plant is controlled by its governor in a tight feedback loop, which counteracts much of the dynamic behavior of the engine. The scope of the work that is described in this thesis is not a detailed investigation of the dynamic response of a particular diesel engine, but rather a more general performance testing of the power grid as a whole. The model of the diesel engine for this use needs to accurately represent the most important dynamical properties of the engine as well as the physical limitations which are impossible for the governor to counteract. The most important such limitation is the turbocharger lag, which limits the amount of oxidizer in the cylinders, and therefore also the maximum effective fuel injection. Other practically important factors include the fuel index rate limit, and a governor response lag. The latter is an inevitable factor in feedback-based governors, since they cannot undertake any correcting action until after a deviation from the velocity setpoint is reliably measured, and the aggressiveness of that correcting action is usually limited by stability considerations.

Such model was was developed by the present author in collaboration with T. A. Johansen and R. Skjetne in [79], and is included (with permission) in the following for completeness. The model is based on [11, 67, 71, 89], and can be considered a simplification of the model in [89].

The benefit of this model compared to other models in the literature is that situations when the engine experiences large load variations are represented with a reasonable degree of fidelity, while in most other respects the model remains fairly simple.

The marine diesel engine manufacturers typically limit the permitted rate of change of the fuel index, both upwards and downwards. This model does not include a rate limiter, and therefore permits variations in the power output that are so large that they would quickly wear down the engine due to thermic variations. Care should be taken in application to limit load variations.

1.3.1 Assumptions and simplifications

Compared to the model in [89], the following assumptions and simplifications are made in this model:

- The angular velocity of the turbine is assumed to depend on the generated power only. In reality this relationship is quite dynamic, with other factors such as thermodynamic relationships incorporated in the exhaust manifold. Still, both generated power and the exhaust volume that drives the tur-

bocharger depend upon how much fuel is burned per unit of time, and both relationships are linear to some degree.

- To calculate the Air-to-Fuel ratio (AF) after each injection, it is assumed that the fuel injected into the cylinder in each cycle is proportional to the fuel index position. The amount of air entering the cylinder is assumed to be linearly dependent on the velocity of the turbocharger compressor. If the compressor velocity is zero, then the amount of air entering will be $m_{a,0}$, and it will linearly increase to a maximum value as the velocity of the compressor approaches its maximum value.
- There is a delay in the order of $(60/N)\cdot(2/z_c)$ seconds from fuel index change until the corresponding change of torque on the drive shaft. The main cause of the delay is that it takes time before the new measure of fuel is injected into the next cylinder in the firing sequence, and in addition it takes some more time before the ignition leads to increased in-cylinder pressure and then increased torque on the drive shaft[63, p. 25]. The nominal RPM of the engines in the simulations was around $N = 1800$, so this delay had little practical consequence and was ignored.
- On older engines, setting a new value for the fuel index involved moving an actual fuel rack, a mechanical device which determined the fuel injection rate into the engine, resulting in a certain amount of lag. On newer engines with direct fuel injection there is no physical fuel rack, so this delay is not included in the model.
- Performance of a diesel engine during a large transient is limited by the performance of the turbocharger, which needs time to increase the pressure in the intake manifold. Until it does, the concentration of oxygen in the combustion chamber will limit the combustion.
- The damping due to friction is mostly a function of the current engine RPM. Since the engine in a power plant normally operates in a narrow RPM range, this friction is not important for the dynamical performance of the engine and was not modeled.

In addition, the EGR (exhaust gas recycling) is assumed to be reduced or disabled during the upward transients.

1.3.2 Variables

The variables used for the diesel engine model are described in Table 1.3.

1.3.3 Mathematical formulation

The proposed diesel engine model is centered around the swing equation that describes the rotation of the drive shaft, (1.12); the drive shaft is driven by the expanding combustion products in the cylinders, and it drives the electric load through the electric generator.

Symbol	Description
p_e	Break mean effective pressure in the cylinders (p.u.)
t_m	Total mechanical torque from an engine (p.u.)
t_e	Electrical torque (p.u.)
$p_{e,r}$	Rated BMEP (Pa)
N	Instantaneous crank shaft RPM
N_r	Nominal engine RPM
z_c	Number of cylinders
V_h	Cylinder volume (m^3)
η_c	Combustion efficiency (non-dimensional, p.u.)
F_r	Fuel rack/fuel index position (nondimensional, p.u.), which determines the amount of fuel injected into the combustion cylinders per diesel cycle.
ω_t	Turbocharger rotational velocity (p.u.)
T_t	Turbocharger dynamics time constant
$m_{a,0}$	Air flow (mass) without the turbocharger as fraction of the maximal airflow
AF_n	Nominal air-to-fuel ratio on max turbocharger velocity and max BMEP
AF_{low}	Air-to-fuel ratio at which the combustion stops due to excessive in-cylinder cooling from the injected fuel.
AF_{high}	Air-to-fuel ratio at which full combustion is achieved. Typical values: 20-27 for HFO, 17-20 for Diesel Oil
P	Current engine power output (Watt)
P_l	Power consumed by the load (Watt)
P_r	Rated engine power (Watt)
I	Moment of inertia of the rotating mass in the genset ($kg \cdot m^2$)
H	Inertia constant of the engine, represented as the time needed for the engine running at nominal power to produce the energy equivalent to the kinetic energy in the rotating mass at nominal speed.

Table 1.3: Variables used for the diesel engine model.

The amount of fuel injected into the cylinders at each combustion cycle determines the energy in the combustion gases, assuming that there is enough air present in the cylinder to burn the fuel efficiently. The fuel rack can change the fuel injection arbitrarily, which roughly translates to a change in BMEP (p_e in per-unit) after a short injection and combustion delay which may not be modeled. Since the cycle-mean torque delivery is proportional to BMEP, the per-unit torque t_m has the same numerical value as p_e, as expressed in (1.8). If the

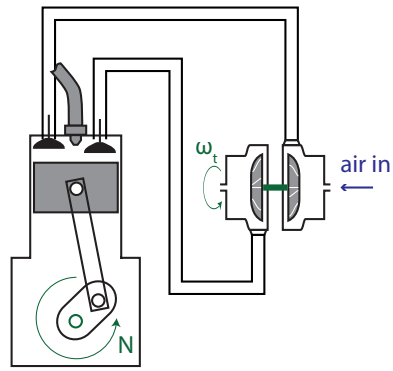

Figure 1.3: A simplified representation of a single diesel engine cylinder

oxidizer concentration is not high enough for efficient combustion, the combustion efficiency η_c will go down per (1.8).

The air to the cylinders is compressed by the turbocharger. The equation (1.9) is a rough representation of the turbocharger lag. This lag includes a large number of effects, such as pressure buildup in the exhaust manifold (if the turbo is not pulse charged), acceleration of the turbocharger shaft and buildup of the pressure in the intake manifold, as well as heating up the engine to the new working temperature.

If the turbocharger didn't have time to increase air delivery sufficiently, then either the combustion efficiency will be reduced as per (1.8), or the fuel rack limiter will be activated and not allow the fuel rack to exceed the maximal efficient value.

The torque from the electric load t_e is an external input to this model and has to come from the model of the generator.

$$AF = \frac{m_{a,0} + (1 - m_{a,0})\omega_t}{F_r} \cdot AF_n \tag{1.6}$$

$$\eta_c = \begin{cases} 1 & AF \geq AF_{high} \\ \frac{AF - AF_{low}}{AF_{high} - AF_{low}} & AF_{low} < AF < AF_{high} \\ 0 & AF \leq AF_{low} \end{cases} \tag{1.7}$$

$$t_m = p_e = \eta_c F_r \tag{1.8}$$

$$\dot{\omega}_t = -1/T_t(\omega_t - p_e) \tag{1.9}$$

$$P = p_{e,r} p_e z_c V_h {}^N/_{60} = P_r t_m {}^N/_{N_r} \tag{1.10}$$

$$H = \frac{\frac{1}{2} I \left(\frac{2\pi N_r}{60}\right)^2}{P_r} \tag{1.11}$$

$$\dot{N} = \frac{\frac{1}{2} N_r (t_m - t_e)}{H} \tag{1.12}$$

1.3.4 Numerical values

The numerical parameters that are used in simulations in this dissertation are matched so that they represent a typical marine diesel engine of the size used in the rest of this work. The stoichiometric ratios AF_* are taken within the range specified in [89, page 23], $AF_{high} = 20$, $AF_{low} = 14$. The air-to-fuel ratio under full power and fully developed turbocharger velocity is set to 27. The naturally perspired efficiency m_{a0} is set to 0.2 to reflect the compression ratio in the modern marine turbochargers, which is around 5 [55]. The losses in the conversion of power from the mechanical to electrical systems are not modeled, so the rated power P_r of each diesel engine can be calculated from the genset rated power.

1.3.5 Diesel engine governor

A diesel engine prime mover for a power plant has to maintain its rotational velocity in presence of variations in the load. This requires a feedback-based controller. The controllers for the diesel engines are conventionally called "governors". Ill-designed governors may create unnecessary variations in the electric frequency, increase fuel consumption on the grid and in the worst scenarios destabilize the plant. Legacy implementations are either distributed droop governors, or isochronous governors. Droop governors are usually implemented as PID controllers that measure the deviation in the electric frequency from a drooped setpoint and control the fuel index accordingly. Isochronous governors have a constant (non-drooped) frequency setpoint but also share information about the average load on each connected bus segment through a separate load sharing line. Introductory texts about marine diesel control systems are available in e.g. [9, 71, 87], and [19, sec 4.4.1]. Texts about general engine modeling and control, such as [17], may also be of interest. More modern control methods for marine power plants, such as those in the recent Kongsberg power management systems, use droop-based governors but rapidly modify the droop curve based on the loading situation. This way, they achieve both the fault tolerance of the droop governors and the frequency stability of the isochronous governors.

1.4 DP control architecture

The vast majority of vessels that are equipped to keep position using the thruster force have a capability to do so automatically, with computers controlling the individual thrusters.

The computer algorithms that are designed for this purpose are usually separated into several levels. First, a high-level motion control algorithm, also called a DP control algorithm, calculates the total force and moment of force that the thruster system should produce. Then, a thrust allocation (TA) algorithm coordinates the thrusters so that the resultant force they produce matches the request from the DP control algorithm.

Achieving the dynamic positioning task may be trivial if the environmental conditions are favorable, positional precision requirements are leisurely and the operator is not too concerned about costs such as fuel and wear-and-tear of the machinery. For the high-level motion controller, one can use three independent PID controllers (one for each degree of freedom), and a simplistic thrust allocation algorithm as described in Subsection 7.2.2.

More advanced algorithms aim to have faster position acquiring and recovery, less rapid variation in the thruster commands, handling of variable-direction thrusters, better handling of thruster limitations, etc. Several well-functioning algorithms for the high-level motion control are known, many of them are described in [25, Subsection 12.2]; also, in [34] the high-level motion control is implemented as an MPC algorithm, resulting in a controller that combines use of leisurely control effort as long as it is sufficient to keep the vessel within a predefined operational area, and more aggressive control effort when dynamic simulations show that the vessel would leave the operational area otherwise. The task of allocating the force

order to the individual thrusters is left with a classical thrust allocation algorithm. A similar MPC-based high-level motion controller was discussed in [16], although without simulating disturbances or including constraints on the position of the vessel [8]. [40] [42]

Thrust allocation remains an active field of research. The most recent trends are towards integration and increased information passing between the control allocation and other systems on the ship. In [65], a thrust allocation method is introduced with a functionality to balance the the thruster load between the different parts of the power plant, allowing a reduction in the total NOx emissions. Using thrust allocation to reduce the load variations on the power plant has been explored in e.g. [56, 78, 79]. Also notably, in [62] the local thruster control was modified to achieve the same purpose, thus bypassing the thrust allocation algorithm. A recent review of the state of the art thrust allocation is available in [39].

1.5 Main contributions

The main contributions found in this thesis are summarized here. Parts of this thesis have been published previously. The present author was responsible for the main research effort, including development and testing of the algorithms and writing all those publications except the one which forms the basis for Chapter 4, in which he had a supporting role. References to these publications are given below.

- Chapter 2 describes a thrust allocation algorithm that facilitates more stable loading on the power plant. This algorithm modulates the power consumption by coordinating the thrusters to introduce load variations that counteract the load variations from the other consumers on the ship. To reduce load variations without increasing the overall power consumption it is necessary to deviate from the thrust command given by the dynamic positioning system. The resulting deviation in position and velocity of the vessel is tightly controlled, and results show that small deviations are sufficient to fulfill the objective of reducing the load variations. The effectiveness of the proposed algorithm has been demonstrated on a simulated vessel with a diesel-electric power plant. A model for simulation of a marine power plant for control design purposes has been developed.

  The results show that the load variations on the power are significantly reduced compared to the existing algorithms in the literature. There are several advantages to reducing the load variations, which include 1) less wear-and-tear of the individual generator sets, which would otherwise be subject to thermic variations, 2) more stable grid frequency allows more reliable connection of additional generators to the grid, which can be crucial in critical situations where additional power is needed to prevent a black-out, 3) load variations may lead to starting up of additional generators, and 4) transients in load variations lead to less efficient combustion.

  The material in this chapter is based on the paper titled “Thrust allocation with dynamic power modulation for diesel-electric ships”, by A. Veksler, T. A. Johansen, E. Mathiesen, and R. Skjetne, which was submitted to IEEE Transactions on Control Systems Technology in October 2013, and resubmit-

ted in a revised version in April 2014 [83]. Intermediate results of this work were also published in [78] and [79].

- Chapter 3 introduces a modification to the TA algorithm from the previous chapter that improves the capability of that algorithm to control its power consumption by continuously monitoring the environmental forces and modifying the setpoint of the dynamic positioning algorithm to place the vessel a short distance (e.g. 20 cm) in the direction of steepest increase of the environmental force potential, thus maximizing the available potential energy. Its contents are based on the conference article "Reducing power transients in diesel-electric dynamically positioned ships using re-positioning", by A. Veksler, T. A. Johansen, R. Skjetne, and E. Mathiesen, which is to be presented at the 40th Annual Conference of the IEEE Industrial Electronics Society in Dallas, Texas [84].
- Whereas the previous chapters examine the practicality of using the thruster system to compensate for the power variations by other consumers mainly through computer simulations, in Chapter 4 the question of practicality is approached from a more theoretical perspective. In this chapter, formulas are derived in order to relate the dynamic energy storage capacity to the maximum allowed ship position deviation, as a function of the frequency of the requested dynamic energy storage. The benefits of DP dynamic energy storage are found to be reduced diesel-generator maintenance need, reduced fuel consumption and emissions, reduced risk for blackout, and increased operational flexibility allowing power-consuming operations such as drilling and lifting to be safely prioritized over DP for short periods of time. The results are largely in agreement with the computer simulations from the previous chapters. Its contents are based on the article "Dynamic Positioning System as Dynamic Energy Storage on Diesel-Electric Ships", by T. A. Johansen, T. I. Bø, E. Mathiesen, A. Veksler, and A. Sørensen, which is currently in press in IEEE Transactions on Power Systems [43]
- In Chapter 5, the diesel engine model that is described in Section 1.3 is used to design an improved diesel engine governor. The proposed governor is centralized, with a single controller for all generator sets that are connected to a bus. It is based on MPC, which allows a consistent handling of preview information about the loading of the power plant. For example, this allows the governor to prepare the power plant for e.g. rapid load increases. Additionally, this governor can be tuned for aggressive response to load variations. Due to the use of feed-forward, this adaption has a potential to remove the frequency variations from the grid almost entirely. This results in excessively heavy use of equipment, but may be helpful in emergency situations, where the benefits – which include larger margins to the under-frequency condition, reduced risk of blackout and more reliable synchronization of additional generating sets – may outweigh the costs. The contents of this chapter are based on the conference article "Governor principle for increased safety and economy on vessels with diesel-electric propulsion" by A. Veksler, T. A. Johansen, E. Mathiesen, and R. Skjetne, which was presented at the European Control Conference in Zürich, Switzerland in 2013 [80].

- The literature on thrust allocation algorithms that is currently available usually focuses on solving only a few of the many facets of the thrust allocation problem at a time. Chapter 6 presents a unified thrust allocation algorithm that solves most of the challenges that are faced by the practitioners in one algorithm. Those challenges include controlling thrusters such as azimuth thrusters and ruddered propellers that can change the direction of the generated thrust slowly as well as thrusters that can generate force in either positive or negative directions; minimizing the power consumption and wear-and-tear in the thrusters; and handling thruster saturations. In particular, when rotable thrusters are present, a functionality to avoid driving the thruster system into singular configurations should usually be included. This functionality requires significant numerical calculations for each iteration of the thrust allocation algorithm. In the presented work those calculations were written in explicit form using a symbolic processor, translated to ANSI C and compiled. This technique was demonstrated to provide acceptable real-time performance.

  The product is a well-functioning thrust allocation algorithm that can handle most of the practical situations.

  The contents of this chapter are largely based on the conference article "Cartesian thrust allocation algorithm with variable direction thrusters, turn rate limits and singularity avoidance", by A. Veksler and T. A. Johansen, and F. Borrelli, which is to be presented at IEEE Multi-conference on Systems and Control in Antibes Juan-les-Pins, France in October 2014 [81].

- The control output produced produced with classical control architecture consisting of a separate high-level motion control algorithm and a thrust allocation algorithm is not always optimal; this may result in a position loss that would not have occurred with a more sophisticated control algorithm. Recent advances in computer hardware and algorithms make it possible to consider model-predictive control algorithm that combines positioning control and thrust allocation into a single algorithm; theoretically this should yield a near-optimal controller output. The work that is presented in Chapter 7 explores advantages and disadvantages of using model predictive control compared to the traditional algorithms.

  The results show a control architecture that is capable of coordinating thrusters with the motion of the hull in ways that do not appear to be possible with the classical control architecture without significant heuristic adaption to the latter.

  The contents of this chapter are based on a paper titled "Dynamic positioning with model predictive control" by A. Veksler, T. A. Johansen, F. Borrelli, and B. Realfsen, which has been submitted to IEEE Transactions on Control Systems Technology in July 2014 [82].

Chapter 2

Thrust allocation with dynamic power modulation for diesel-electric ships

2.1 Introduction

A marine vessel is said to have dynamic positioning (DP) capability if it is able to maintain a predetermined position and heading automatically exclusively by means of thruster force [4]. DP is therefore an alternative, and sometimes a supplement to the more traditional solution of anchoring a ship to the seabed. The advantages of positioning a ship with the thrusters instead of anchoring it include:

- Immediate position acquiring and re-acquiring. A position setpoint change can usually be done with a setpoint change from the operator station, whereas a significant position change for an anchored vessel would require repositioning the anchors.
- Anchors can operate on depths of only up to about 500 meters. No such limitations are present with dynamic positioning.
- No risk of damage to seabed infrastructure and risers, which allows safe and flexible operation in crowded offshore production fields.
- Accurate control of position and heading.

The main disadvantages are that a ship has to be specifically equipped to operate in DP, and that dynamically positioned ships consume a lot more energy to stay in position, even though anchored vessels also have to expend energy to continuously adjust the tension in the mooring lines.

DP is usually installed on offshore service vessels, on drill rigs, and now increasingly on production platforms that are intended to operate on very deep locations.

To maximize the capability of the DP system, the thrusters should be placed on distant locations on the ship, which makes mechanical transfer of power from the engines less practical compared to electrical distribution. This and other operational advantages [19, p. 6] result in electric power distribution being almost ubiquitous in offshore vessels with DP today.

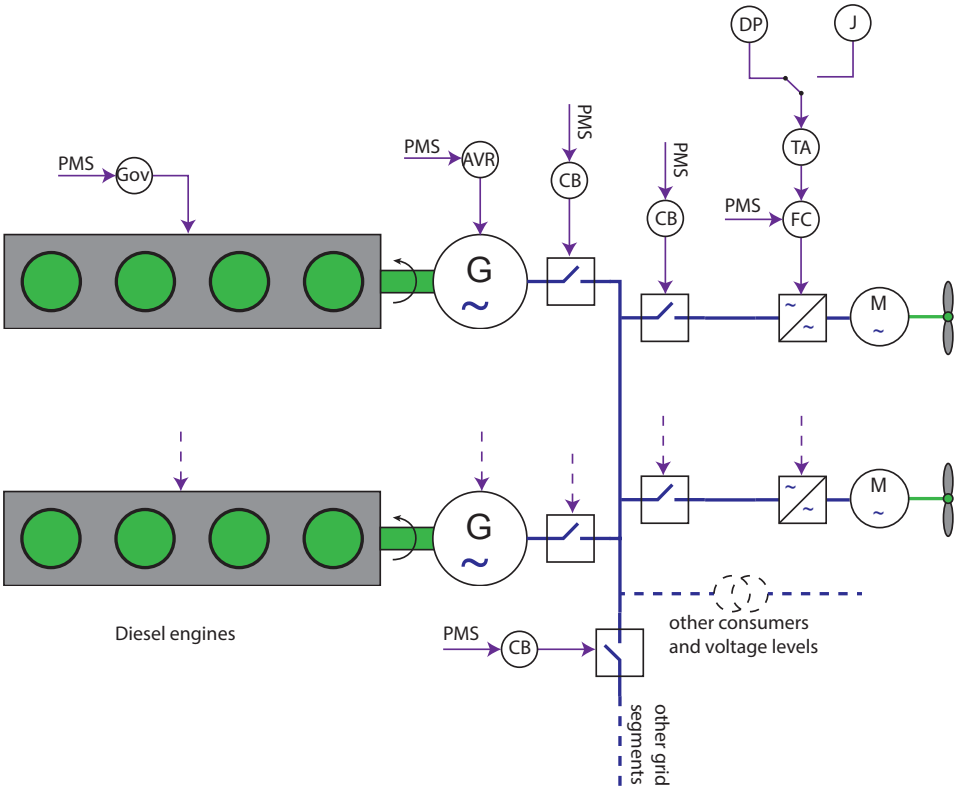

Figure 2.1: An illustration showing some of the controllers on the electric grid. A diesel engine speed controller, conventionally called governor (Gov), adjusts the amount of fuel injected into the engines; An Automatic Voltage Regulator (AVR) adjusts the magnetization of the rotor coils of the generators (G); various circuit breakers (CB) connect and disconnect equipment and also isolate faults such as short circuits; the Frequency Converters (FC) are used for local control of the thruster motors (M), and receive commands from both the Thrust Allocation (TA) and the Power Management System (PMS). Finally, the TA can receive the generalized force command from either the DP control system or from a Joystick (J).

The type of prime mover predominantly in use is the diesel engine, although other types such as gas engines and gas turbines are also available. A power grid on a DP vessel typically consists of several diesel generators connected to the thrusters and other consumers through a reconfigurable distribution network with several separable segments and several voltage levels. Often, the thruster system requires more power from the generators than all the other consumers on the grid combined. The control architecture for the resulting system is highly distributed, with independent controllers for diesel engine fuel injection, generator rotor magnetization, circuit breakers, centralized and local thruster controllers, etc. An example of such network with controllers is shown on Figure 2.1. In legacy implementations in the literature and the industry, many of the controllers do not directly communicate with each other, but instead gain information about the state of the grid by monitoring voltage levels, currents and the frequency on the bus. This has changed in the recent years with increased communication between the individual controllers through data networks.

While diesel engines are efficient in terms of fuel consumption [46], use of primarily diesel electric power grid introduces a range of challenges for the control system in terms of both stability and fuel efficiency. Stability relates to maintaining stable frequency and voltage on the grid in presence of large and sometimes unpredictable disturbances in load, as well as stable load sharing when a grid segment is powered by more than one generator set. Modern marine diesel engines are almost always turbocharged. Turbocharging limits how fast the engine can increase its output because increasing the output requires building up pressure in the scavenging receiver, which puts a physical limit on how fast a diesel-electric power plant can increase its output. A rapid load increase can therefore lead to a mismatch between the generated mechanical and consumed electrical power. This mismatch can become unrecoverable even if the load rate constraints on the governors are disabled. The result of this mismatch is deficit consumption that extracts energy from the rotating masses in the engines and the generators. If unchecked, it will lead to a rapid drop in frequency, and then a blackout due to engine stall or protection relay disconnect.

Economic and environmental concerns are somewhat coupled, because factors that lead to pollution often also lead to increased economic costs. Increased fuel consumption leads to both increased fuel expenses and (under most circumstances) more pollution. Pollutants such as carbon monoxide, unburned hydrocarbons, soot and NO_X emissions constitute a minor part of the combustion process in terms of energy, and have therefore a negligible impact on the engine process [21, p. 194]. However, those emissions tend to increase during load transients, especially upwards transients [63, ch. 5 and p. 37]. Those transients also increase wear-and-tear on the engines because of the resulting thermic expansion and contraction. In addition, load variations on the power plant as a whole may lead to excessive start and stop of generator sets, with additional pollution and wear-and-tear due to cold start transients.

Because of this, variations in the power consumption have recently received increased attention in the literature. A cost term for variations in force produced by the individual thrusters is included in [42], which has a dampening effect on the combined load variations. In [37] functionality to handle power limitations in the

optimization process and other power-related features are introduced.

Thrust allocation algorithms such as [42] and [40] do their best to produce the commanded generalized force at all times, most often by passing this command as a constraint to a numerical optimization solver. In practice, the high inertia of a ship makes it possible to deviate from this command over short periods of time without affecting the position and velocity of the ship significantly[43]. This makes it possible to exploit the thrusters to improve the load dynamics on the power grid. In terms of energy preservation, the short-term transfer of energy from the thrusters can be thought of as coming from the potential energy stored in the mass of hull in the field of the environmental forces. The amount of energy that can be made available is thus proportional to the mass of the vessel and the square of the permissible velocity deviation. The distance the ship is allowed to deviate from the setpoint determines the length of time until the thrusters will need to use energy to stop the ship and then turn it around. Several approaches to realizing this has been attempted in the literature. In [62], the local thruster controllers were modified to counteract the variations in frequency on the grid by deviating from the orders they receive from the thrust allocation algorithm. Approaching this problem on the local thruster controller level precludes the possibility of estimating and limiting the resulting deviations in the position of the ship, since the individual thruster controllers do not have the information about the actions that the other local controllers are undertaking and can not compute the deviation in the resultant generalized force. Because of this limitation, in this work the power redistributing functionality is moved to the thrust allocation algorithm. In [56], information on the maximum available power from the PMS to the local thruster controllers was used to reduce thruster loads in order to compensate for load variations elsewhere.

The present work combines and expands the contributions in [78], [79]. It describes and tests a thrust allocation algorithm that coordinates the thrusters to introduce load variations that counteract load variations from the other consumers on the ship, thus reducing the total load variations on the power plant.

In order to produce the counteracting load variations, the thrusters have to be able to both increase and decrease their power consumption at will. Increasing the power consumption can be achieved by biasing the thrusters as described in Subsection 2.4.4, thus simply wasting the superfluous energy. Reducing the power consumption is more complicated. For any feasible thrust command given to the thrust allocation algorithm there exists a minimal value for the power consumption needed to achieve this thrust. The existing thrust allocation algorithms usually attempt to minimize the power consumption, and in practice the power consumption is for this reason very close to the minimum. This presents two options to control variations in power consumption. The first option is to maintain a thruster bias reserve for this purpose. When a reduction in power consumption is requested to compensate for an increase elsewhere, the thrust allocation algorithm can release some or all of this bias. This will increase the overall power consumption. The second option is to let the power consumption go below the minimal value needed to execute the thrust command, allowing a temporary deviation between commanded and generated thrust. The thrust allocation algorithm presented here explores the second option. It estimates the resulting error introduced in velocity and position of the vessel, and constraints this error to stay within acceptable parameters.

In cases where the surges in power consumption are too large to be compensated by the thrusters, they get delayed. The thrust allocation algorithm sends a feedforward signal to the generator speed controllers (governors), allowing them to prepare for the delayed load increases.

This chapter also introduces a practical and generic model for the turbocharger lag modeling, which is used for power plant simulation. In order to focus on the power management aspects of the method, the study has been limited to thrusters with fixed direction. Several methods for handling variable-direction thrusters have been described in the literature, see e.g. [39].

The structure of this article is as following: first, the architecture of the relevant control systems on a dynamically-positioned ship is presented in Section 2.2; a mathematical model that describes the motion of a ships at the low velocities that are characteristic of the dynamic positioning applications is developed in Section 2.3; this model is used to formulate an estimate of how much deviations in the thrust allocation affect the velocity and position of the vessel in Subsection 2.3.2; the thrust allocation algorithm is described in Section 2.4 and a simulation study is presented in Section 2.5. The simulation study includes a description of the simulated vessel Subsections 2.5.1 – 2.5.6. The specifics of the diesel engine model are given in Section 1.3.

To keep the presentation concise, following notation is used:
For $x \in R^N$, $Q = Q^T \in R^{N \times N} \succ 0$, $Q = LL^T$

$$|x|^p \triangleq [|x_1|^p, |x_2|^p, \dots |x_N|^p]^T \tag{2.1}$$

$$|x|^p \, sign(f) \triangleq \begin{bmatrix} |x_1|^p \, sign(f_1) \\ |x_2|^p \, sign(f_2) \\ \vdots \\ |x_N|^p \, sign(f_N) \end{bmatrix} \tag{2.2}$$

Notice that $|x|^p \in \mathbb{R}^N$, and is not a vector norm. Also,

$$\|x\|_Q^2 \triangleq x^T Q x = \|Lx\|_2^2 \tag{2.3}$$

$\mathcal{L}$ is the one-sided Laplace transform operator. For a function $f : \mathbb{R} \to \mathbb{R}$,

$$\mathcal{L}[f(t)](s) = \int_0^\infty e^{-st} f(t) dt \tag{2.4}$$

2.2 Control system architecture

This section describes the control architecture of a typical DP vessel, and places the presented thrust allocation algorithm within this framework.

Figure 2.2 shows how the proposed thrust allocation algorithm (highlighted in blue) fits within the overall control strategy of the DP and the power plant. A high level motion control algorithm receives the ship position and velocity reference from e.g. GPS, and generates the force and moment of force (collectively generalized force) reference τ_d that can bring the vessel to the setpoint location. The thrust

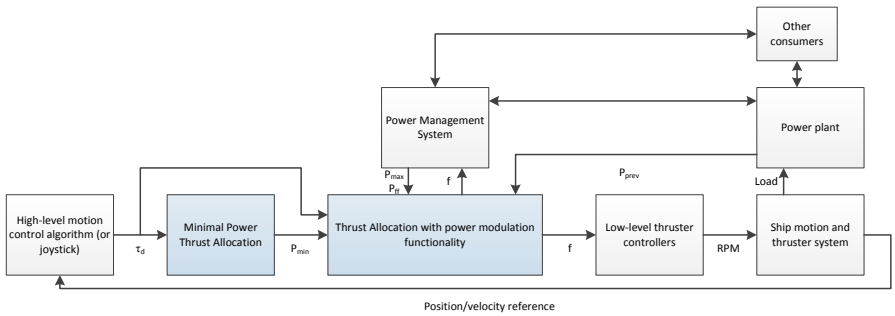

Figure 2.2: A general overview of the control architecture.

allocation algorithm attempts to coordinate the thrusters so that the resultant generalized force τ they generate matches that reference.

Most thrust allocation algorithms in the literature follow that reference strictly, however the proposed thrust allocation algorithm introduces small deviations from the reference to improve the conditions for the power plant. Sometimes it reduces the power consumption below the minimal consumption needed to follow the reference (P_{min}), resulting in a temporary deviation in the position of the vessel.

The power management system normally has to approve large variations of load from the largest consumers, and in the proposed implementation it informs the thrust allocation algorithm about imminent variations in the load P_{ff} from other consumers, which, from the point of view of the thrust allocation algorithm, is a feedforward signal. The power management system also informs the thrust allocation algorithm about the maximum available power P_{max}, and the current power consumption P_{prev}.

The local thruster controllers should map the thruster force command f to an RPM command to the local thruster power supply, typically frequency converters. This mapping is non-trivial. For example, [59] proposes a feedback-based strategy that ensures the propeller torque can be set as needed, and in [54] the thruster-hull interactions are modeled, which could make it possible to create local thruster controllers that could compensate for those effects automatically.

2.3 Consequence analysis of a deviation from the commanded generalized force

In this section, a low-speed mathematical model of surface vessel is presented. This presentation can be seen as a summary of the more thorough discussions about marine vessel modeling that are available in the literature, such as [22, 24, 25, 31].

The model is then used to estimate the results of a deviation from the command in the thrust allocation algorithm.

Symbol	*Description*
$\eta = \begin{bmatrix} N & E & \psi \end{bmatrix}^T \in \mathbb{R}^3$	Position and orienation of the vessel in an inertial frame of reference, in this case North-East-Down.
$\nu = \begin{bmatrix} u & v & r \end{bmatrix}^T \in \mathbb{R}^3$	Velocity of the vessel in its own (body) frame of reference.

Table 2.1: Abbreviations that are used to describe the position and velocity of the vessel, as per convention from [1] and [25, especially p. 19].

2.3.1 Mathematical model

For the purposes of dynamic positioning, a ship is usually modeled as a rigid body in three degrees of freedom: Surge (forward), Sway (sideways) and Yaw (turn around the vertical axis). The model is separated into kinematic and dynamic equations.

Kinematics

The position of the ship is described in a locally-flat Cartesian coordinate system, with the origin near the DP setpoint, x-axis pointing towards the North and y-axis pointing towards the East. The orientation of the ship is described as a clockwise rotation with the bow pointing towards the North as the reference. This system of coordinates is called NED. The last letter is an abbreviation for the Down direction.

The velocity of the ship is described in the hull-bound frame of reference, called "body", with the velocity vector composed of forward velocity, lateral velocity and clockwise rotation. This nomenclature was formalized in [1]. A summary of the relevant terms and the conventional abbreviations is presented in Table 2.1.

The relationship between the position in the NED coordinate system and the velocity in the body coordinate system can be represented as

$$\dot{\eta} = R(\psi)\nu \tag{2.5}$$

where

$$R(\psi) = \begin{bmatrix} \cos(\psi) & \sin(\psi) & 0 \\ -\sin(\psi) & \cos(\psi) & 0 \\ 0 & 0 & 1 \end{bmatrix} \tag{2.6}$$

Dynamics

It is usually most convenient to express the forces that are acting on the ship in the "body" coordinate system.

$$M\dot{\nu} + C(\nu)\nu = \tau_{tot^*} \tag{2.7}$$

where M is the mass matrix including the hydrodynamic added mass, and τ_{tot^*} is the total resultant generalized force that is acting on the vessel. The centripetal and coriolis term $C(\nu)\nu$ is defined in e.g. [25] or (expanded in the scalar form) in [1].

For low-speed applications the hydrodynamic damping (water resistance) force can be approximated as proportional to the ship velocity, that is $-D\nu$ with D being a constant matrix. The negative sign is purely conventional. The coriolis and centripetal forces may also be ignored. This allows representing (2.7) as

$$M\dot{\nu} + D\nu = \tau_{tot} \tag{2.8}$$

where $\tau_{tot} = \tau_{tot^*} + D\nu$.

Thruster forces

Let a thruster i located on the ship at the point $\begin{bmatrix} l_{xi} & l_{yi} \end{bmatrix}^T$ and at orientation α_i produce a force equal $K_{ii}f_i$, where $f_i \in \begin{bmatrix} -1 & 1 \end{bmatrix}$. Then, the force this thruster exert on the ship may be represented as $K_{ii}f_i \begin{bmatrix} \cos\alpha_i & \sin\alpha_i \end{bmatrix}^T$. The torque around the origin of the coordinate system will be $K_{ii}f_i\left(-l_{yi}\cos\alpha_i + l_{xi}\sin\alpha_i\right)$. Collecting the terms above yields

$$\tau_i = K_{ii}f_i \begin{bmatrix} \cos\alpha_i \\ \sin\alpha_i \\ -l_{yi}\cos\alpha_i + l_{xi}\sin\alpha_i \end{bmatrix} \tag{2.9}$$

Summing up the generalized force from all active thrusters yields the expression for the resultant generalized force from the thrusters which is fairly standard in dynamic positioning literature,

$$\tau = B(\alpha)Kf \tag{2.10}$$

where the columns of the matrix $B(\alpha) \in \mathbb{R}^{3\times N}$ consist of $\begin{bmatrix} \cos\alpha_i, & \sin\alpha_i, & (-l_{yi}\cos\alpha_i + l_{xi}\sin\alpha_i) \end{bmatrix}$

2.3.2 Consequences of a force deviation

In this subsection, an approximate expression for the consequences of a small deviation τ_e in the resultant generalized thruster force from the command τ_d to the thrust allocation algorithm is formulated.

If τ_e is small enough that the differences in the hydrodynamic forces can be ignored, the deviation in acceleration $\dot{\nu}_e$ can be extracted from (2.8)

$$\dot{\nu}_e = M^{-1}\tau_e \tag{2.11}$$

A solution of the thrust allocation algorithm is applied on the vessel for a time period δt, until a new solution is calculated. In typical industrial implementations the thrust allocation problem is solved every second, i.e. $\delta t = 1\,\text{sec}$. Defining T as the time when the current iteration of the thrust allocation algorithm is solved and the output is sent to the thruster controllers, let $T_e = T + \delta T$ be the time when the output from the next iteration of the thrust allocation algorithm is available to the thruster controllers.

If T_e is small enough to assume constant orientation of the ship from 0 to T_e, the deviation in velocity at time T_e can be approximated per

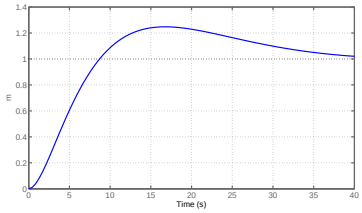

(a) The step response for a surge excitation the high-level motion control algorithm (closed loop) from the simulation in Section 2.5.7.

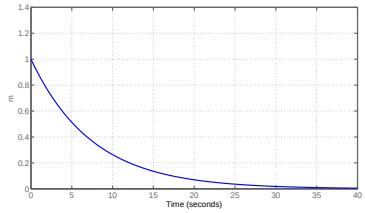

(b) Step response of the high-pass filter, with T_{dp}=8.5 seconds

Figure 2.4

$$\nu_e = \int_0^{T_e} \dot{\nu} dt \tag{2.12}$$

Under the same assumptions, the deviation in position η_e can be estimated per

$$\eta_e = \int_0^{T_e} \nu_e dt \tag{2.13}$$

The high-level motion control algorithm will also detect the deviations ν_e and η_e introduced by the proposed modifications in the thrust allocation algorithm, and will work to correct them. It will do so on a longer time scale than the thrust allocation algorithm. The thrust allocation algorithm should not correct for the deviations that are corrected by the high-level motion control algorithm. To estimate how much the position and velocity of the ship deviate from what they would have been had the thrust allocation algorithm followed its command exactly, deviation that is corrected by the high-level motion control algorithm has to be discarded. One way is to set a specific "hard" time window starting at T_s, and assume that any deviation that was before that time was corrected by the high-level motion control algorithm

Figure 2.3: The timescape of the real-time implementation. The thrust allocation algorithm is solved iteratively. The output signal is sent to the local thruster controllers at time T, and stays constant until time T_e when the output from the next iteration of the thrust allocation algorithm is available.

$$\nu_{e,\,h} = M^{-1} \int_{T_s}^{T_e} B(\alpha) K f(t) - \tau_d(t) dt \tag{2.14}$$

$$\eta_{e,\,h} = \int_{T_s}^{T_e} \nu_e dt \tag{2.15}$$

where T_s is a point in time before which it can be assumed that the dynamic positioning algorithm will correct any error. This timeline is illustrated in Figure 2.3. The approximation is valid as long as $T_e - T_s$ is small enough to assume constant orientation of the ship from T_s to T_e. This approximation was used in [79]. Alternatively, the separation can be done with a soft temporal separation between the TA and the high-level motion control algorithms by using a high pass filter on the deviation terms,

$$\nu_e(s) = \left[\frac{T_{dp}s}{T_{dp}s+1}\right] \mathcal{L}\left[M^{-1}\int_0^{T_e} B(\alpha)Kf(t) - \tau_d dt\right](s) \tag{2.16}$$

$$\eta_e(s) = \left[\frac{T_{dp}s}{T_{dp}s+1}\right] \mathcal{L}\left[\int_0^{Te} \nu_e dt\right](s), \tag{2.17}$$

where T_{dp} is a time constant which represents the bandwidth on which the high-level motion control algorithm operates. Observing that both ν_T and η_T are known and determined at the current time T, and that $f(t)$ and thus also the inner part of the integral (2.16) are constant from current time T until the time $T_e = T + \delta t$ when the solution from the next iteration of the thrust allocation algorithm becomes available, the integrals can be separated into past and future terms. High-pass filtering of the future signal can be reasonably discarded since $T_{dp} \gg \delta t$, resulting in the following estimates for the velocity and position deviation due to TA deviating from the command it receives:

$$\begin{aligned}\hat{\nu}_{e,\,T_e}(s) = \left[\frac{T_{dp}}{T_{dp}s+1}\right] \mathcal{L}\left[M^{-1}\left(B(\alpha)Kf(t) - \tau_d\right)\right](s) \\ + \frac{1}{s}\left(M^{-1}B(\alpha)Kf(T) - \tau_d\right)\delta t\end{aligned} \tag{2.18}$$

$$\begin{aligned}\hat{\eta}_{e,\,T_e}(s) = \left[\frac{T_{dp}}{T_{dp}s+1}\right] \mathcal{L}\left[\nu_e\right](s) + \frac{1}{s}\nu_{e,\,T}\delta t \\ + \frac{1}{s}\left(M^{-1}\left(B(\alpha)Kf(T) - \tau_d\right)\right)(\delta t)^2/2\end{aligned} \tag{2.19}$$

The Laplace transform should be evaluated at time T.

2.4 Thrust allocation with power modulation

In this section, a thrust allocation algorithm with a functionality to assist the power management system is described. The numerical optimization problem that is at the core of the method is introduced in Subsection 2.4.1. Certain implementational aspects are discussed in later subsections.

Decision variables	Slack variables	Controllable variables	Parameters that change between iterations	Physical parameters	Tuning parameters
f	s, τ_e	τ_d, P_{bias}, $\dot{P}_{ff}$, α	$f(T-\mathrm{t})$, $P_{th}(T-t)\ \forall t>0$ (used to calculate $\dot{f}$ and $\dot{P}_{th}$ with the selected discretization scheme)	P_c, K, $\underline{f}$, $\overline{f}$, P_{max}	Θ, Q_2, Q_3, Q_4, $\nu_{e,\,max}$, $\eta_{e,\,max}$

Table 2.2: Breakdown of the variables in optimization problems (2.20)–(2.22) and (2.24)–(2.29)

2.4.1 Numerical optimization problem

This subsection presents a mathematical description of the proposed method, with some implementational details left for later. The variables that are used for the thrust allocation algorithms are described in Table 2.2.

Minimal power thrust allocation

As the first step, the thrust allocation problem is solved for minimal power consumption without regard to variation in the power consumption:

$$P_{min} = \min_{f,s} P_c K \left|f\right|^{3/2} + \|s\|_{Q_1}^2 \tag{2.20}$$

subject to

$$B(\alpha)Kf = \tau_d + s \tag{2.21}$$

$$\underline{f} \leq f \leq \overline{f} \tag{2.22}$$

where the power consumption in thrusters is estimated by the nonlinear relationship

$$P_{th} = P_c K \left|f\right|^{3/2} \tag{2.23}$$

which is similar to what was used in [40]. This thrust allocation method is well-documented in the literature, usually with a quadratic power cost function; see [24]. Ideally, the solution of (2.20)–(2.22) should fulfill the thrust command τ_d exactly, which would imply that the slack variables satisfy $s \equiv 0$. This may not be possible

without violating the constraint (2.22). Therefore, s must be allowed to be non-zero, with the cost matrix Q_1 being large enough to ensure that s is significantly larger than zero only when constraints (2.21), (2.22) would otherwise be infeasible. The constraint (2.21) therefore ensures that the produced generalized force τ is for practical purposes equal to the commanded force τ_d unless the commanded force is infeasible, while (2.22) ensures that the thrusters are not commanded to produce more thrust than their maximal capacity. The solution to this optimization problem provides a minimum P_{min} to which the power consumption can be reduced while delivering the requested thrust τ_d, at least as long as the condition $s \approx 0$ holds. This minimum value is used in the following to calculate a control allocation with a specified power bias, P_{bias}, and a feedforward P_{ff} to compensate for power variations in other consumers. The choice of these inputs will be described shortly.

Power modulation functionality

The following optimization problem is used to solve for the actual thrust output:

$$\begin{aligned}\min_{f,s_1,s_2,\tau_e} P_c K \left|f\right|^{3/2} + \left\|K\dot{f}\right\|_{\Psi}^2 + \Theta\left(\dot{P}_{th} - \dot{P}_{ff}\right)^2 \\ + \left\|\tau_e\right\|_{Q_2}^2 + \left\|s_1\right\|_{Q_3}^2 + \left\|s_2\right\|_{Q_4}^2\end{aligned} \tag{2.24}$$

subject to

$$-\nu_{e,\,max} \leq \nu_e + s_1 \leq \nu_{e,\,max} \tag{2.25}$$

$$-\eta_{e,\,max} \leq \eta_e + s_2 \leq \eta_{e,\,max} \tag{2.26}$$

$$B(\alpha)Kf = \tau_d + \tau_e \tag{2.27}$$

$$P_{max} \geq P_c K \left|f\right|^{3/2} \geq P_{min} + P_{bias} \tag{2.28}$$

$$\underline{f} \leq f \leq \overline{f} \tag{2.29}$$

Table 2.2 presents a breakdown of the variables that are used in the two optimization problems above. The main decision variable from that controller is the vector f.

The generalized force order from DP or joystick is represented as τ_d. Contrary to the situation in (2.20)–(2.22), significant deviations are expected between the setpoint generalized force τ_d and the actual generalized force $B(\alpha)Kf$. This means that the slack variable in the generalized force constraint (s in (2.21)) is not longer expected to be close to zero. To emphasize this, it was replaced with τ_e in (2.27), and weight matrix Q_1 was replaced with Q_2, which presumably has smaller numerical values.

If the operational situation requires a power bias, the constraint (2.28) ensures that the power consumption in the thrust allocation can be reduced by a selectable parameter P_{bias} while still allocating the commanded thrust. This constraint is only necessary if the bias is required; if it is not it can safely be left out.

If $P_{bias} > P_{max} - P_{min}$, the optimization problem becomes infeasible. Preferably this should be avoided by having enough power available (P_{max}) both to allocate the commanded thrust and to create the required bias, but as a fail-safe the bias

could be forced to $P'_{bias} = min(P_{bias}, P_{max} - P_{min})$. A situation with a negative value of P'_{bias} is fine for the optimizer, but a position loss would likely be imminent.

2.4.2 Position and velocity contraint handling

Expressions (2.18), (2.19) are used to estimate ν_e and η_e in (2.25), (2.26). Ideally one would want to fulfill the constraints continuously during the entire period δt during which the solution is to be applied on the vessel, but in practice it is sufficient to evaluate them at the end of this period. This choice admits the possibility that constraints would be violated during this period. The calculation for ν_e in (2.12) integrates over a constant term from T to T_e. This means that if the constraint (2.25) is not violated at either T or T_e, it can not be violated between T and T_e. This does not apply to the position constraint (2.26) since (2.13) integrates over velocity, but this violation will not be large enough to be practically significant since δt is typically too small to allow significant changes in the velocity of the ship during that period.

Due to the short horizon, when the constraints (2.25), (2.26) are approached, avoiding violation in the next time step could either be infeasible or would require too much energy. In a practical implementation, the constraints (2.25), (2.26) are replaced with a heuristically chosen cost term which is to be added to (2.24):

$$J_{\nu,\eta} = \|K_p \hat{\nu}_{e,\,T_e}\|^2_{Q_J} + \|K_i \hat{\eta}_{e,\,T_e}\|^2_{Q_J} \tag{2.30}$$

where Q_J is a weighing matrix to ensure prioritization between the degrees of freedom, while K_p and K_i are scalar constants. The effect of the factors K_p and K_i is analogous to the gains in the PI controller, although the relationship to the controller output is not linear.

2.4.3 Power feedforward

The feedforward request of power consumption increase or decrease rate $\dot{P}_{ff}$ is one of the goals for the thrust allocation algorithm. Preferably, the rate of change in the power consumption by the thrusters $\dot{P}_{th}$ should always match $\dot{P}_{ff}$, which implies a constant load on the power plant. This is of course not possible, so a near match most of the time is the actual goal of the thrust allocation algorithm. Both of those derivatives, as well as $\dot{f}$, should be calculated by discretization; forward Euler was used in by the authors for testing purposes, i.e. $\dot{f} \approx {}^{f(T)-f(T-\delta t)}/_{\delta t}$. Notice that $f(T) = f$ is the decision variable, while $f(T - \delta t)$ is a constant parameter, equal to $f(T)$ from the previous iteration of the algorithm.

The power feedforward term P_{ff} signals a "soft" requirement for thrust allocation to increase or decrease its power consumption compared to power consumption in the previous iteration. Two applications for this signal may be considered. One use is to stabilize network frequency by setting it to

$$\dot{P}_{ff} = -k_{gp}(\omega_g - \omega_{0g}) \tag{2.31}$$

where k_{gp} is a positive constant. A similar control strategy is employed in [62] on the level of the local thruster controllers. The other way to use this signal is to

compensate for other power consumers that vary their consumption in a way that can be known in advance. The signal $\dot{P}_{ff}$ is used to reduce variations in the total power consumption by setting

$$\dot{P}_{ff} = -\dot{P}_{others} \tag{2.32}$$

where P_{others} is the power consumption by other consumers on the vessel. Since the power plant is able to handle rapid load reductions much better than rapid load increases, in this chapter the cost of load variation downwards is set to a fraction of load variation upwards, by changing the value of Θ in (2.24) depending on whether $\dot{P}_{th} - \dot{P}_{ff}$ is positive or negative.

2.4.4 Thruster biasing

To bias the thrusters is to deliberately increase the power consumption in the thrusters without changing the total produced force and moment on the ship, effectively forcing the thrusters to push against one another.

The combined force vector and angular momentum produced by the thrusters for a given azimuth and rudder angle vector α is given by (2.10),

$$\tau = B(\alpha)Kf \tag{2.33}$$

and is a linear combination of the forces f generated by the individual thrusters. If the ship is equipped with at least four thrusters, then the matrix $B(\alpha)K$ is guaranteed to have a non-trivial null space F_0. Additionally, if f^* is a strict global minimizer of the power consumption for a given τ, then for any $f_0 \in F_0 \backslash \mathbf{0}$ the power consumption for $f^* + f_0$ will be higher than for f^*, with the resultant generalized force remaining the same. Therefore, biasing can always be achieved as long as there are at least four non-saturated thrusters available for the purpose. Fewer than four thrusters are sufficient for configurations in which the columns of the matrix $B(\alpha)K$ are not independent.

Two practical applications for thruster biasing are discussed in this work: one is maintain a reserve capacity that the system can accept sudden load increases or power losses such as generator failures or short circuits of the part of the power system; the other one is to limit the rate of variations in load on the power plant.

Bias to keep a reserve capacity

Depending on the DP class, a DP vessel may be required to be able to continue operation uninterrupted after any single fault in the equipment. A typical worst case fault to be considered is a sudden disconnection of a single generator set or a single switchboard from the grid. Barring an emergency power source, this implies that at least two generator sets and switchboards must be operating at all times.

A marine diesel engine is unable to accept load steps above a certain limit, mainly due to the time required to build up the pressure in the turbocharging system. A blackout can only be prevented if the load step on the remaining generators after the fast load reduction (FLR) system is activated does not exceed the load step capacity of the remaining diesel engines, also assuming that the FLR is able

to reduce the load before the frequency variation tolerance is exceeded[60, p. 12]. It is up to the power management system to avoid the condition where a single fault may lead to blackout, which it can do by bringing more generator sets online so that a load step can be distributed between more engines. This can be done either by pre-calculated load-dependent start tables as in [61], or based on real-time worst-case scenario calculations as in [7].

Starting additional generators increases the wear-and-tear on the system. Also, when diesel engines are loaded far below their rated capacity, they are quite inefficient both in terms of specific fuel consumption and emissions. Biasing thrusters and allowing the FLR to release the bias when needed may allow the power plant to run with fewer generator online, which may be enough to compensate for the energy that is wasted in biasing. This approach is extensively applied in the industry, among others by Kongsberg, and is mentioned in publications such as [69, 70, 78]. A contribution of the present work is a fairly general formulation of thruster biasing for the purpose of keeping a power reserve in the optimization problem.

Bias to cushion load drops

As discussed previously, sharp decreases in power consumption may affect the power plant negatively. Therefore, it makes sense to even out load decreases by burning off some of the energy. This obviously incurs costs in terms of fuel consumption and in many cases in wear-and-tear on the thruster units. The proposed thrust allocation algorithm automatically weighs those costs against the benefits, and biases the thrusters if this is optimal.

Force variation

Because of the bias, the second cost term in (2.24), $\left\|K\dot{f}\right\|_{\Psi}^2$, is necessary because the addition of the constraint (2.28) can otherwise under some circumstances turn the solution of (2.24)–(2.29) into a continuous set with an infinite number of solutions. Without (2.28) , a specific thruster command f will be a global minimizer of the optimization problem. However, the bias request can typically be achieved by addition to f of any permutation f_0 from a continuous set – and all of them may minimize (2.24) without $\left\|K\dot{f}\right\|_{\Psi}^2$. The third term, $\Theta\left(\dot{P}_{th}-\dot{P}_{ff}\right)^2$, helps the situation a little because it attempts to drive $\dot{P}_{th}=P_cK\left|\dot{f}\right|^{3/2}$ towards a specific value. It is however at best one equality for N (number of thrusters) degrees of freedom, so the solution set f may not always be a point.

With many numerical solvers, this would lead to chatter in the output. This complication can be illustrated on a simplified problem

$$\min_x \frac{1}{2}x^TGx \tag{2.34}$$

subject to

Symbol	*Description*
T	Current time, i.e. time when the thrust allocation problem is solved.
T_e	Time when the solution from the next iteration of the thrust allocation algorithm will be applied to the thrusters.
$\nu_e(t)$, $\eta_e(t)$, $\nu_{e,\,T}$, $\eta_{e,\,T}$	Deviation in, respectively, velocity and position of the vessel from the nominal trajectories, i.e. from what the velocity and position would have been if thrust command was allocated exactly. $\nu_{err}(t)$, $\eta_{err}(t) \in \mathbb{R}^3$ contain longitudinal, lateral, and heading components; $\nu_{e,\,T} \triangleq \nu_e(t=T)$, $\eta_{e,\,T} \triangleq \eta_e(t=T)$.
$\nu_{e,\,max}$, $\eta_{e,\,max}$	Maximal allowed values for $\nu_e(t)$ and $\eta_e(t)$.
τ, τ_d	Actual and desired generalized force produced by all thrusters. τ, $\tau_d \in \mathbb{R}^3$ contain surge and sway forces, and yaw moment.
N	Number of thrusters installed on the ship.
f	$f \in \mathbb{R}^N$, the force produced by individual thrusters. The elements of f are normalized by their maximal values into the range $[-1, 1]$.
K	$K \in \mathbb{R}^{N\times N}$ such that Kf is the vector of forces in Newtons.
$B(\alpha)$	Thruster configuration matrix[24]. It is a function of the vector α consisting of orientations of the individual thrusters. In this chapter, α is assumed to be constant.
P_c	$P_c \in \mathbb{R}^{1\times N}$ such that (2.23) holds.
P_{th}	The total power consumed by the thrusters per (2.23)
$\dot{P}_{ff}$	The desired rate of change of power consumption by the thrusters. This signal can be used to reduce either frequency or load variations on the electrical network.
P_{min}	Minimal power consumption by the thrusters needed to produce commanded thrust.
P_{max}	The maximal power available for thrust allocation.
ω_g, ω_{0g}	Respectively actual and desired angular frequency of the voltage on the electrical network. Typically, $\omega_{0g} = 2\pi \cdot 60$.
Ψ	$\Psi \succ 0$, quadratic cost matrix of variation in force produced by individual thrusters.
Θ	$\Theta \in \mathbb{R}^+$ is the cost of variation in total power consumption.

Table 2.3: Variables used in the thrust allocation model

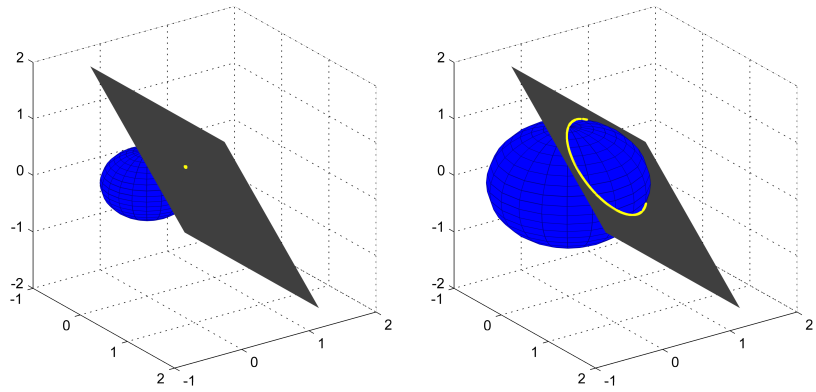

(a) For $z_{min} = z^*_{min}$, the solution set is a point.

(b) For $z_{min} > z^*_{min}$, the solution set is a circle.

Figure 2.5: The set of solutions of the simplified optimization problem (2.34)–(2.36) with $N = 3,\ M = 1$ shown in yellow. If the second problem were to be used in optimization-based control, the output of the controller would likely vary a lot between the samples. The original problem (2.24)–(2.29) would exhibit a similar structure without the cost on time derivative of the individual thruster outputs f.

$$Ax = b \tag{2.35}$$

$$\frac{1}{2}x^T Gx \geq z_{min} \tag{2.36}$$

where $G \in \mathbb{R}^{N\times N}$, $A \in \mathbb{R}^{M\times N}$ are matrices of full rank with $N \geq M + 2$, and z_{min} a scalar which is larger than the global minimum z^*_{min} of this optimization problem without the constraint (2.36). The solution to this problem is a connected set. For $N = 3,\ M = 1$ this is illustrated on Figure 2.5. If the left hand side of (2.36) is not identical to the cost function but instead a slight permutation of it, the solution of the optimization problem would in general be unique, but sensitive to changes in the permutation between the iterations, which would also result in chatter.

2.5 Simulation – case study

The proposed thrust allocation algorithm was tested in a simulation, on a model of SV Northern Clipper, featured in [24].

A model of a diesel-electric power plant was developed as part of this work. It is introduced in Subsection 2.5.4.

Figure 2.6: Thruster system on the simulated ship.

2.5.1 Hull and thruster system

The simulated vessel is 76.20 meters long, with a mass of $4.591 \cdot 10^6$ kg. It has four thrusters, with two tunnel thrusters near the bow and two azimuth thrusters at the stern. The maximal force for each thruster was set to $1/60$ of the ship's dry weight.

The ship is illustrated in Figure 2.6.

2.5.2 Motion control algorithm

The applied high-level motion control algorithm is a set of three PID controllers, one for each degree of freedom.

2.5.3 Power plant and distribution

The power plant installed on the simulated vessel consists of three generator sets. Two of them are rated at 1125 kVA, and the third one at 538 kVA. All gensets are connected to a single distribution bus. The engine governors were set in droop mode with the setpoint frequency of 60 Hz and a 5% droop. This power plant is sufficiently complex for testing control principles. It is more complex than the illustration in Figure 2.1, but still much simpler than found on most practical vessels.

The power management system supplied a feed-forward signal to the thrust allocation algorithm per (2.32).

2.5.4 Diesel engine model

In this subsection, the main principles of modeling of a marine diesel engine are discussed, with additional details available in Section 1.3.

A very accurate model for a turbocharged diesel engine can be constructed using a CFD simulation of the process fluids in the engine combined with a model of the dynamic behavior of the mechanical parts throughout the combustion cycles. Less accurate but more practical cycle-mean quasi-steady models, such as those examined in [74, 75, 89], are capable of reasonable quantitative prediction of the diesel engine behavior on the time scales comparable to a drive shaft revolution.

A diesel engine deployed in a power plant is controlled by its governor in a tight feedback loop, which counteracts much of the dynamic behavior of the engine. The scope of this work is not a detailed investigation of the dynamic response of a particular diesel engine, but rather a more general performance testing of the power grid as a whole. The model of the diesel engine needs to accurately represent the most important dynamical properties of the engine as well as the physical limitations which are impossible for the governor to correct. The most important such limitation is the turbocharger lag, which limits the amount of oxidizer in the cylinders, and therefore also the maximum effective fuel injection. Other practically important factors include the fuel index rate limit, and a governor response lag. The latter is an inevitable factor in feedback-based governors, since they cannot undertake any correcting action until after a deviation from the velocity setpoint is measured, and the aggressiveness of that correcting action is usually limited by stability considerations.

The authors could not find a fitting model in the literature, so a model was developed in [79], and is included in Section 2.5.4 for completeness. It is based on [11, 67, 71, 89], being a simplification of the model in [89]. The same model was used in [80] as a prediction model for an MPC governor.

The benefit of this model compared to other models in the literature is that situations when the engine experiences large load variations are represented with a reasonable degree of fidelity, while in most other respects the model remains fairly simple.

From the practical perspective, this model does not include a rate limiter, and therefore permits load variations that are so large that they would quickly wear down the engine due to thermic variations. The marine diesel engine manufacturers typically limit the permitted rate of change of the fuel index, both upwards and downwards. The thrust allocation algorithm presented in this work attempts to keep the variations in load on the power plant as low as possible, and there is no reason to push them lower than that.

If the EGR (exhaust gas recycling) is installed on the engine, it is assumed to be reduced or disabled during the upward transients.

2.5.5 Diesel engine governor

A diesel engine prime mover for a power plant has to maintain its rotational velocity in presence of variations in the load. This requires a feedback-based controller. The controllers for the diesel engines are conventionally called “governors”. Ill-designed governors may create unnecessary variations in the electric frequency, increase fuel consumption on the grid and in the worst scenarios destabilize the plant. Legacy implementations are either distributed droop governors, or isochronous governors. Droop governors are usually implemented as PID controllers that measure the deviation in the electric frequency from a drooped setpoint and control the fuel index accordingly. Isochronous governors have a constant (non-drooped) frequency setpoint but also share information about the average load on each connected bus segment through a separate load sharing line. Introductory texts about marine diesel control systems are available in e.g. [9, 71, 87], and [19, sec 4.4.1]. More modern control methods for marine power plants, such as those in the recent Kongsberg

power management systems, use droop-based governors but rapidly modify the droop curve based on the loading situation. This way, they achieve both the fault tolerance of the droop governors and the frequency stability of the isochronous governors.

The governor used in conjunction with this thrust allocation algorithm is a droop governor, with a functionality for feedforward from the loads. The proposed feedforward implementation measures the total electric load, distributes it between the available generator sets, calculates the approximate fuel index which would produce the electric power currently consumed, and adds this value to the output of the PID controller. This way, when the power consumption changes, the fuel index rapidly changes to a value close to what is needed to match the produced mechanical power and the consumed electrical power. With these nearly balancing each other out, the torques on the rotating parts of the generating set will approximately match, resulting in a near-constant rotational velocity. The remaining deviation is due to modeling inaccuracies and will be corrected by the PID controller. In a practical implementation, the output from the feedforward could be passed through a low-pass filter to avoid excessive fuel index movement.

Tests were conducted both with and without the feedforward. Without the feedforward, a droop governor can only respond to changes in load after these changes affect the frequency. This leads to frequency variations that do not originate in the physical limitations of the system.

This architecture bears a certain resemblance to an isochronous controller since the feedforward term is similar to the value on the load sharing line. However, the value on the load sharing line in an isochronous governor is passed through the PID of the governor, which does not appear to be necessary.

As mentioned in Subsection 2.5.4, the density of the air injected into the cylinders limits how much fuel can be effectively injected into the cylinder. It is assumed that the diesel engine fuel limiter informs the governor about the maximum efficient fuel index, and the governor is never allowed to exceed this value.

The introduced thrust allocation algorithm reduces the load variations in the network essentially by delaying some of the power consumption. In situations with large and rapid load increases, this results in the governor first reacting less than it would have with a standard thrust allocation algorithm, for instance the one described by (2.20)–(2.22). Afterwards it is unable to move the fuel index enough to deliver power for the delayed consumption due to the limitations mentioned above. In simulation tests, this situation often resulted in unnecessarily large frequency drops. To avoid this, the feedforward implementation was modified to use the information of the power the thrust allocation would have used if it had fulfilled the command exactly, i.e., P_{min} from (2.20) is distributed to the governors. Since an amount similar to that difference is likely to be requested by the thrusters shortly, it is prudent for the governor to prepare for the coming load increase. In this chapter, this was done by integrating the power difference in time to acquire an energy quantity, and changing the setpoint frequency so that the resulting change in the kinetic energy of the rotating machinery would be equivalent to the energy difference produced by the thrust allocation algorithm.

Simulation case	Governor feedforward	TA power modulation	Uncompensated environmental disturbances
1	no	no	no
2	active	no	no
3	active	active	no
4	active	active	yes
5	no	no	yes

Table 2.4: Tested configurations

2.5.6 Adaption for a split bus tie configuration

The algorithm was only tested on a fully connected bus. It could be adopted to a split bus configuration by using a separate power feedforward term $\Theta \left(\dot{P}_{th} - \dot{P}_{ff} \right)^2$ in the cost function (2.24) for each of the bus segments. Similarly, the biasing and power limit constraint (2.28) has to be applied individually for each of the bus segments.

2.5.7 Simulation results

The simulation was implemented in Simulink, and the Matlab Optimization Toolbox was used to solve the numerical optimization problem. The update frequency for thrust allocation was set to 0.2 seconds. The simulation was run on a laptop computer with an Intel i7 Q820 CPU.

Five configurations were tested with different combinations of options, as presented in Table 2.4. In the first configuration, the governors were run with feedback-only control and a classical droop implementation, and no attempt by the thrust allocation algorithm to reduce the load variations. In the second simulation, the governors received a feedforward from the loads, but again with no assistance from the thrust allocation. The first and the second configurations functioned as a baseline to evaluate the effect of the proposed features in the thrust allocation algorithm. In the third configuration, the thrust allocation introduced counter-acting load variations as proposed in this chapter. A stochastic disturbance representing environmental disturbances that were not compensated by the wind feedforward or wave filter [25] was added in simulations four and five.

The initial position in the simulations is two meters away from the setpoint in surge, with no deviation in sway or heading. An constant environmental (wind) force from the stern of the vessel equivalent to 2% of the ship's weight, that is $\begin{bmatrix} 0.02 & 0 & 0 \end{bmatrix}^T$ in the bis system normalization [25, table 7.2] was present in all simulation cases. The azimuth thrusters are oriented 45 degrees towards the center line of the the ship. Since the presented thrust allocation algorithm does not include methods for rotating those thrusters, they remain at that orientation for the entire course of the simulation.

In addition to the thrusters, a periodic, fast-rising load of 1.5 MW was present on the grid to emulate the load from a heave-compensated platform or a similar

wave-induced load typical for a drilling vessel. This load stays at 1.5 MW for two seconds before subsiding to 0.2 MW where it stays for additional two seconds, after which it drops to zero. The fuel rate limiters were not enabled on the governors. The tolerances for deviation in position were set to 1 meter in each direction, while the tolerances in deviation in velocity were set to 0.3 m/s. The weight factors in (2.30) were set such that deviation in either $\hat{\nu}_{e,T_e}$ or $\hat{\eta}_{e,T_e}$ equal the respective tolerances would incur a cost equivalent to all thrusters running at full power. The cost of power variations downwards was set to be very low in order to avoid increased specific fuel consumption compared to the base scenarios.

Figure 2.7 shows the total load on the bus in the first three test cases. In the first two, the thrusters don't do anything except compensating for the slowly-varying environmental force. Because of that, their load does not vary a lot, and the periodic 1.5 MW load enters the power plant unhindered. In the third case, when the thrust allocation algorithm power control is activated, the total load variations are significantly more smooth.

The modified thrust allocation algorithm informs the governors that it is delaying power consumption. As shown on Figure 2.9, this gives the governors time to increase the power production, as well as accelerate the turbocharger shaft and increase the pressure in the scavenging receiver. This initially leads to an increase in frequency, resulting in a slight overfrequency but also some additional energy being stored in the rotating masses. The resulting frequency variations are displayed in Figure 2.8. Had the fuel index rate limiter been activated, this would instead lead to a lower mismatch between generated and consumed energy, and therefore lower frequency deviation.

Without the feedforward from the loads, an abrupt change in load leads to a change in the frequency setpoint due to the droop. This is a fundamental limitation of the droop governors, because during a load transient, a local governor does not have enough information to determine if e.g. a load increase it observes on it own terminals is due to an increase in the load on the bus or due to it having taken a larger share of the load from the other generators. Those conditions require opposite actions, and it is not possible to determine which is correct until the frequency on the grid decreases due to the increased load. This is less of an issue in isochronous mode since a load increase does not lead to a setpoint frequency drop, but the governor still have to wait until it observes a frequency deviation until it can change the position of the fuel index.

The position of the vessel in surge for test cases 1-3 is shown in Figure 2.10. Use of the proposed thrust allocation algorithm leads to small variations being superimposed on the trajectory of the vessel, which in this simulation are well within required precision for most offshore operations. The largest acceleration the ship experiences during the simulation is $0.11 \mathrm{m/s^2}$. This happens during the initial setpoint acquiring, and is not connected to the load variation compensation features of the algorithm. Since the initial deviation is in the direction of surge and the environmental disturbance is deterministic and acts strictly in the same direction, there are no forces acting in either sway or in yaw. For this reason there will be no deviation in those directions in test cases 1-3, and the respective plots are omitted. This scenario was selected to make the power-related effects more emphasized – returning a ship to the setpoint from any desired starting point is

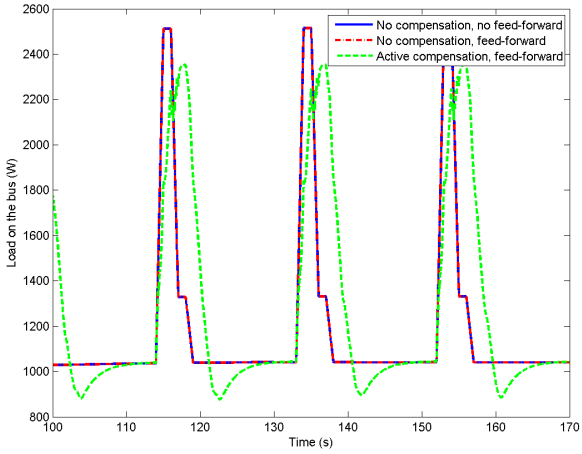

Figure 2.7: Total load; test cases 1, 2, 3

not a new challenge, and the proposed algorithm does not behave differently from other algorithms in the literature in that regard.

Deviation in sway and in yaw (the latter being rather small) were present when a random component was added to the environmental forces. The main motivation for adding the random component to the environmental force is the fact that the environmental forces are not deterministic in reality. The position of the vessel in surge with and without the random environmental disturbances is shown in Figure 2.11. It shows that the disturbances due to the thrust allocation PMS assistance are not large compared to typical random disturbances. The effect of the thrust allocation algorithm modification on the frequency is not qualitatively affected by the random disturbances, as shown on Figure 2.14.

2.6 Discussion and conclusion

The proposed thrust allocation algorithm has been demonstrated to reduce load variations on a marine power plant by making the thrusters produce counteracting load variations that partially cancel the load variations from the other consumers. This can be taken advantage of either through reducing frequency variations as has been demonstrated in simulation, or by reducing the variations in the fuel index, thus reducing wear-and-tear on the engine, emissions and sooting. The optimization is done with regards to the current state only, so the response may not be optimal with regards to how the load continues to evolve. For example if there is a load increase, the algorithm has no way of knowing if it is a very short load peak or a load step. If the former is the case it would have been preferable to allow the ship to mostly drift while the load peak lasts, and then slowly bring the ship back to the setpoint position. If the latter is the case, then it is more optimal to "spread out" the load reduction in the thrusters over a longer period of time to allow a

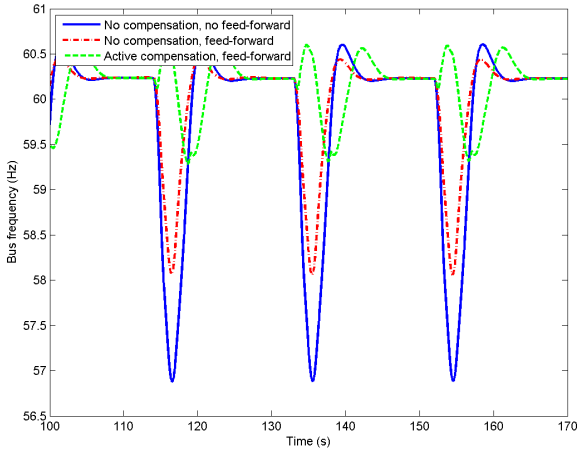

Figure 2.8: Bus frequency; test cases 1, 2, 3

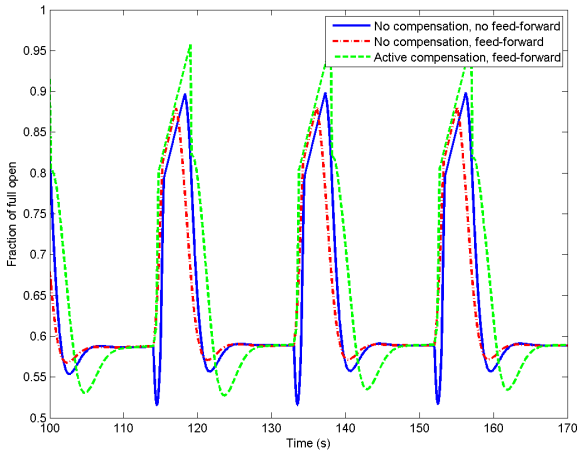

Figure 2.9: Fuel injection rate on one of the generators; test cases 1, 2, 3

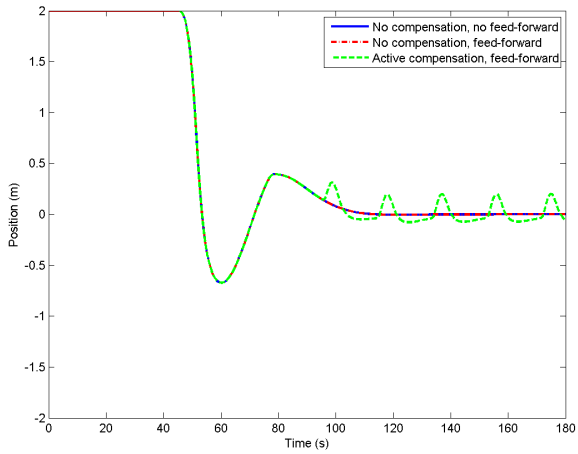

Figure 2.10: Position of the vessel in surge; test cases 1, 2, 3

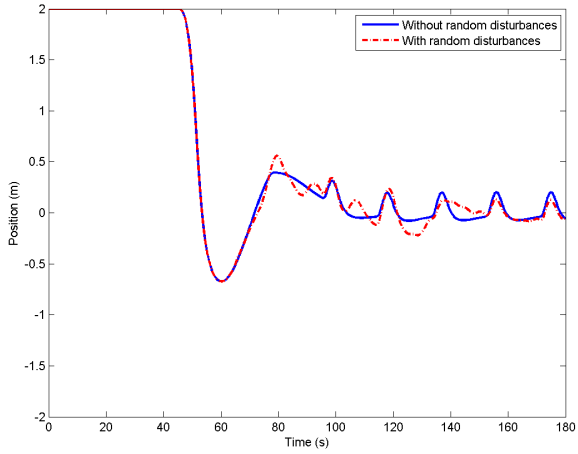

Figure 2.11: Position of the vessel in surge with and without uncompensated environmental disturbances, with PMS assistance activated; test cases 3, 4

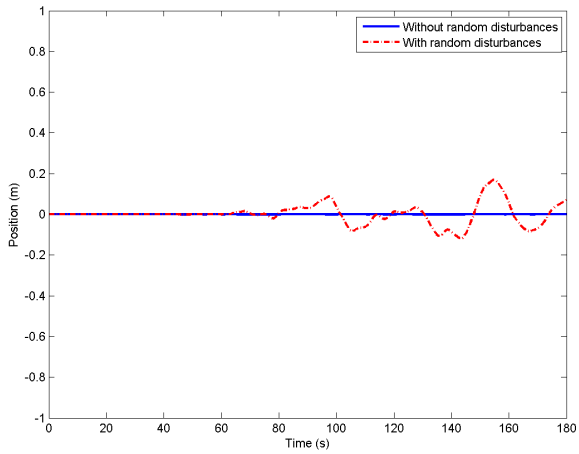

Figure 2.12: Position of the vessel in sway with and without uncompensated environmental disturbances, with PMS assistance activated, repositioning deactivated; test cases 3, 4

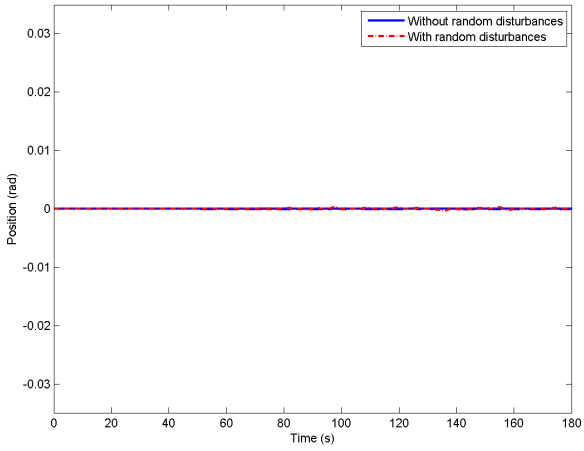

Figure 2.13: Orientation of the vessel in yaw with and without uncompensated environmental disturbances, with PMS assistance activated, repositioning deactivated; test cases 3, 4

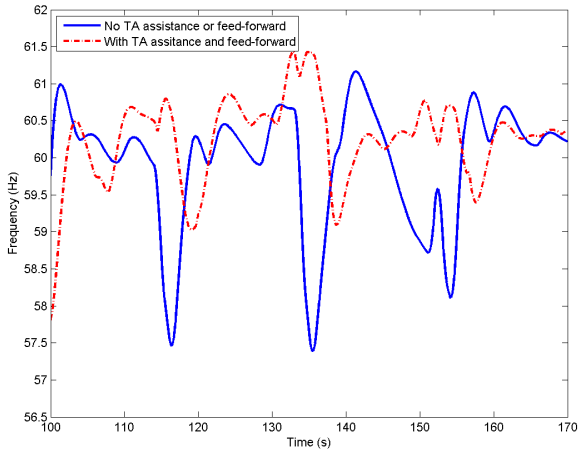

Figure 2.14: Frequency on the grid with uncompensated environmental disturbances; test cases 4, 5

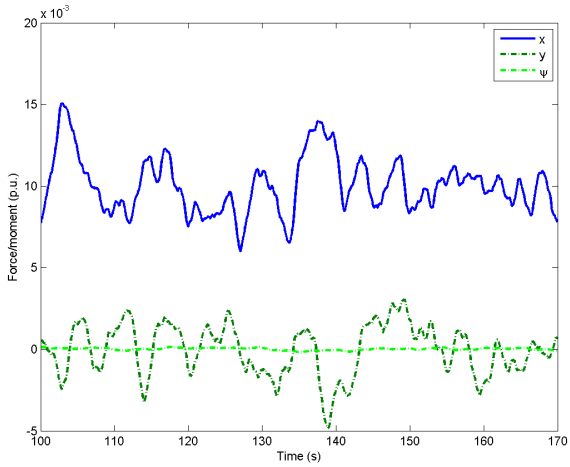

Figure 2.15: Environmental disturbances, including random uncompensated disturbances; test case 4 (test case 5 is qualitatively similar but driven by a different random noise realization)

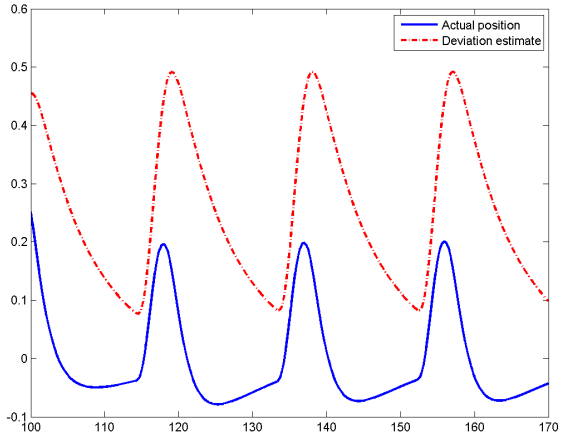

Figure 2.16: Position deviation estimate in surge due to effects of the thrust allocation deviations, superpositioned on the actual position shows the interaction between the dynamic positioning algorithm and the deviation in thrust allocation; test case 3

smoother load increase.

The algorithm was tested in fairly realistic conditions, which resulted in some practical challenges. In particular, tuning of the algorithm was time-consuming. The cost terms in (2.24) and in (2.30) have to be carefully balanced against each other to ensure that the thrust allocation does not respond to the load variations elsewhere too aggressively or too calmly. It is typical for marine control systems which are in general difficult to tune for a wide range of operational scenarios, but the proposed algorithm does add a layer of complexity to the control system.

Chapter 3

Reducing power transients in diesel-electric dynamically positioned ships using re-positioning

3.1 Introduction

A marine vessel is said to have dynamic positioning (DP) capability if it is able to maintain a predetermined position and heading automatically exclusively by means of thruster force [4]. DP is therefore an alternative, and sometimes a supplement to the more traditional solution of anchoring a ship to the seabed. The advantages of positioning a ship with the thrusters instead of anchoring it include:

- Immediate position acquiring and re-acquiring. A position setpoint change can usually be done with a setpoint change from the operator station, whereas a significant position change for an anchored vessel would require repositioning the anchors.
- Anchors can operate on depths of only up to about 500 meters. No such limitations are present with dynamic positioning.
- No risk of damage to seabed infrastructure and risers, which allows safe and flexible operation in crowded offshore production fields.
- Accurate control of position and heading.

The main disadvantages are that a ship has to be specifically equipped to operate in DP, and that dynamically positioned ships consume a lot more energy to stay in position, even though anchored vessels also have to expend energy to continuously adjust the tension in the mooring lines.

DP is usually installed on offshore service vessels, on drill rigs, and now increasingly on production platforms that are intended to operate on very deep locations.

To maximize the capability of the DP system, the thrusters should be placed on distant locations on the ship, which makes mechanical transfer of power from the engines less practical compared to electrical distribution. This and other operational advantages [19, p. 6] result in electric power distribution being almost ubiquitous in offshore vessels equipped with DP today.

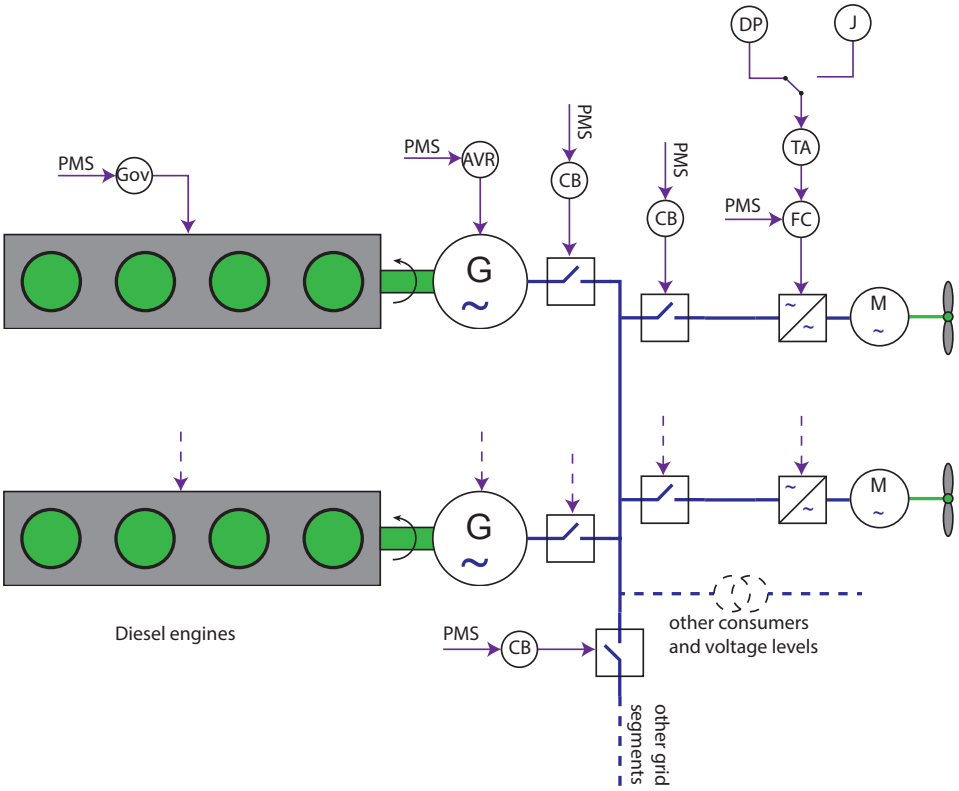

Figure 3.1: An illustration showing some of the controllers on the electric grid. A diesel engine speed controller, conventionally called governor (Gov), adjusts the amount of fuel injected into the engines; An Automatic Voltage Regulator (AVR) adjusts the magnetization of the rotor coils of the generators (G); various circuit breakers (CB) connect and disconnect equipment and also isolate faults such as short circuits; the Frequency Converters (FC) are used for local control of the thruster motors (M), and receive commands from both the Thrust Allocation (TA) and the Power Management System (PMS). Finally, the TA can receive the generalized force command from either the DP control system or from a Joystick (J).

The type of prime mover predominantly in use is the diesel engine, although other types such as gas engines and gas turbines are also available. A power grid on a DP vessel typically consists of several diesel engines mechanically coupled to electrical generators, delivering power to the thrusters and other consumers through a reconfigurable distribution network with several separable segments and several voltage levels. Often, the thruster system requires more power from the generators than all the other consumers on the grid combined.

The control architecture for the resulting system is highly distributed, with independent controllers for diesel engine fuel injection, generator rotor magnetization, circuit breakers, centralized and local thruster controllers, etc. First, a high-level motion control algorithm considers the current position and orientation of the ship, and determines the total force and moment of force (together called "generalized force") that needs to be applied on the ship. After the generalized force is calculated by the motion control algorithm it is passed as an input to a lower-level thrust allocation algorithm, which determines the forces and angles the individual thrusters should produce. The main goal of the thrust allocation algorithm is to ensure that the combined generalized force that the thrusters generate matches the output from the high-level motion control algorithm. The output from the thrust allocation algorithm is then sent to the local thruster controllers. An example of such network with controllers is shown on Figure 3.1.

While diesel engines are efficient in terms of fuel consumption [46], use of primarily diesel electric power grid introduces a range of challenges for the control system in terms of both stability and minimizing fuel consumption. Stability relates to maintaining stable frequency and voltage on the grid in presence of large and sometimes unpredictable disturbances in load, as well as stable load sharing when a grid segment is powered by more than one generator set. Modern marine diesel engines are almost always turbocharged. Turbocharging limits how fast the engine can increase its output because increasing the output requires building up pressure in the scavenging receiver, which puts a physical limit on how fast a diesel-electric power plant can increase its output. A rapid load increase can therefore lead to a mismatch between the generated mechanical and consumed electrical power. This mismatch can become unrecoverable even if the load rate constraints on the governors are disabled. The result of this mismatch is deficit consumption that extracts energy from the rotating masses in the engines and the generators. If unchecked, it will lead to a rapid drop in frequency, and then a blackout due to engine stall or protection relay disconnect.

Economic and environmental concerns are somewhat coupled, because factors that lead to pollution often also lead to increased economic costs. Increased fuel consumption leads to both increased fuel expenses and (under most circumstances) more pollution. Pollutants such as carbon monoxide, unburned hydrocarbons, soot and NO_X emissions constitute a minor part of the combustion process in terms of energy, and have therefore a negligible impact on the engine process [21, p. 194]. However, those emissions tend to increase during load transients, especially upwards transients [63, ch. 5 and p. 37]. Those transients also increase wear-and-tear on the engines because of the resulting thermic expansion and contraction. In addition, load variations on the power plant as a whole may lead to excessive start and stop of generator sets, with additional pollution and wear-and-tear due to cold

start transients.

Because of this, variations in the power consumption have recently received increased attention in the literature. A cost term for variations in force produced by the individual thrusters is included the thrust allocation optimization problem in [42], which has a dampening effect on the combined load variations. The thrust allocation that is described in [37] includes functionality to handle power limitations and other power-related features in the optimization process.

Additional improvements are possible if one considers that the very large inertia of a typical marine vessel means that short-term deviations of the force output in the thrusters result in relatively insignificant deviations in the position of the vessel[43]. Deviating from the command from the high-level motion control algorithm allows a certain measure of control over short-term power consumption in the thrusters, which can be used to dampen the high-frequency components in the load on the power plant. Several recently-proposed implementations explore this possibility. [62] introduced a modification directly in the local thruster controllers, allowing them to deviate from the orders they receive from the thrust allocation algorithm. In [78] the task of counteracting the frequency variations was moved up to the thrust allocation algorithm. In [79], the modified thrust allocation algorithm was tested on a simulated vessel with a power plant consisting of three generator sets. In [56], a similar effect was achieved by using the available power signal from the power management system to the local thruster control. [65] introduced a modification of the thrust allocation algorithm that allows control of power distribution between the electric buses by adjusting the cost of using different thrusters in the thrust allocation optimization task.

The method in [78] works by adjusting the load from the thrusters by modifying the thrust allocation algorithm. The thrust allocation algorithms in the literature usually attempt to minimize the amount of power that the thrusters use, and in practice they do not use significantly more power than is necessary to fulfill the orders that the thrust allocation algorithm receives from the dynamic positioning or the joystick. This means that to be able to temporarily reduce the load from the thrusters that method must allow the thrust allocation to deviate from the orders; provisions are made to ensure that the ship does not drift further than permissible by the operational requirements from what the position would have been if the orders to the thrust allocation were executed exactly. The resulting deviation should typically be on the scale of 1m. The goal of adjusting the load is to reduce the variations in the total load on the power generation system. This method effectively uses the hull of the vessel as an energy storage.

In the present work, the effectiveness of this algorithm is further improved by continuously observing the direction of the environmental force, and modifying the setpoint to the DP control algorithm to increase the operational margins for the modified thrust allocation algorithm. This is illustrated in Figures 3.2–3.3. Within the analogy of using the hull as an energy storage, this modification allows more energy to be recovered from the hull before the deviation in position and velocity becomes unacceptably large.

The thrust allocation algorithm from [78] is described in Section 3.2, while the modifications introduced in this chapter are described in Section 3.3. The results are presented in Section 3.4.

3.2 Power management-aware thrust allocation

The trust allocation algorithm in [78] expands on the idea of allowing the thruster system to deviate from the commanded thrust over a short time in order to improve the dynamics of the power distribution system. This idea was first explored in [61], where deviations were introduced on the level of the local thruster controllers. Coordinating the deviation from the dynamic positioning controller orders in the thrust allocation algorithm makes it possible to estimate and limit the resulting deviations in the velocity and the position of the ship.

This algorithm is based on solving a nonlinear optimization problem, similar to [40].

$$P_{min} = \min_{f,s} P_c K \left|f\right|^{3/2} + \left\|s\right\|_{Q_1}^2 \tag{3.1}$$

subject to

$$B(\alpha)Kf = \tau_d + s \tag{3.2}$$

$$\underline{f} \leq f \leq \overline{f} \tag{3.3}$$

This method is well-documented in the literature – although usually with quadratic cost function; see [24].[1] The cost matrix Q_1 must be large enough to ensure that the slack vector s is significantly larger than zero only when constraints (3.2)–(3.3) would otherwise be infeasible. The solution to this optimization problem provides a minimum P_{min} to which the power consumption can be reduced while delivering the requested thrust τ_d, at least as long as the condition $s \approx 0$ holds. Power consumption in the thrusters is estimated by the nonlinear relationship

$$P_{th} = P_c K \left|f\right|^{3/2} \tag{3.4}$$

which is similar to what was used in [40]. The variables P_c, K, f, $B(\alpha)$, K, $\underline{f}$, and $\overline{f}$ are defined in Table 3.1.

In [78], the following thrust allocation optimization problem is used for thrust allocation when there is no thruster power bias requirement:

$$\begin{aligned} \min_{f,\tau_e,s_1,s_2} P_c K \left|f\right|^{3/2} + \left\|K\dot{f}\right\|_{\Psi}^2 + \Theta\left(\dot{P}_{th} - \dot{P}_{ff}\right)^2 + \\ \left\|\tau_e\right\|_{Q_2}^2 + \left\|s_1\right\|_{Q_3}^2 + \left\|s_2\right\|_{Q_4}^2 \end{aligned} \tag{3.5}$$

subject to

$$-\nu_{e,\,max} \leq \nu_e + s_1 \leq v_{e,\,max} \tag{3.6}$$

$$-\eta_{e,\,max} \leq \eta_e + s_2 \leq \eta_{e,\,max} \tag{3.7}$$

[1] The notation used here and in the following is that $\left\|x\right\|_A^2 \triangleq x^T A x$ and $\left|x\right|^p \triangleq \begin{bmatrix} x_1^p & x_2^p & \cdots & x_N^p \end{bmatrix}^T$ for any x, A and p of suitable dimension.

Symbol	*Description*
T	Current time, i.e. time when the thrust allocation problem is solved.
T_s, T_e	Lower and upper limits for the integrals in (3.6), (3.7) which calculate deviations in velocity and position at time T_e.
$\nu_e(t)$, $\eta_e(t)$, $\nu_{e,\,T}$, $\eta_{e,\,T}$	Deviation in respectively velocity and position of the vessel from what they would have been if thrust command was allocated exactly, as functions of time. $\nu_e(t)$, $\eta_e(t) \in \mathbb{R}^3$ contain longitudinal, lateral and heading components; $\nu_{e,\,T} \triangleq \nu_e(t = T)$, $\nu_{e,\,T} \triangleq \nu_e(t = T)$
$\nu_{e,\,max}$, $\eta_{e,\,max}$	Maximal allowed values for $\nu_e(t)$ and $\eta_e(t)$
τ, τ_d	Actual and desired generalized force produced by all thrusters. τ, $\tau_d \in \mathbb{R}^3$ contain surge and sway forces, and yaw moment.
ω_g, ω_{0g}	Respectively actual and desired angular frequency of the voltage on the electrical network. Typically, $\omega_{0g} = 2\pi \cdot 60$.
$B(\alpha)$	Thruster configuration matrix. It is a function of the vector α consisting of orientations of the individual thrusters. In this chapter, α is assumed to be constant.
N	Number of thrusters installed on the ship.
f	$f \in \mathbb{R}^N$, the force produced by individual thrusters. The elements of f are typically normalized into the range $\left[\ \underline{f},\ \ \overline{f}\ \right] = \left[\ -1,\ \ 1\ \right]$.
K	$K \in \mathbb{R}^{N \times N}$ such that Kf is the vector of forces in Newtons.
P_c	$P_c \in \mathbb{R}^{1 \times N}$ such that equation (3.4) holds.
Ψ	$\Psi \succ 0$, quadratic cost matrix of variation in force produced by individual thrusters.
Θ	$\Theta \in \mathbb{R}^+$ is the cost of variation in total power consumption.
P_{th}	The total power consumed by the thrusters per equation (3.4)
$\dot{P}_{ff}$	The desired rate of change of power consumption by the thrusters. This signal can be used to reduce either frequency or load variations on the electrical network.
P_{min}	Minimal power consumption by the thrusters needed to produce commanded thrust.

Table 3.1: List of abbreviations

$$B(\alpha)Kf = \tau_d + \tau_e \tag{3.8}$$

$$P_{max} \geq P_c K \left|f\right|^{3/2} \tag{3.9}$$

$$\underline{f} \leq f \leq \overline{f} \tag{3.10}$$

This optimization problem includes cost for variations in power consumption and in force produced by individual thrusters. It uses a smaller cost Q_2 on deviation from thrust allocation command τ_d, that is $Q_2 \ll Q_1$. This is to allow the produced generalized force τ to deviate from τ_d when beneficial.

The deviations in the produced generalized force result in deviations in velocity and position of the ship from what they would have been if the thrust allocation algorithm followed the command from the motion control algorithm exactly. Assuming approximately constant orientation of the dynamically-positioned ship, those deviations can be approximated per

$$\nu_e(T_e) = M^{-1} \int_{T_s}^{T_e} \left[B(\alpha)Kf(t) - \tau_d\right] dt \tag{3.11}$$

$$\eta_e(T_e) = \int_{T_s}^{T_e} \nu_e(t) dt \tag{3.12}$$

In an exact physical interpretation T_s must be the time when the thrust allocation started running. In practice it can be noted that the motion control algorithm will also detect and attempt to correct the deviations. It will do so on a time scale that is relatively slow compared to that of the thrust allocation algorithm. This can be represented as "forgetting" deviations that happened before a certain point in time. In the implementation, the choice was made to let integration start five seconds in the past relative to when the thrust allocation is solved, therefore assuming that a deviation in velocity and position that was present before that would have been corrected by the motion control algorithm. The constraints (3.6)–(3.7) are only evaluated at the time T_e when the solution from the next iteration of the thrust allocation algorithm is available. This is further discussed in Section IV of [78].

The velocity deviation is constrained within a predefined range by imposing (3.6), and the position deviation is constrained in (3.7). The constraint (3.7) is illustrated in Figure 3.2

A limit on maximal power consumption has to be imposed; it is introduced as P_{max} in (3.9). This limit necessitates the slack variables s_1 and s_2 in the constraints (3.6) and (3.7), with cost matrices Q_3 and Q_4 large enough to ensure that s_1 and s_2 will significantly deviate from zero only if the constraints (3.6) and (3.7) would otherwise be infeasible.Thruster bias is not used in this work, but if it was then the power consumption $P_c K \left|f\right|^{3/2}$ in (3.9) would have to be constrained from below as well.

Without the $\dot{P}_{ff}$ signal, the third term in (3.5) would be zero if the thrust allocation consumed exactly the same amount of power as in the previous iteration of the algorithm (assuming forward Euler discretization). The power feedforward

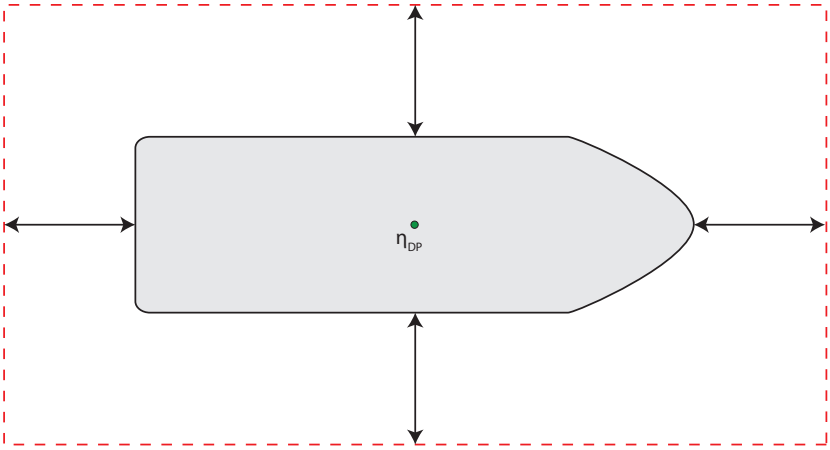

Figure 3.2: The DP setpoint and safety margins. Typically, the safety margins are significantly smaller than illustrated.

term P_{ff} signals a "soft" requirement for thrust allocation to increase or decrease its power consumption compared to power consumption in the previous iteration. Two applications for this signal are discussed in [78]; however, the only way this signal is used in this work is to compensate for other power consumers that rapidly vary their consumption in predictable patterns. The signal $\dot{P}_{ff}$ is used to reduce variations in the total power consumption by setting

$$\dot{P}_{ff} = -\dot{P}_{others} \tag{3.13}$$

where P_{others} is the power consumption by other consumers on the vessel. Since the diesel-electric power plant is able to handle rapid load reductions much better than rapid load increases, in this chapter the cost of a load reduction is set to a fraction of the cost of a load increase, by changing the value of Θ in (3.5) depending on whether $\dot{P}_{th} - \dot{P}_{ff}$ is positive or negative.

3.3 Repositioning

The direction of the environmental forces tends to change slowly. This can be exploited by repositioning the vessel away from the initial DP setpoint towards the environmental forces. This way, when it becomes necessary to reduce the power consumption of the thrusters, the environmental forces will initially push the vessel towards the original setpoint. This allows more time before the thrusters have to increase their consumption again, which is important since the turbocharged diesel engine has an asymmetric step response during large load steps. In [36] the operator is instead provided with a drift-off analysis tool to help him or her determine manually if the setpoint position should be modified to improve the time margins to a drift-off error. Doing this would however require a constant attention from the operator, leaving the operation vulnerable to human error. In this chapter, the

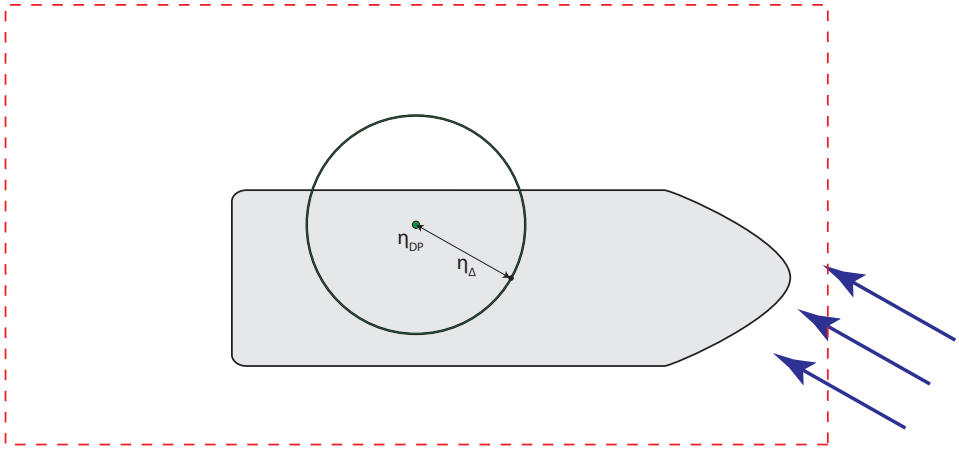

Figure 3.3: The original DP setpoint η_{DP} is dynamically modified by η_Δ as the environmental forces, here illustrated with blue arrows, change. Typically, the magnitude of η_Δ is much smaller than illustrated.

repositioning can optionally be performed automatically, requiring only minimal attention from the operator.

It is not possible to introduce a constant offset in position by modifying the thrust allocation algorithm alone, because the dynamic positioning control algorithm would detect a constant deviation and attempt to compensate it. The offset is therefore introduced in the dynamic positioning control algorithm. After calculating the offset, the dynamic positioning algorithm informs the thrust allocation algorithm that it now has better margin of safety in some directions and smaller margin of safety in others. This is equivalent to replacing (3.7) with

$$-\eta_{e,\,max} + \eta_\Delta \leq \eta_e + s_2 \leq \eta_{e,\,max} + \eta_\Delta \tag{3.14}$$

where $\eta_\Delta \in \mathbb{R}^3$ is the repositioning vector in surge, sway and yaw. This is illustrated in Figure 3.3. In practice, the repositioning in yaw is usually kept at zero to avoid increasing the wind and wave drag. For improved performance, the constraint (3.6) was also modified to allow larger velocity deviation in the direction where the safety margin is larger. The repositioning distance should be chosen according to a trade-off between maximum allowed position deviation and the variability of environmental forces. Its choice will depend on the vessel location e.g. relative to other installations, weather conditions and the requirements of the operation, a choice which is best left to the operator.

This modification can be summarized as following:

Figure 3.4: Thruster layout of the simulated vessel

1. Start the dynamic positioning operation with the thrust allocation algorithm as described previously.
2. Detect the resultant direction of the combined environmental forces. If the dynamic positioning algorithm is PID-based, this can be done simply by measuring the integrator states.
3. Modify the setpoint for the dynamic positioning by moving it a predetermined distance against the environmental forces. Define η_Δ as the vector from the original setpoint to the new one.
4. Replace the constraint (3.7) with (3.14).
5. Possibly allow a similar asymmetric modification of constraint (3.6) to allow a larger velocity deviation in the direction in which the safety margin is larger.

3.4 Results

The new algorithm was tested on a simulated vessel with a diesel-electric power plant, same one as in [79]. It is based on SV Northern Clipper, featured in [24]. It is 76.2 meters long, has four thrusters, with two tunnel thrusters near the bow and two azimuth thrusters at the stern. Since this thrust allocation algorithm does not handle thrusters with variable thrust angle, the azimuth thrusters were locked in position 45 $^\circ$ towards the center line. This layout is illustrated in Figure 3.4. All the thrusters are assumed to be symmetric, each capable of producing a thrust equivalent to 1/40 of the ship's weight. The simulated ship is in dynamic positioning mode, dynamic positioning being implemented with three independent PID controllers, one in each degree of freedom. The following limits on velocity and position errors were selected: $\nu_{e,\,max} = \begin{bmatrix} 0.1 & 0.1 & 0.1 \cdot \pi/180 \end{bmatrix}^T$, $\eta_{e,\,max} = \begin{bmatrix} 0.5 & 0.5 & 0.5 \cdot \pi/180 \end{bmatrix}^T$.

The setpoint for the dynamic positioning algorithm was set to the origin, and the repositioning distance was set to 0.5 meters. The propulsion system had to compensate for an environmental force on the vessel, which was equivalent to 1% of the weight of the vessel. In addition to the thrusters, the load consisted of a constant load of 300 kVA and periodic load spikes of 1.4 MVA, which after two

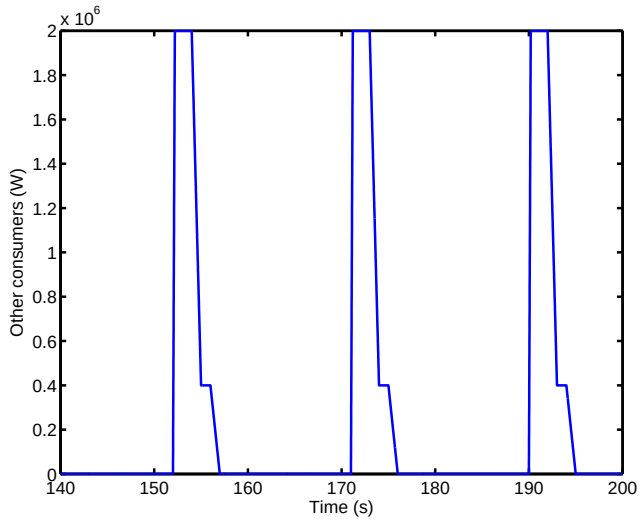

Figure 3.5: Load from the other consumers

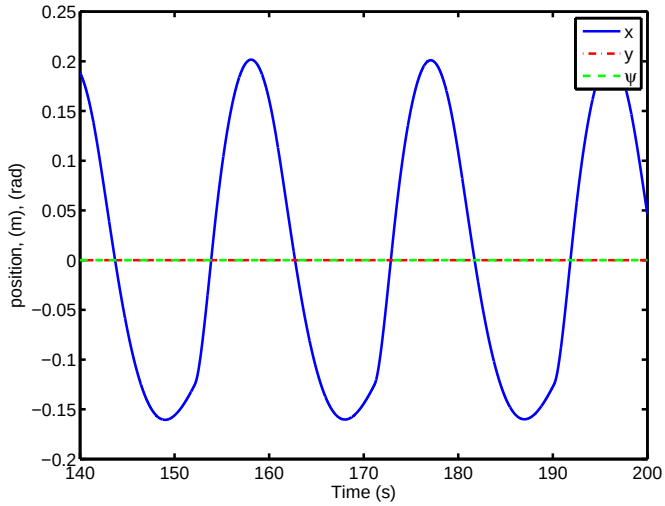

Figure 3.6: Position of the vessel with repositioning disabled

seconds dropped to 0.2 MVA and after two additional seconds to zero. The power factor was set to 0.95 for the thrusters and 0.75 for the other consumers. The other consumers loaded the vessel as shown on Figure 3.5. The position of the vessel relative to the set point is shown on Figures 3.6–3.7, and the electric bus frequency is shown in Figures 3.8–3.9.

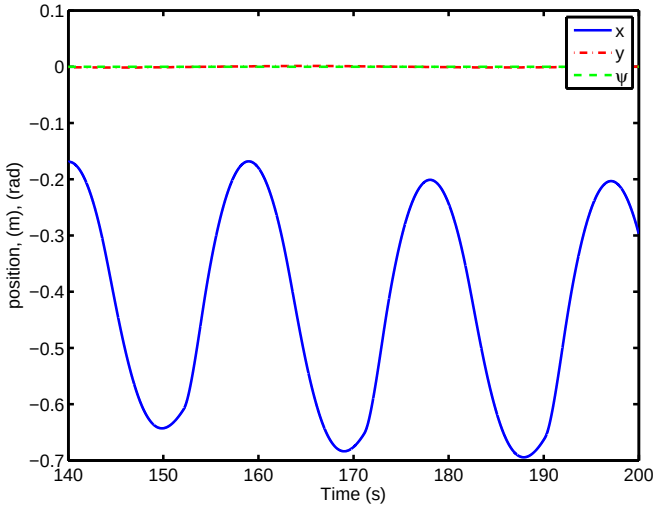

Figure 3.7: Position of the vessel with repositioning enabled

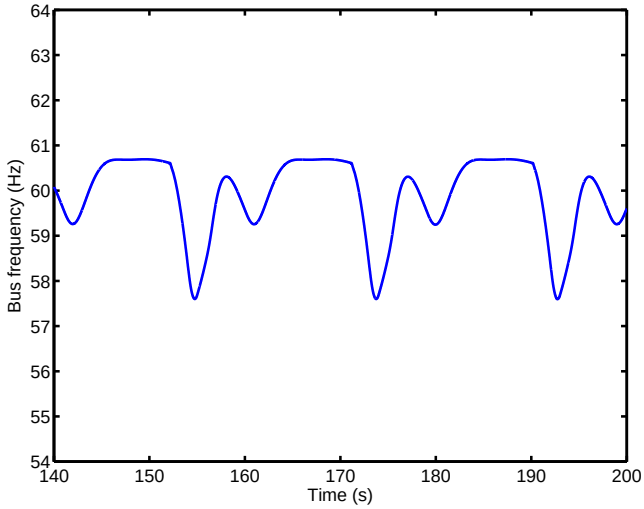

Figure 3.8: Bus frequency with repositioning disabled

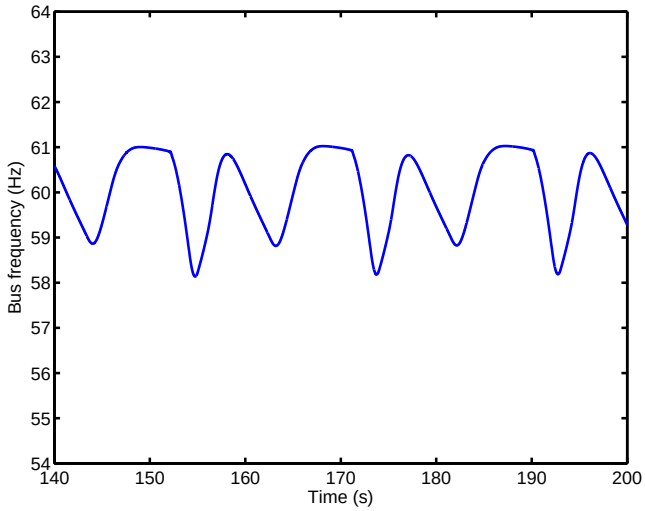

Figure 3.9: Bus frequency with repositioning enabled

3.5 Concluding remarks

Introduction of a repositioning scheme allowed larger absolute variations in the position of the vessel, which allowed some reduction in the fluctuation of the electric bus frequency. The improvement is not overwhelming, but significant in certain operating conditions.

Chapter 4

Dynamic Positioning System as Dynamic Energy Storage on Diesel-Electric Ships

4.1 Introduction

Dynamically positioned (DP) vessels with diesel-electric power and propulsion systems are commonly used in offshore operations in order to keep the ship position and heading at their references. While the DP system is often the main consumer of electric power on the ship, other variable power consumers are connected on the same power buses as the electric thrusters. The relatively weak electric grid on a vessel is therefore subject to significant variations in voltage and frequency caused by the dynamics of several more or less independent consumers. This causes challenges due to increased wear and tear, maintenance costs, emissions, and fuel inefficiency of diesel generators in combination with increased risk for blackout due to over- or under-frequency condition causing protection relays to trip generators. Common variable load consumers include drilling drives, heave compensators, cranes, pumps and winches whose operation are often influenced by wave-induced ship motions and other external disturbances.

From a DP ship operator's point of view, the main goal is to maximize the operationally useful time of a DP vessel in order to maximize operational income, hence minimizing inefficient and costly downtime resulting from loss of position incidents. At the same time, minimizing running hours on equipment such as power generators and thrusters will reduce maintenance costs. Historically, these two goals have been in conflict because the demand to maximize operational uptime has required a conservative and redundant use of power and thruster equipment, as required by the International Maritime Organization (IMO) rules for DP vessels [3]. A new and more flexible DP notation called DYNPOS ER (Enhanced Reliability), [20], has recently been launched. It is "... developed to allow owners to optimize fuel usage and reduce operational costs, while maintaining high integrity towards loss of position and heading" and enables a more "... flexible, redundant and fuel-efficient way of structuring DP systems". Such a new development on the classification side,

which is a result of new technological developments, opens up new possibilities for improved and integrated DP and power control functionality, thus motivating the dynamic energy storage on DP vessels.

Although large resistor banks and thrust allocation with thruster biasing are sometimes used to waste of power on DP ships in order to reduce the effects of power transients on the system, e.g. [37], it is clear that more efficiency and flexibility could be achieved with dynamic energy storage. While several concepts are currently being investigated, such as DC grids (e.g. [28]), hybrid power systems (e.g. [90]), battery banks, capacitive storage and increased mechanical inertia such as fly-wheels, the purpose of this chapter is to study a much simpler approach that does not require any new equipment, i.e. the use of the inertia of the vessel hull itself as dynamic energy storage controlled by the DP system.

The forces that act on a DP vessel can be assumed to be limited to the environmental forces and the thruster forces commanded by the DP controller. Further, assume that the slowly-varying components of the environmental forces are sufficiently large. The vessel hull itself is an effective dynamic energy storage due to its inertia. For example, accelerating the vessel forward by an electrical thruster will convert electric energy to mechanical energy that is at first stored as kinetic energy (due to velocity resulting from the acceleration caused by the thrust) and later as potential energy (a change in position in the presence of the slowly-varying environmental force field) that can be converted back by returning the vessel back to the original position. Temporary energy storage can therefore be provided by the DP system by allowing the vessel to move away from the set-point within a given position tolerance. This is not a new idea, and some power control and thrust allocation methods that exploits this mechanical energy storage capacity have been studied and implemented in various forms [13, 62, 78, 79]. A benefit of dynamic energy storage is increased operational flexibility as it allows these consumers to have higher priority than DP thrusters with respect to load reduction and load shedding, without reduced safety or operational performance, for short periods of time. Dynamic energy storage is currently also much considered for power and energy management in micro-grids and for integration of renewable energy sources, e.g. [48, 49].

The main contribution of this chapter is derivation and verification of a new and simple analytical formula that relates the amplitude of the position deviations that need to be allowed to achieve a given capacity of the dynamic energy storage characterized by the frequency and amplitude of the stored power. This allows bounds on the dynamic energy storage capacity provided by methods such as [13, 62, 78, 79] to be quantified using a very simple formula. Consequently, the need and benefits of new concepts for dynamic energy storage can be more easily discussed and compared in a wider perspective, as dynamic energy storage capacity can be provided within a reasonable range of frequencies and amplitudes simply through functions that can be realized in DP software without the need for any new power system hardware or other equipment.

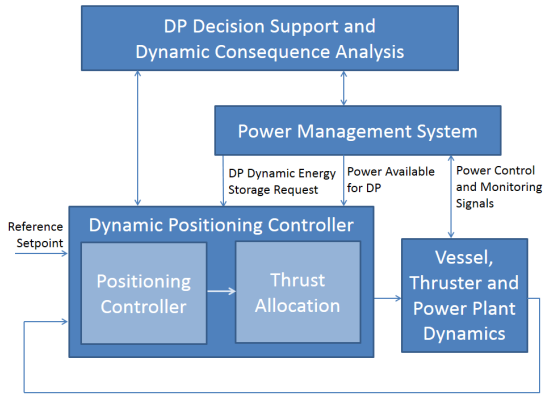

Figure 4.1: The Power Management System is allowed to request dynamic energy storage from the DP controller. A supervisory control and monitoring systems may provide advice and control in order to minimize risk for DP loss of position and other hazards due to electric power shortage resulting from equipment failure or operational issues.

4.2 A conceptual control architecture for dynamic energy storage in dynamic positioning

Figure 4.1 shows a control architecture that intends to illustrate the main idea. In a DP system there is a positioning controller that commands forces in surge and sway directions, as well as the yaw moment, in order to keep position and heading at their specified set-point, [25, 72]. Conventionally, a thrust allocation module allocates these forces to the individual thrusters in order to meet these commands whenever possible, where exceptions would be when the thrust demands cannot be met due to the static or dynamic limitations in the thruster system, machinery, or the electric power system. Those limitations are commonly managed through a power available signal from the power management system (PMS) that has the basic function of preventing overloading of the power plant due to equipment failures or protection trips due to under-frequency or under-voltage that would potentially lead to loss of position and emergency operation.

The architecture in Figure 4.1 deviates from conventional DP architectures since it allows the PMS to request dynamic energy storage to the DP controller. Such dynamic energy storage requests would typically either be issued to compensate for known or predictable load variations in other electric power consumers, e.g. heave compensators, or in response to failures or operational issues such as loss of generator capacity or partial blackout. Some further discussion on the potential benefits of dynamic energy storage in provided in section 4.5. The DP controller can then implement dynamic energy storage functionality in many different ways, for example

- Modify the position set-point slightly to increase or decrease the power con-

sumption during the transient.

- Modify the thrust request to the thruster controllers, [62], without any analysis of consequences for positioning errors.
- Modify the thrust request to the thrust allocation with an amount that corresponds to the requested dynamic energy storage rate. This is the approach that will be used in this chapter for demonstration and analysis, for simplicity.
- Modify the power available and limits to the thrust allocation in order to implement the dynamic energy storage request in a smooth and efficient way with minimum impact on the operation of the system, [13, 78, 79].

Dynamic storage of energy as kinetic and potential energy in a DP vessel has some inherent limitations. First, the energy storage cannot change faster than the thruster dynamics. While the electric thruster power can be changed in much less time than one second using frequency converters, it should be realized that persistent fast changes will cause mechanical stress on the system and increased tear and wear. Hence, in practice we expect that energy storage dynamics faster than about 0.2 - 0.5 Hz cannot normally be accommodated by the DP system. Note that higher frequencies than this would be effectively handled by the mechanical inertia of the diesel-generators, and the capacitances and inductances in the electric system, [60]. In emergency situation the functionality with significant risk of black-out the functionality could be allowed fast energy storage regardless of thruster wear considerations. On the other hand, the DP system typically has a control bandwidth corresponding to a response time of 15-60 seconds for a typical diesel-electric vessel. This bandwidth is chosen due to the dynamics of thrusters as well as the desire to avoid to act against the first order wave induced motions, which is commonly achieved with wave filtering, [72]. Hence, dynamics slower than about 0.05 rad/sec, or about 0.01 Hz, will be typically counteracted by the DP controller unless special functionality is implemented to allow certain position deviations. Consequently, the DP dynamic energy storage will typically be mostly effective for power variations in the range of 0.01 Hz to 0.2 Hz. Although this is a limited frequency band, it is still very useful since it captures important dynamics such as heave compensation systems, some drilling drive systems, and other large consumers. Dynamic energy storage requests of lower frequency can be effectively handled by load changes on the diesel generators, including start of standby generators, as they typically will be able to follow frequencies of 0.01 Hz.

4.3 Dynamic energy storage capacity analysis

Consider a vessel with mass m that is under DP control. For simplicity of analysis, we assume the vessel is headed against the weather (i.e. against the resultant steady-state environmental force vector) and consider only the surge axis position x. Assume further that a PID controller is used [72], and wind variations and first order forces due to ocean waves are neglected. It can be simplified as $F_{DP} = -(K_p x + F_I + K_d \dot{x})$ where a slowly time-varying force F_I (due to integral action) is assumed to cancel the slowly time-varying total environmental force F_E such that $F_I + F_E = 0$. Assume further that the DP system allocates a thrust

according to F_{DP} except for a component that is requested as dynamic energy storage to compensate for electric power variations outside the DP:

$$F_{alloc} = F_{DP} + K_0 P_{req} \tag{4.1}$$

where P_{req} is the requested dynamic energy storage (power), and K_0 $[N/W]$ is the thrust/power factor that is assumed to be constant for a given thruster configuration near some operating point. The equation of motion for the ship along the surge axis is

$$m\ddot{x} + D\dot{x} = F_{alloc} + F_E \tag{4.2}$$

where D is the hydrodynamic damping coefficient. This leads to

$$m\ddot{x} + (D + K_d)\dot{x} + K_p x = K_0 P_{req} \tag{4.3}$$

Next, consider the allocated (stored) power that is derived directly from (4.1):

$$\begin{aligned} P_{alloc} &= P_{DP} + P_{req} && (4.4)\\ &= F_{DP}/K_0 + P_{req} && (4.5)\\ &= -\frac{1}{K_0}\left(K_p x + F_I + K_d \dot{x}\right) + P_{req} && (4.6) \end{aligned}$$

Disregarding the stationary power F_I/K_0 needed to compensate for stationary environmental forces F_E, and transforming eqs. (4.3) and (4.6) to the Laplace domain gives the following equations:

$$\begin{aligned} \frac{1}{K_0}\left(ms^2 + (K_d + D)s + K_p\right) X(s) &= P_{req}(s) && (4.7)\\ P_{alloc}(s) + \frac{1}{K_0}(K_p + K_d s)X(s) &= P_{req}(s) && (4.8) \end{aligned}$$

Combining with (4.4) leads to the following transfer functions after some straightforward algebra:

$$\begin{aligned} \frac{X}{P_{alloc}}(s) &= \frac{K_0}{ms^2 + Ds} && (4.9)\\ \frac{P_{alloc}}{P_{req}}(s) &= \frac{ms^2 + Ds}{ms^2 + (K_d + D)s + K_p} && (4.10) \end{aligned}$$

Simulations in section 4.4 show that for a typical vessel and DP controller, the hydrodynamic damping force corresponds to less than 1-2 % of the power, so we get the following approximate transfer functions:

$$\begin{aligned} \frac{X}{P_{alloc}}(s) &\approx \frac{K_0}{ms^2} && (4.11)\\ \frac{P_{alloc}}{P_{req}}(s) &\approx \frac{ms^2}{ms^2 + K_d s + K_p} && (4.12) \end{aligned}$$

Assuming the dynamic energy storage request is sinusoidal $P_{req}(t) = P_a \sin(\omega_1 t)$, we get that for $\omega_1 >> \omega_0 = \sqrt{K_p/m}$

$$P_{alloc}(t) \approx P_{req}(t) \tag{4.13}$$

$$x_a \approx \frac{K_0}{m\omega_1^2} P_a \tag{4.14}$$

where x_a is the amplitude of the resulting sinusoidal motion $x(t) = x_a \sin(\omega_1 t + \phi)$ of the ship. By also accounting for the hydrodynamic damping, a slightly more accurate approximation can be made

$$x_a \approx \frac{K_0}{\sqrt{m^2\omega_1^4 + D^2\omega_1^2}} P_a \tag{4.15}$$

Based on these simple formulas, some observations can be made.

- The dynamic energy storage capacity P_{alloc} decreases when the dynamic power load frequency ω_1 decreases, in particular when it becomes smaller than the bandwidth ω_0 of the DP controller. For ω_1 much larger than ω_0 we have $P_{alloc} \approx P_{req}$, i.e. full capacity is available. For ω_1 much smaller than ω_0 we get $P_{alloc}/P_{req} \approx 0$, cf. (4.12).
- The amplitude x_a of the ship motion required to accommodate the dynamic energy storage decreases rapidly as ω_1 increases, cf. (4.14). This is a natural physical interpretation since high-frequency motions require relatively higher force and power than low-frequency motions of the same amplitude. Conversely, smaller high-frequency motion amplitudes will be generated using the same power.
- Net power savings are possible only when the environmental force $F_E \neq 0$, and full dynamic energy storage capacity is available only when $|F_E| \geq K_0 P_a$. This may not be seen as a practical limitation since large dynamic energy storage capacity may primarily be needed when there are high waves, which usually result from high winds that also lead to large $|F_E|$.

The calculations can be easily generalized for dynamic power load variations that are not sinusoidal by considering power spectra or Fourier series.

4.4 Verification - case study

The simulation example considers a case where a sinusoidal electric power system disturbance, corresponding to a given power amplitude and period, is added to the thrust commanded by the DP controller to implement dynamic energy storage according to (4.1). The modification to the thrust command is allocate to the surge force only, before the command is sent to the thrust allocation module.

The simulations are conducted using Matlab and the six-degrees-of-freedom Marine Systems Simulator, [25]. The DP vessel considered is a typical drillship, $m = 43,7 \cdot 10^6$ kg, where the main need for dynamic energy storage comes from active heave compensation of the drill-string or riser. The simulations consider a typical situation with a steady-state (constant) environmental force resulting from

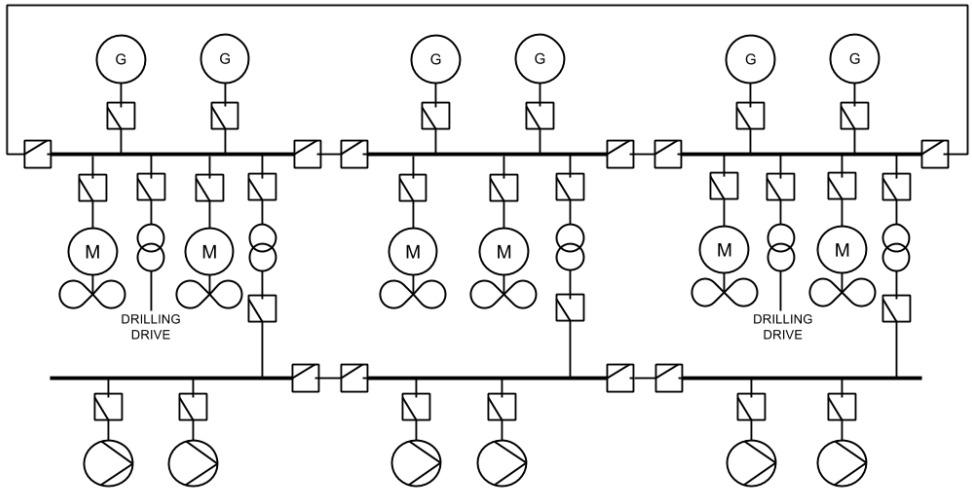

Figure 4.2: Power plant of simulated drilling vessel used in case study.

mean wind and current forces. In order to accurately analyze the dynamic energy storage functionality by itself, we have not included dynamic disturbance forces due to ocean waves and wind variations in the simulations. These forces could be super-positioned on the simulated forces to give additional dynamic variations in position, thrust and power consumption. In addition to the 6-degrees-of-freedom model of vessel motion with hydrodynamic and aerodynamic loads, the simulator contains a PID-based DP controller and a thrust allocation algorithm based on the pseudo-inverse. A simple model of the power plant dynamics is given by the diesel generators momentum balance, [79], inlet air pressure restrictions, [62] and electric system power balances, [9]. Based on this, other variables such as voltages and currents can be computed.The DP system is designed with a bandwidth in surge, sway and yaw of $\omega_0 = 0.033$ rad/s and critical relative damping $\zeta = 1.0$.

The power plant with diesel generators, distribution and consumers is illustrated in Fig. 4.2, and is characterized as follows

- There are three main 11 kV buses/switchboards with 2 diesel-generators having circuit breakers that allows them to be connected or disconnected. The generators operates with frequency-control by governors in droop mode.
- There is a ring bus and bus-tie breakers that allows the bus segments to be connected in as a single bus, or in 2-split or 3-split modes. In the simulations we operate with closed bus-ties.
- There are six azimuth thrusters arranged in a standard geometric layout, two for each power bus segment.
- There are several additional consumers connected through transformers or 440 V switchboards that are fed by the main switchboards. For simplicity

the figure only shows some main other drilling consumers, i.e. active heave draw-works drive, mud pumps and top drive.

$P_{alloc}[MW]$	$P_{req}[MW]$	$\omega_1[rad/s]$	x_a $[m]$ (sim)	x_a $[m]$ (eq. (4.14))	x_a $[m]$ (eq. (4.15))
0.65	1.26	0.033	1.04	1.09	1.04
2.06	3.99	0.033	5.20	5.42	5.18
3.60	3.99	0.100	1.02	1.03	1.03
8.82	9.78	0.100	2.05	2.06	2.05
9.63	9.78	0.330	0.19	0.21	0.21
3.94	3.99	0.500	0.03	0.04	0.04
9.58	9.78	1.000	0.04	0.02	0.02

Table 4.1: Numerical results from case study.

Simulation results are shown in Table 4.1. They consider a number of cases with different power storage request amplitudes and frequencies, corresponding to different drilling loads that may result from compensation for wave-induced ship motions:

- Dominating wave amplitudes commonly correspond to the range 0.33 rad/s - 1.0 rad/s, e.g. [25, 76].
- Power variations with frequencies in the range 0.033 rad/s - 0.1 rad/s correspond to low-frequent wave motions such as swells or more exceptional waves that may occur in some geographical regions.
- Even in rough sea states an active heave drawwork and drilling drives has power consumption variations with amplitudes of less than 5 MW. The scenarios simulated are therefore to be considered as conservative worst cases.

The table reports the simulated and analytic (using (4.14)) position deviation amplitudes as well as dynamically stored energy. The simulations confirm that several megawatts of power variations can be managed by the power management and DP system by accepting relatively small position deviations on a typical mobile offshore drilling unit. Note that typical position deviation for a DP system in normal conditions is about 1 meter. At $\omega_1 = \omega_0 = 0.033\ rad/s$ the dynamic energy storage only has about 50% effect as the allocated (stored) power is only half of the requested dynamic energy storage, due to interactions resulting from the conflict with the primary position control objectives of the DP controller.

The simulations confirm the accuracy of the simple analytic formula (4.14) with accuracy typically better than 5 % error. For cases with very small surge amplitudes, the deviation between x_a predicted by the simple model and the advanced simulation model is relatively large in percent (up to 50 %) but negligible in absolute position deviations (a couple of cm). The main reason why higher relative deviations are observed in these cases is the "higher order" dynamic effects of couplings between surge/pitch (longitudinal) and sway/roll (lateral) ship motions included by variations in thruster forces and moments.

The simulations also verify that the dynamic energy storage has the benefit that it makes the variations in electric frequency very small (less than 1 % for all cases) and even less variations in voltage. Moreover, the dynamic energy storage it balances out the difference between consumed and produced power that results due to the dynamics of the diesel generators.

It has been verified by simulations that the formulas (4.14)-(4.15) qualitatively are in good agreement also with more advanced implementation of DP dynamic energy storage, [78, 79].

4.5 DP Decision Support and Dynamic Consequence Analysis

According to established industry standard system design and operational procedures for dynamically positioned ships, [3], it is up to the operator to enable or disable a sufficient amount of thrusters based on the DP decision support tools such as on-line consequence analysis, capability analysis, and motion prediction, while the PMS ensures that a sufficient amount of generators are running at all times to serve both operational and positioning power needs. Conventionally, a redundant number of on-line generators and thrusters are employed to guarantee safety and operational availability. However, such a redundancy leads to equipment running at low and inefficient loads, and increases both fuel and maintenance costs as well as exhaust gas emissions.

By increasing the information exchange and actively taking advantage of the dynamic energy storage capacity offered by the DP system, a less conservative use of generators and thrusters can be achieved. In particular, the following enhancements can be envisioned within the framework presented in Figure 4.1, see [10, 13] for further details. An on-line simulation-based dynamic consequence analysis can take into account information about the vessel dynamics, the weather situation (wind, waves and current), load situation, startup time of standby generators and thrusters, etc. to realistically calculate an optimal position reference for the DP system which minimizes the chance of drift-off or drive-off while simultaneously maximizing the available operational time after generator or switchboard failure, i.e., how long it is possible to prioritize the operational drives in favor of the thruster drives before safety is compromised. This knowledge can be used to reduce the amount of on-line generators and thrusters while still achieving operational availability and safety in case of a failure, sending the information back to PMS system for consumer load control.

Such integrated and simulation-based power management functionality can for instance be employed by drilling vessels, which have flexibility in positioning depending on the water depth and the corresponding length of the drill string. For such vessels, the functionality will ensure that safety will not be compromised if equipment fails even if a minimum power and thrust configuration is used, because there will be enough time to remedy the failure situation by enabling/disabling relevant power/thrust equipment. Examples include:

- If a generator fails and results in insufficient power, the power consumption must be reduced to avoid a blackout. In order to continue the drilling

operation, the thrust consumption must be reduced instead of the drilling consumption. Hence, the vessel will experience a drift-off. However, using a simulator-calculated position reference, e.g. [10], the vessel is already located such that it can safely be allowed to drift for a certain period of time without having to reduce the drilling power consumption in favor of the positioning. During this time frame, the vessel will be able to start the necessary standby generators in order to restore sufficient power to stop the drift-off and bring the vessel back into position.

- In the worst case, if the vessel moves close to the safety limit during a drift-off, the power to the operational drives (e.g. drilling drives and mud pumps) must be reduced in favor of power to the thruster drives, in order to maintain the safety of the vessel, equipment and crew. Hence, the integrated system will automatically prioritize drilling versus positioning needs depending on the vessel drift pattern, in order to continue the drilling operation as long as safely possible.

4.6 Conclusions

Simple formulas are derived in order to related the dynamic energy storage capacity to the maximum allowed ship position deviation, as a function of the frequency of the requested dynamic energy storage. The formulas are verified using a high-fidelity vessel simulator, and show that for dynamic energy storage requests at wave frequencies (resulting e.g. from an active heave compensation system) that power variations of several megawatt will result in position deviations that are no larger than normal position deviations resulting from the dynamics of ocean waves and winds, as well as inaccuracies in sensors and position reference systems.

The main advantage of this integrated approach is to maintain operational availability and safety while minimizing power consumption, which translates into lower fuel costs and exhaust gas emissions, as well as minimizing wear and tear of generators and thrusters, which translates into lower maintenance costs. Relevant applications include marine operations with positioning flexibility such as drilling.

It could also be mentioned that the method can be directly extended to other energy storage capacities on-board ships in order to allow more low-frequency dynamic energy storage requirements, e.g. thermal storage in cooling, cargo, ventilation, air conditioning and other systems. Such functionality is enabled by integrated automation systems that allows the required software functionality to be implemented.

Chapter 5

Governor principle for increased safety and economy on vessels with diesel-electric propulsion

5.1 Introduction

Diesel-electric power plants have become the de facto standard primary power source for ships in the offshore industry that are expected to spend a large part of their time in dynamic positioning. This operational mode is important for ships that perform functions such as supplying offshore installations, drilling and oil production, laying pipes, supporting divers or ROV operations, or performing surface-based measurements or exploration. The main benefits of diesel-electric propulsion and thrusters are reduced power consumption under operational conditions typical for certain vessel types, resilience to equipment failures, lighter engines, and less noise [19]. Ensuring fuel-optimal operation during normal conditions as well as continued fulfillment of the operational requirements and safety despite equipment failures introduces challenges for the control system.

A diesel-driven power plant operates optimally when the load is large and close to being constant. The diesel engine may be physically unable to respond to large and sudden load increases due to the relatively slow turbocharger dynamics. Dependent upon the tuning, the governor may also respond slowly to changes in load, resulting in frequency fluctuations. Although small frequency fluctuations are acceptable, the protection relays typically set a limit of $\pm 10\%$ on the maximal frequency deviation from the nominal value. If this limit is exceeded, the generators and some of the consumers will disconnect from the power grid.

A thrust allocation algorithm that attempts to assist the power management system in reducing the load variations on the power plant by counteracting the load variations from other consumers on the ship has been introduced in [78] and [56], while in [62] the counteracting of the load variations is performed by the local thruster controllers.

A diesel-electric power plant typically consists of several generator sets connected to one or more electric buses, in a configuration that allows the gensets

to be connected and disconnected as the operational conditions change. The connection and disconnection of gensets can be performed for example according to a precalculated optimal start-stop table as in [61] or by ensuring through a dynamic simulation that the power plant is at all times capable of continuing operations in a predefined worst case scenario, as in [7]. The operation of the power plant is supervised by the power management system (PMS). Legacy industrial implementations rely on distributed control to ensure a stable frequency, load sharing and fault tolerance on the electric bus. A typical way of implementing this is to use droop, ie every governor has a set point that depends on its current power output.

This mechanism has several drawbacks. A drooped governor relies exclusively on feedback control. A significant improvement can be achieved with use of a feed-forward of the load variations. A feed-forward from the load measurements on the terminals of each generator was tested in [79], and a feed-forward from the load preview information from the PMS was tested in [56].

Large variations in the power output of the diesel engine will increase the specific fuel consumption, wear-and-tear, soot and particle emissions. Unfortunately, on the marine power plants there are large and often rapid variations in the consumed power, and if those variations are not closely matched by the diesel engines, the electric bus frequency will fluctuate. The use of a centralized control system as suggested in this chapter allows better balancing between those considerations.

In normal operational conditions it is preferable to accept some frequency variations. However, under circumstances with high blackout risk it will be beneficial to temporarily disregard the operational costs and keep the frequency as steady as physically possible.

Such circumstances could arise during activation of the fast load reduction system, activation of the power constraint in the thrust allocation algorithm, a significant drop in frequency (that should have been avoided, but wasn't), closing of a bus tie that may cause faults to be exposed, or any other signs that the operational safety needs to prioritized.

The main contribution of this chapter is an application of a receding horizon control strategy on a marine power plant, allowing a more precise control in presence of predictable load fluctuations, as well as a capability to temporarily disregard the wear-and-tear and economic concerns to aid recovery to safe operational conditions. The biggest challenge with implementing this control strategy was developing a model that is suitable for use in the receding horizon control. The modelling is discussed in Section 5.2. The proposed controller architecture is described in Section 5.3. The results from simulation tests are presented in Section 5.4.

5.2 Modeling

High fidelity models of most of the individual components that constitute a diesel-electric power plant are readily available in the literature. The control engineering challenge is thus to find a simple model with sufficient fidelity to predict the behavior of aspects of the controlled system that are relevant on the time scale that is

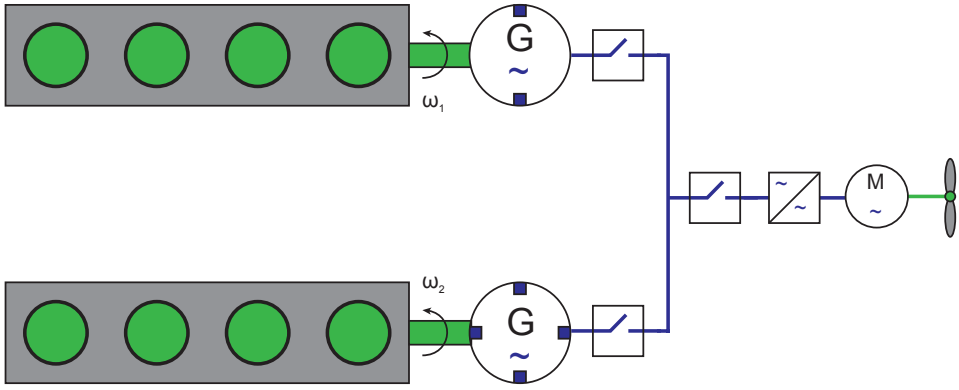

Figure 5.1: A simple example of a diesel-electric propulsion system. Two four-cylinder diesel engines each drive its own electric generator. When both circuit breakers are connected, the engine that drives the two-poled generator has to rotate twice as fast as the one that drives the four-poled generator, i.e. $\omega_1 = 2\omega_2$.

relevant. Although higher fidelity is in general desirable, an overly complex model would impede the engineering task.

A state-space model of a connected bus will be introduced in Subsection 5.2.4, and a model for the torque output from a diesel engine will be introduced in Subsection 5.2.5.

5.2.1 Abbreviations and Normalization

Normailization parameters in this chapter are as follows:

Description	Abbreviation	Unit
Nominal mechanical angular velocity of engine number i.	$\omega_{r,i}$	$^{\text{rad}}/_{\text{s}}$
Nominal electrical angular velocity of the bus.	$\omega_{r,e}$	$^{\text{rad}}/_{\text{s}}$
Nominal mechanical power output of engine number i.	$P_{r,i}$	W
Total nominal mechanical power connected to the bus.	$P_r = \sum_i P_{r,i}$	W
Inertia time constant of engine number i.	$H_i = \frac{\frac{1}{2} I_i \omega_r^2}{P_r}$	s

A typical marine power plant runs at 60 Hz, so normally $\omega_{r,e} = 2\pi \cdot 60$. The nominal mechanical angular velocity of each connected engine depends on the number of poles in the generator, such that $\omega_{r,i} = k_i \omega_{r,e}$ with a constant k_i. The inertia time constant is defined as a function of the moment of inertia I_i of the rotating mass in the genset. The parameter H_i is usually available in the specifications of a genset.

The following state variables are defined both in S.I. units and in the normalized units, with the subscript "pu" used to separate the variables expressed in per-unit scale:

Description	Normalization
Mechanical angular frequency of engine i.	$\omega_i = \omega_{pu}\omega_{r,i}$
Electrical angular frequency on the bus	$\omega_e = \omega_{pu}\omega_{r,e}$
Total power generated by the engines	$P = p_{pu}P_r$
Mechanical torque produced by engine i	$\tau_{m,i} = \tau_{pu,m,i}\tau_{r,i}$
Mechanical power produced by engine i	$p_{m,i} = p_{pu,m,i}p_{r,i}$

The reason why ω_{pu} is used as the per-unit rotational velocity for all gensets as well as the electrical frequency will be explained in Subsection 5.2.4.

5.2.2 Equations for a single genset

The rotational dynamics of a single genset are described by the swing equation. Its representation in the SI units and the per-unit form are listed in the table below. The difference between the delivered mechanical torque τ_m and the load torque τ_l is represented as $\Delta\tau$ and $\Delta\tau_{pu}$ respectively for SI and per-unit representation.

Description	SI units	Per-unit
Swing equation	$I\dot{\omega} = \Delta\tau$	$2H\dot{\omega}_{pu} = \Delta\tau_{pu}$
Power as function of rotational velocity	$P = \omega\tau$	$p_{pu} = \omega_{pu}\tau_{pu}$

5.2.3 Losses

The diesel engines are connected to the loads through the generator and a dynamic electric distribution network that may have many possible configurations and voltage levels. The distribution system is not modeled in this chapter, but is assumed to transfer the power from generators to consumers with losses being proportional to the transferred power. This implies that a system with losses is equivalent to a lossless system with a smaller power output, making the losses largely irrelevant to the dynamical behavior of the system.

5.2.4 Connected bus

The dynamics of a bus connection are such that if one of the engines for some reason increases its speed relative to the other engines, it would quickly overtake a larger share of the load, forcing it to slow down while the other engines increase their speeds because they would get a lower share of the load. This dynamic restricts all the gensets connected to a single bus to rotating at the same electrical frequency. For example, if a four-poled and a two-poled genset are connected to the same bus, then the two-poled genset will be forced to spin two times faster than the four-poled genset. This is illustrated in Figure 5.1.

It is therefore possible to represent the speed of each engine in terms of the electrical frequency as $\omega_i = k_i\omega_e$. In per-unit terms, $\omega_i/\omega_{i,r} = k_i\omega_e/k_i\omega_{e,r} = \omega_{pu}\forall i$. Thus,

$$I_i\dot{\omega}_i = \Delta\tau_i = \Delta p_i/\omega_i \tag{5.1}$$

$$I_i k_i^2 \dot{\omega}_e \omega_e = \Delta p_i \tag{5.2}$$

Where $\Delta p_i = \Delta \tau_i \omega_i$ is the difference between the power consumed by the load and power produced by the diesel engine on genset i. Summation over all gensets connected to a bus yields

$$\sum_i \{I_i k_i^2\} \dot{\omega}_e \omega_e = \Delta P \tag{5.3}$$

$$\sum_i \{I_i k_i^2\} \omega_{r,e}^2 \dot{\omega}_{pu} \omega_{pu} = \Delta p_{pu} P_r \tag{5.4}$$

where Δp_{pu} is the per-unit difference between the load on the bus and the total mechanical power that is generated. Note that since this equation concerns the entire bus, the total rated power on the bus $P_r = \sum_i P_{r,i}$, is used for normalization. Next, defining the inertia time constant for a system of connected gensets as

$$H = \frac{\frac{1}{2} \sum_i I_i \omega_{r,i}^2}{\sum_i P_{r,i}} \tag{5.5}$$

and then substituting $\omega_{r,i} = k_i \omega_{r,e}$, the equation above can be transformed to

$$H = \frac{\frac{1}{2} \sum_i \left\{I_i k_i^2\right\} \omega_{r,e}^2}{P_r} \tag{5.6}$$

Inserting this into (5.4) yields

$$2H \dot{\omega}_{pu} \omega_{pu} = \Delta p_{pu} \tag{5.7}$$

The electrical torque does not represent any measurable physical quantity, but is defined in analogy to the mechanical torque as $\tau_{pu,e} \triangleq \frac{p_{pu}}{\omega_{pu}}$. This can be used to transform the equation above to

$$2H \dot{\omega}_{pu} = \Delta \tau_{pu,e} \tag{5.8}$$

which is analogous to the swing equation for a single engine, as defined in Subsection 5.2.2.

Additionally, to calculate the load on individual generators, we can make use of the fact that for each genset, the following holds:

$$2H_i \dot{\omega}_{pu} \omega_{pu} = \Delta p_{pu,i} \tag{5.9}$$

Since we have that $\Delta p_{pu,i} = p_{pu,m,i} - p_{pu,l,i}$, the load $p_{pu,l,i}$ on each generator can be calculated.

5.2.5 Mechanical power from the engine

Many types of engines can be used as a prime mover in a marine power plant, however the type of prime mover dominantly utilized in the maritime industry is the diesel engine.

The model in this text is based on the model presented in [79], which is in turn based on the quasi-steady cycle-mean-value model from [89]. With small variations it is widely available in the literature, such as [27]. The dynamics of a diesel engine are such that as long as there is sufficient pressure in the scavenging receiver it is possible to set the torque delivery of a diesel engine essentially at will by changing the amount of fuel that enters the next cylinder in the firing sequence. The delay before the new torque will be put on the shaft depends on when the next cylinder in the firing sequence will be available for fuel injection, and a short fuel evaporation and ignition delay.

Oxidizer concentration in the scavenging receiver does however set a physical limit on how fast the torque output of an engine can increase. The turbocharger compressor is driven by a turbine, which derives its energy from the exhaust gas of the engine. For a given engine power output at a given engine RPM, the pressure in the scavenging receiver will converge to an equilibrium point. The time it takes to build up the pressure severely limits the dynamic response of the engine. As in [79], we assume that for control purposes it is sufficient to estimate a linear relationship between the engine power output at a given RPM and the equilibrium pressure in the scavenging receiver, and then assume that the pressure will converge to the equilibrium pressure exponentially.

The exact mathematical description of the dependence of the combustion efficiency on the air-to-fuel ratio and the combustion efficiency varies somewhat between different models. What matters for the purposes of this chapter is that there is an upper limit on how much the torque can be increased over a very short period of time.

The relevant equations from [79] are restated here

$$\tau_m = \eta_c F_r \tag{5.10}$$

$$\dot{\omega}_t = -\kappa_1(\omega_t - p_{pu,m}) \tag{5.11}$$

$$AF = \frac{m_{a,0} + (1 - m_{a,0})\omega_t}{F_r} \cdot AF_n \tag{5.12}$$

$$\eta_c = \begin{cases} 1 & AF \geq AF_{high} \\ \frac{AF - AF_{low}}{AF_{high} - AF_{low}} & AF_{low} < AF < AF_{high} \\ 0 & AF \leq AF_{low} \end{cases} \tag{5.13}$$

The new variables are defined in the table below. When they are applied to the individual engines, a subscript index i is used.

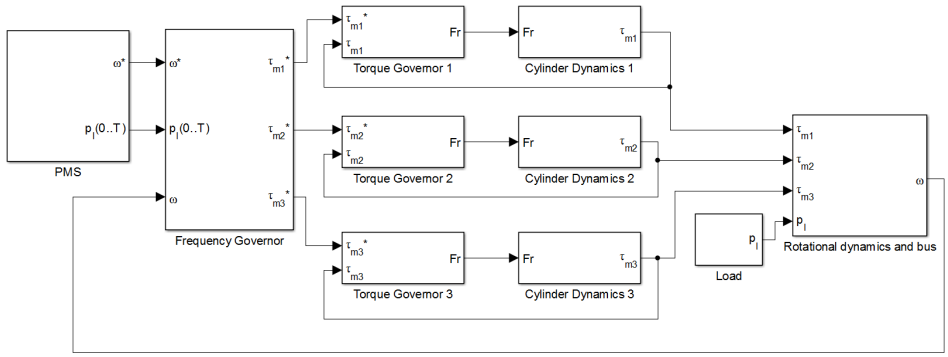

Figure 5.2: The proposed control architecture, illustrated on a powerplant with three connected generator sets.

Description	Abbreviation
Fuel index of engine. This is the variable that is directly under the control of the governor.	F_r
The combustion efficiency	η_c
Per unit turbocharger velocity	ω_t
The inverse of the time constant of the turbocharger	κ_1
Air-to-fuel ratio	AF
The minimal air-to-fuel ratio needed to achieve full combustion, the minimal air-to-fuel ratio needed to achieve combustion at all, the normal operating point of the engine at full load (disregarding the throttling of the supply air and exhaust gas recirculation)	AF_{high}, AF_{low}, AF_n
Air flow fraction without the turbocharger	$m_{a,0}$

5.3 Control architecture

The control architecture for a single distribution bus is illustrated in Figure 5.2. The power management system sets a bus frequency set point, and it provides a prediction of the load over a time horizon T. The task of governing the engines is separated into torque control and frequency control. The local torque controllers need to have a thorough knowledge of the dynamics of the diesel engines that they control. For example, in [47] the engine torque output as a function of the governor current and engine speed is obtained experimentally, and used to tune a PID controller. As long as a sufficient amount of air is provided by the turbocharger, a torque controller is able to change the torque output of an engine very quickly, on the time scale of a fraction of a single crank shaft revolution. For medium or high speed engines which are usually employed in the diesel-electric power plants, this delay is negligible. The advantage of this approach is that the centralized frequency governor does not need to consider the particulars of each engine except for the limitations imposed by the intake air supply.

An even lower level controller sets variables such as combustion timing and throttle openings based on the fuel index. Algorithms for such controllers are available in the litterature, for example [15, 38, 50].

The task of the centralized frequency governor is to maintain a stable bus frequency, a task which has to be balanced against the wear-and-tear of the engines, emissions, soot, and specific fuel consumption. A precise model for those variables would have to be either very complex or ad hoc parameter matching. A study measuring fuel consumption and emissions during transients in load and speed on two full-sized diesel engines that were originally mounted on heavy equipment machines was conducted in [52]. In this work, it is assumed that for a given power output level the economic and environmental costs are generally minimized by reducing the variations in the power output, and the controller implemented in this chapter contents itself with this.

$$\min_{\vec{\tau}} \int_0^T \left[Q\tilde{\omega}_{pu}^2(t) + \left\| \frac{d\vec{\tau}}{dt}(t) \right\|_R^2 \right] dt + P\tilde{\omega}_{pu}^2(T) \tag{5.14}$$

Subject to

$$\text{For each of the gensets, equations (5.10)-(5.13)} \tag{5.15}$$

$$\text{Equation (5.7)} \tag{5.16}$$

$$|\tilde{\omega}_{pu}(t)| \leq \tilde{\omega}_{max} \tag{5.17}$$

$$\tilde{\omega}(0) = \tilde{\omega}_0 \tag{5.18}$$

$$\omega_t(0) = \omega_{t,0} \tag{5.19}$$

Here, $\vec{\tau} = \begin{bmatrix} \tau_1 & \tau_2 & \cdots & \tau_N \end{bmatrix}^T$ is the setpoint vector for the local torque governors , $\tilde{\omega}_{pu}(t)$ is the deviation between the desired and the actual frequency on the bus, $\tilde{\omega}_0$ is this deviation measured at the current time at every iteration of the moving receding controller, and $\omega_{t,0}$ is the estimated turbocharger velocity at the current time at every iteration of the receding horizon controller. The variables Q, R and P are weighing scalars and matrices of appropriate dimensions.

5.4 Results

This proposed algorithm was tested in simulation on a bus powered by three generator sets, two of them rated at 1 MW, and the third one rated at 2 MW. The inertia time constants for the three generators were 10, 8 and 9 seconds. The load changes are described in Figure 5.3. Two configurations of the governor were tested. One configuration had a normal weighing of the engine torque variations relative to the bus frequency in the cost function. The other one, and emergency mode ("eager") configuration, had a low cost on the engine torque variations. In the normal

configuration, $Q = 1$, $R = I_{3\times3} \cdot 5 \cdot 10^{-3}$, $P = 20$. In the eager configuration the value for R is set to $I_{3\times3} \cdot 10^{-8}$, with all the other parameters remaining the same. A load preview horizon T of one second was used.

The simulation was implemented in Simulink, and the receding horizon controller was implemented in Acado [6].

When a load is increased by a relatively small amount five seconds into the simulations, the normal governor prepares for the load increase by slightly increasing the torque output, and then adjusts it to the new equilibrium over a period of about three seconds. It does essentially the same thing with a larger load increase; however since the diesel engines are physically unable to produce the power that is consumed by the load, a drop in the frequency is inevitable. The governor then pushes the engines as hard as physically possible until the frequency recovers.

In the eager configuration the governor is more aggressive in stabilizing the frequency, and acts somewhat counterintuitively. Before a load increase, it will first create a dip in the generated torque and thus a very small dip in the bus frequency. Then, just before the inrush load, it will increase the torque to the maximal physically possible value. This maneuver gives a two-fold advantage. Firstly, this means the torque output can be increased more just before the inrush. Without the prior dip, it would result in a larger overfrequency. Secondly, since the preparation for the inrush load involves an initial increase in the frequency above the setpoint, and this cost is proportional to the square of the deviation, this cost can be minimized by minimizing the time spent with a large value of the deviation. The cost of this small dip in frequency in terms of the time integral of the square of the deviation is negligible, while it allows for faster transition of the period with a large overfrequency.

5.5 Conclusions

The proposed governor is able to increase the power output quite substantially before the load increase hits the bus, both in the normal and in the eager configuration. By doing this it is increasing the energy stored in the rotating machinery and giving the turbocharger a head start to compress more air. The eager configuration provides a larger safety margin to blackout due to underfrequency, at the cost of wearing down the engine. It is therefore best suited for emergency situations. Although only variations in consumer load on the bus were tested, the effect from a sudden disconnection of a generator is expected to be essentially identical.

5.6 Future work

The assumptions made in this chapter about the diesel engine dynamics and emission model need verification. Experiments on a high fidelity simulator with a physical diesel engine in the simulation loop are currently being conducted by the research group.

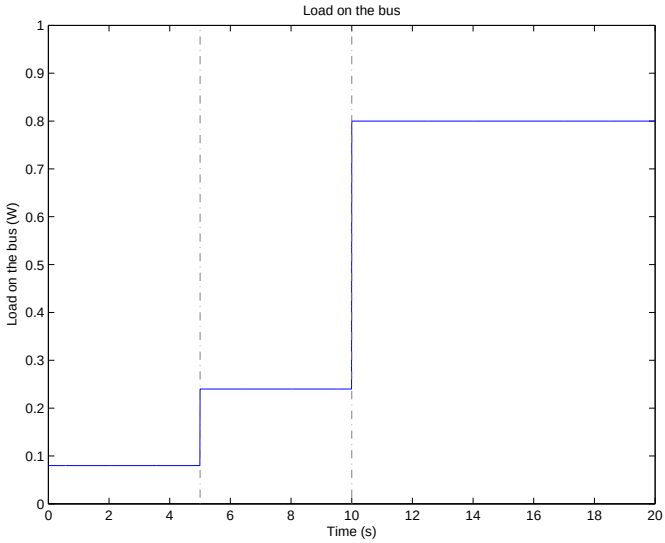

Figure 5.3: Load on the bus

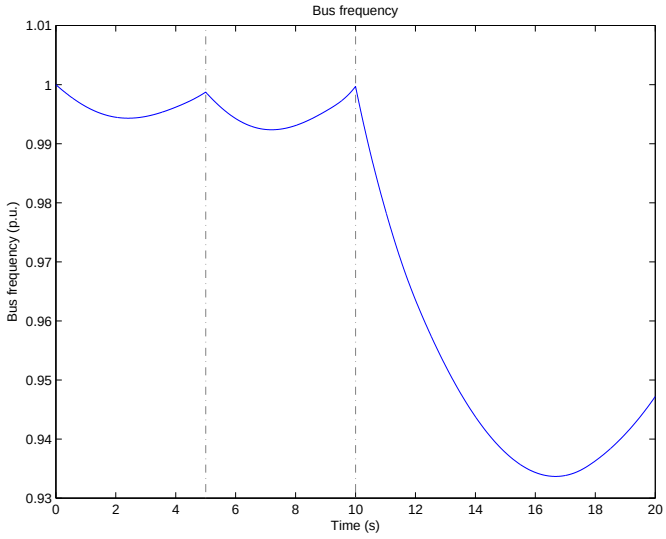

Figure 5.4: Bus frequency, normal configuration.

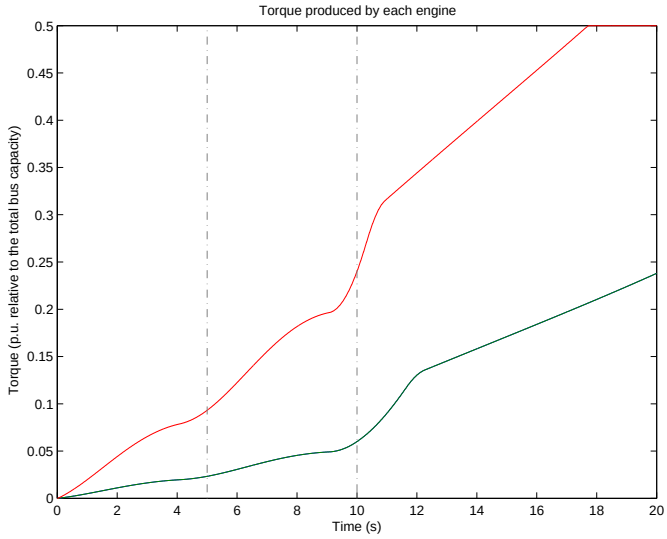

Figure 5.5: Torque output of the engines, normal configuration. The two of the smaller engines follow an identical trajectory, displayed in green.

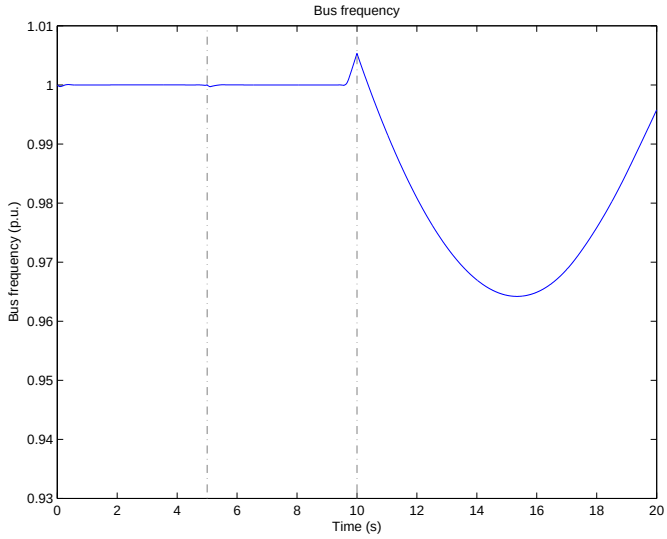

Figure 5.6: Bus frequency, eager configuration.

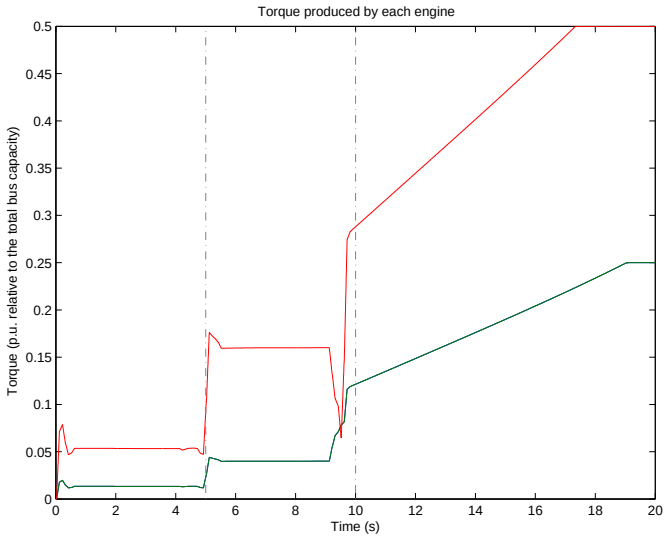

Figure 5.7: Torque output of the engines, eager configuration. The two of the smaller engines follow an identical trajectory, displayed in green.

Chapter 6

Cartesian thrust allocation algorithm with variable direction thrusters, turn rate limits and singularity avoidance

6.1 Introduction

Designing control systems for ships in dynamic positioning (DP) is subject to a long-lasting and ongoing research effort, with Project Mohole in the early sixties being one of the first practical implementations [35, 58]. The more recent efforts were directed towards designing algorithms that systematically resolve complications such as coordination of rotable thrusters [40, 73], control of ruddered propellers [42], power consumption optimization [66] and other power management-related issues [56, 65, 78, 79], sector constraints and other issues that were earlier resolved heuristically. An introductory textbook is available in [25] and a recent review of the topic is available in [39]. These developments allow DP operations with better safety, economy, positioning precision and reliability, allowing the DP-equipped vessels to perform more complex tasks in deeper waters [18] and on arctic latitudes.

DP algorithms are often divided into several parts, one of which is a thrust allocation (TA) algorithm. The task of the TA algorithm is to receive a command telling it how much force and moment of force (together called "generalized force" in this context) the thruster system should produce, and generate commands to the individual thrusters so that the resultant force and moment of force on the ship is equal to the commanded.

This chapter proposes a TA algorithm that combines and integrates the elements from the earlier contributions, thus providing an implementation with singularity avoidance functionality that is able to control both azimuth thrusters and ruddered propellers. This algorithm is based on [42] and represents the thruster forces in Cartesian coordinates. This allows a consistent representation of the thruster forces between different types of thrusters including tunnel thrusters, azimuth thrusters, ruddered propellers and Voith Schneider propellers. The extension

for the azimuth thrusters is based on [68], and the singularity avoidance is based on [40]. This work also contributes a theoretical and a practical examination of singularity avoidance functionality implementation as a singularity proximity penalty in the cost function of the optimization problem.

6.2 Thrust allocation algorithm

The most important variables used in this chapter are introduced in Table 6.1. Defining the control u_k for thruster k as

$$u_k = \begin{cases} [X_k, Y_k]^T & \text{if the thruster with index } k \text{ is rotable} \\ T_k & \text{otherwise} \end{cases} \tag{6.1}$$

and then defining the extended thrust vector u as $u = \begin{bmatrix} u_1^T & u_2^T & \dots & u_p^T \end{bmatrix}^T \in \mathbb{R}^n$, where $n = 2p_r + p_f$ is the number of degrees of freedom available to the control system. The resultant generalized force from the thrusters is given by

Abbreviation	Description
p	The number of thruster devices on the vessel.
p_r, p_f	The number of rotable and the number of fixed-direction thruster devices.
$r_k = [l_{k,x}, l_{k,y}]^T$	The location of the thruster device with index k.
α_k	The angle of the thruster device with index k; α_k is constant for thruster devices with fixed direction and variable otherwise.
$T_k \in \mathbb{R}$	The force (magnitude) produced by device with index k.
X_k, Y_k, $N_k \in \mathbb{R}$	The force components in surge and sway, and the moment of force in yaw produced by the device with index k.
$\tau = \sum_k \begin{bmatrix} X_k, & Y_k & N_k \end{bmatrix}^T \in \mathbb{R}^3$	The resultant generalized force produced by all thrusters on the vessel.
τ_c	The generalized force order to the thrust allocation algorithm from the high-level motion control algorithm or from a joystick.
$u \in \mathbb{R}^{2p_r+p_f}$	The extended thrust vector.
u_0, $u_{k,0}$	The extended thrust vector from the previous iteration of the algorithm and the control u_k from the previous solution of the thrust allocation algorithm.

Figure 6.1: Nomenclature

$$\tau = Bu \tag{6.2}$$

where

$$B = \begin{bmatrix} B_r, & B_f \end{bmatrix} \tag{6.3}$$

with

$$B_r = \begin{bmatrix} 1 & 0 & \cdots & 1 & 0 \\ 0 & 1 & \cdots & 0 & 1 \\ -l_{1,y} & l_{1,x} & \cdots & -l_{p_r,y} & l_{p_r,x} \end{bmatrix}$$

and

$$B_f = \begin{bmatrix} \cos\alpha_{p_r+1} & \cdots & \cos\alpha_p \\ \sin\alpha_{p_r+1} & \cdots & \sin\alpha_p \\ l_{p_r+1} & \cdots & l_p \end{bmatrix} \tag{6.4}$$

The matrix B describes the location and the orientation of all the thrusters on the vessel, and it is called the thruster configuration matrix.

6.2.1 Thruster saturation

As in [42], the constraints representing the thruster saturation for each rotable thruster is a polygonal approximation to the circular region, which is illustrated in Figure 6.2. This approximation can be done with arbitrary precision, and represented as a linear constraint in the form

$$A_k u_k \leq 1 \tag{6.5}$$

for a thruster with index k. Representing the saturation constraints for the non-rotable thrusters in the form (6.5) is straightforward.

6.2.2 Rotation rate constraint

Some rotable devices such as azimuths and rudders have a limited rate of rotation. This limitation is introduced as a constraint on the sector within which the force from such thrusters can be allocated in the iteration of the thrust allocation algorithm that is being calculated. Let angles $\alpha_{-,k}$ and $\alpha_{+,k}$ specify the sector in which the rotable thruster with index k will be able to produce force. Typically, $\alpha_{+,k} = \alpha_{k,0} + \Delta\alpha_{max}$ and $\alpha_{-,k} = \alpha_{k,0} - \Delta\alpha_{max}$, where $\alpha_{k,0}$ is the angle at which the thruster was in the previous thrust allocation and $\Delta\alpha_{max}$ is the maximal angle it can travel in the period between two allocations. If there are forbidden sectors that the thruster cannot enter, then the constraints on the allowed sector can be modified accordingly. As in [68, eqns (4.38), (4.39)], the sector constraint is represented as

$$\begin{bmatrix} \sin(\alpha_{-,k}) & -\cos(\alpha_{-,k}) \\ -\sin(\alpha_{+,k}) & \cos(\alpha_{+,k}) \end{bmatrix} u_k \leq 0 \tag{6.6}$$

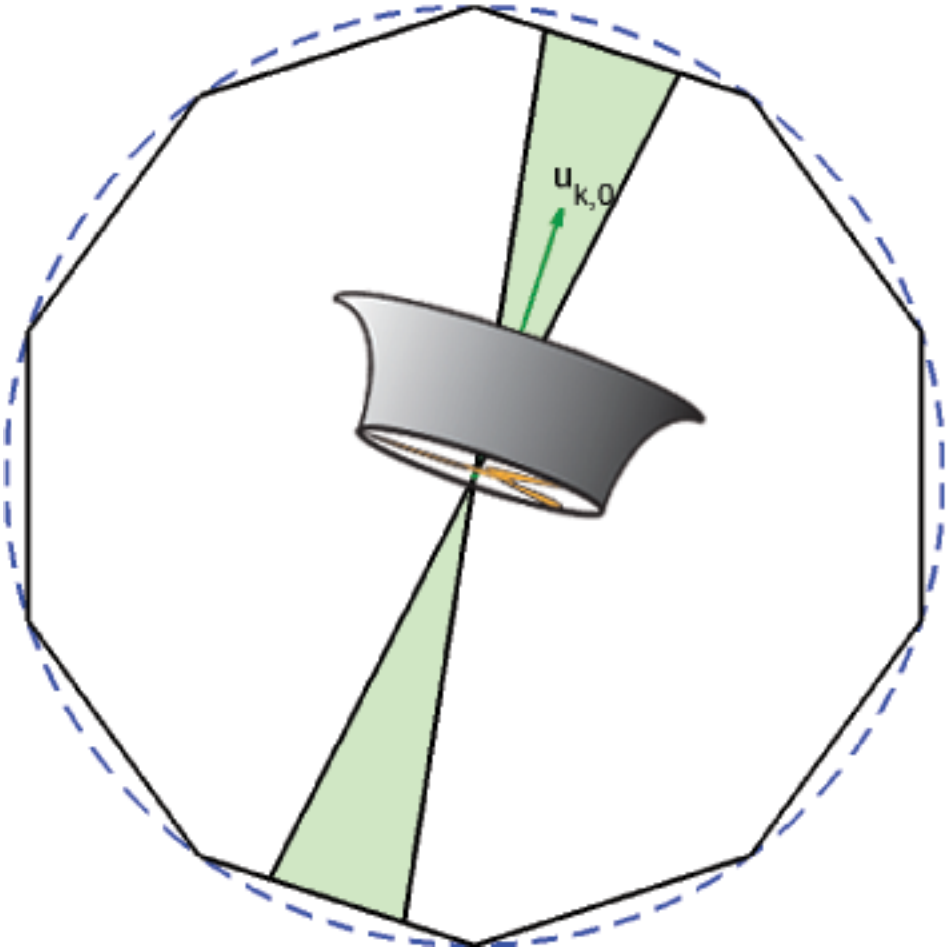

Figure 6.2: An illustration of the constraints on the force that can be produced by an azimuth thruster. The force that was produced by that thruster in the previous iteration is shown as vector $u_{k,0}$. The dashed blue line is the saturation limit and the inscribed polygon is the linear approximation of that region. The light green sectors represent region within which a bidirectional thruster can produce force within the update interval. A unidirectional thruster can only produce force in one direction, which is the opposite of the direction in which it can push water.

6.2.3 Bidirectional thrusters

The sector constraint (6.6) automatically ensures that the corresponding thruster can only generate force in the direction that is opposite to where it is pointing. Some thrusters can reverse their direction by setting negative propeller speed or negative pitch. The constraint (6.6) can be modified to allow negative direction instead of positive by replacing it with

$$-\begin{bmatrix} \sin(\alpha_{-,k}) & -\cos(\alpha_{-,k}) \\ -\sin(\alpha_{+,k}) & \cos(\alpha_{+,k}) \end{bmatrix} u_k \leq 0 \tag{6.7}$$

For some thrusters either the sector constraints, the saturation constraints, or both are not symmetric, and have to be modified accordingly when the thrust is reversed.

A bidirectional thruster has to satisfy either (6.6) or (6.7), and in a special case it can satisfy both. In the simplest implementation, the trust allocation algorithm can be solved for all possible combinations of positive and negative thruster directions. For a configuration with $\overleftrightarrow{p_r}$ bidirectional thrusters this leads to $2^{\overleftrightarrow{p_r}}$ QP problems to be solved at each iteration.

6.2.4 Singularity avoidance

A situation where the thruster system that is constructed to be over-actuated cannot generate significant forces or moments in some directions without first rotating the thrusters is called a singularity situation. When in this situation, the vessel is vulnerable to e.g. rapid changes in the environmental forces, to which it may not be able to respond for a period of a few seconds.

A singularity situation may happen with a thruster system if its unrotable thrusters are not able to avoid this situation alone. Mathematically, the singularity situation is characterized by the thruster configuration matrix B becoming numerically close to being rank deficient.

The singularity avoidance technique that is used in this work is similar to [40]. The algorithm that is presented in that article introduces a penalty for proximity of the current configuration matrix to a singular configuration, as measured by

$$\frac{\varrho}{\epsilon + det(B_\alpha B_\alpha^T)} \tag{6.8}$$

where ϱ is a configurable cost parameter, ϵ is a small positive number that prevents the possibility of division by zero, and B_α is the configuration matrix in polar coordinates, with rows $B_{\alpha,i}$ defined as

$$B_{\alpha,i} = \begin{bmatrix} \cos\alpha_i \\ \sin\alpha_i \\ -l_{yi}\cos\alpha_i + l_{xi}\sin\alpha_i \end{bmatrix} \quad \forall i \in 1 \ldots p \tag{6.9}$$

In this work, by defining

$$\tilde{u}_k = {}^{u_k}/_{\|u_k\|} = \begin{bmatrix} \cos(\alpha_k), & \sin(\alpha_k) \end{bmatrix}^T \tag{6.10}$$

it can be noted that

$$B_\alpha = \begin{bmatrix} B_{\alpha,rotable} & B_{\alpha,unrotable} \end{bmatrix} \tag{6.11}$$

with

$$B_{\alpha,rotable} = \begin{bmatrix} B_{1,1}\tilde{u}_1 + B_{1,2}\tilde{u}_2 & \cdots & B_{1,2p_r-1}\tilde{u}_{2p_r-1} + B_{1,2p_r}\tilde{u}_{2p_r} \\ B_{2,1}\tilde{u}_1 + B_{2,2}\tilde{u}_2 & \cdots & B_{2,2p_r-1}\tilde{u}_{2p_r-1} + B_{2,2p_r}\tilde{u}_{2p_r} \\ B_{3,1}\tilde{u}_1 + B_{3,2}\tilde{u}_2 & \cdots & B_{3,2p_r-1}\tilde{u}_{3p_r-1} + B_{3,2p_r}\tilde{u}_{2p_r} \end{bmatrix} \tag{6.12}$$

$$B_{\alpha,unrotable} = \begin{bmatrix} B_{1,2p_r+1}\tilde{u}_{2p_r+1} & \cdots & B_{1,n}\tilde{u}_n \\ B_{2,2p_r+1}\tilde{u}_{2p_r+1} & \cdots & B_{2,n}\tilde{u}_n \\ B_{3,2p_r+1}\tilde{u}_{2p_r+1} & \cdots & B_{3,n}\tilde{u}_n \end{bmatrix} \tag{6.13}$$

According to Corollary 1 in the Appendix B, the quantity $\sqrt{det(B_\alpha B_\alpha^T)}$ is the volume of the 3-dimensional parallelepiped that is spanned by the row vectors of the matrix B_α, which approaches zero as B_α approaches a rank-deficiency. Thus, the quantity

$$J_{sing}(u) = \frac{\varrho}{\epsilon + det\,(B_\alpha \cdot B_\alpha^T)} \tag{6.14}$$

is a good penalty function for approaching the singularity condition. By linear approximation at the current azimuths the change in cost will be

$$\bar{J}_{sing}(u) = J_{sing}(u_0) + \left.\frac{dJ_{sing}(u)}{du}\right|_{u_o}^{T} \cdot (u - u_0) \tag{6.15}$$

Equation (6.10) assumes that $u_k \neq \mathbf{0}$ even if the magnitude of the thruster force is zero. This can be ensured in an implementation by replacing that magnitude with a nonzero but physically insignificant number, so that the vector u_k always carries the information about the direction of the thruster.

6.2.5 Optimization problem formulation

Collecting the cost and constraint terms from the previous sections and writing it as a standard QP thrust allocation formulation yields

$$\min_{u,s} \quad J(s,u) \tag{6.16}$$

Subject to

$$\tau_c = Bu + s \tag{6.17}$$

$$\pm \begin{bmatrix} \sin(\alpha_{-,k}) & -\cos(\alpha_{-,k}) \\ -\sin(\alpha_{+,k}) & \cos(\alpha_{+,k}) \end{bmatrix} u_k \leq 0 \quad \forall k \leq p_r \tag{6.18}$$

$$A_k u_k \leq 1 \forall k \tag{6.19}$$

where

$$J(s,u) = u^T H u + (u-u_0)^T M(u-u_0) + s^T Q s + \left.\frac{dJ_{sing}(u)}{du}\right|_{u_0} \cdot u \tag{6.20}$$

with positive semidefinite cost matrices H, M and Q of appropriate dimension. For rotable thrusters which are only capable of producing force in the positive direction, the constraint (6.18) has to be satisfied with a positive sign. For thrusters which are capable of producing thrust in both positive and negative direction, the constraint (6.18) has to be satisfied with either positive or negative sign. An instance of the optimization problem can be solved with every possible combination of positive and negative constraints for each applicable k; normally the one with the lowest optimal cost $J^*(s,u)$ should be selected.

The slack vector s is present to ensure that the optimization problem does not become infeasible even if the thruster system is physically unable to produce the generalized force order τ_c. The weight matrix Q should be selected such that the optimal value of s is small unless the problem without s would be infeasible.

The cost function (6.20) also includes a quadratic approximation to the power consumption in the thrusters ($u^T H u$), a penalty for variations in the extended thrust vector that is indended to reduce wear-and-tear in the thrusters $\Big((u-u_0)^T M(u-u_0)\Big)$, and the part of the linearized singularity avoidance penalty (6.15) that is not constant in u.

The output from the optimization problem can be trivially converted to desired thruster forces and angles when applicable (except when u_k for a rotable thruster is 0, then the previous angle can be used). Mapping from the desired thruster force to the RPM setpoint for the frequency converter that feeds that thruster can be done with a model-based controller e.g. [59] or the inverse thrust characteristic.

6.3 Thrust allocation logic

Ideally, repeated iterations of the optimization problem (6.16)–(6.18) will converge the azimuth thrusters to an orientation that is optimal to counteract the environmental forces, possibly with some adjustments due to the singularity avoidance functionality. This does not happen in all situations. Detecting those situations, and implementation of other functionality is often implemented by computer logic that adds or modifies constraints and parameters within the numeric optimization framework. This includes:

- **Turning around bi-directional azimuth** thrusters that are running in reverse over extended periods of time. Although an electrical thruster can quickly revert direction, its propeller is in many cases optimized to push water in one specific direction. Pushing it in the opposite direction is energetically inefficient and also reduces the maximum capacity of the thruster. Turning a thruster around involves having that thruster point in a suboptimal direction over the time interval it takes to turn it around, incurring a significant short-term cost. Taking the decision to turn the thruster effectively means guessing how much the thruster would otherwise be pointing in the

wrong direction in the future, how much it would affect efficiency of the said thruster and if those losses are enough to justify incurring the short-term cost of turning the thruster around. The exact answer depends on random wind variations, how the weather and the sea state continue to evolve and future decisions of the operator. This means that any decision would be inherently heuristic. A simple resolution to this issue is to turn around a thruster that has been running in reverse over a given period of time, or leave it to the operator to issue a reversal request. A more complex algorithm would make a statistical model of the environmental forces and even the operator, similar to applications in the automotive industry such as [51].

- **Crossing the forbidden sectors**. A thruster may not be allowed to push water in certain directions, e.g. into other thrusters, divers, or sensitive equipment. In order to pass a forbidden sector, a thruster may have to be set to zero RPM, which of course leads to a short-term loss of optimality. A heuristic algorithm should consider if this loss of optimality is worth the possible gain from having the thruster point in a more optimal direction in the long run.
- Using the thrust allocation algorithm to **improve the dynamics of the load on the power plant** through additional constraints and cost terms, as is done in [78, 79]. In many cases the power plant is separated into multiple segments. An efficient load distribution between the segments may lead to large reductions in fuel consumption. In [66], this is achieved by modifying the cost parameter H in (6.20) between the iterations of the algorithm depending on how the specific fuel consumption of the generators changes with their load.
- **Allowing the operator additional liberty** with regards to how he or she operates the ship. Operational aspects that are beyond the scope and indeed beyond the concern of the control algorithm designer may be managed by allowing the DP system to control only some of the thrusters,while keeping the rest under manual control or turning them off. In other circumstances, the operator may wish to fix the direction of some of the rotable thrusters, which corresponds to one additional constraint per thruster in the thrust allocation algorithm. Thrust allocation logic usually keeps track of which thrusters are ready to be used, which ones are running, and which ones are actually in use by the dynamic positioning system. Those three parameters may be combined in a number of ways.

6.4 Simulation study

The proposed thrust allocation algorithm was tested in a simulation, on a model of SV Northern Clipper, featured in [24]. It is 76.20 meters long, with a mass of $4.591 \cdot 10^6$ kg. It has four thrusters, with two tunnel thrusters near the bow and two azimuth thrusters at the stern. The maximal force for each thruster was set to $1/60$ of the ship's dry weight. The dynamic positioning control algorithm that was used was a set of three PID controllers.

An explicit symbolic expression for the derivatives of the singularity avoidance cost (6.14) with respect to u was formed using MuPad. The expression is very long, in fact fairly measured by kilobytes. However, profiling demonstrated that on a laptop computer it takes 16 milliseconds to evaluate this expression as a Matlab function handle, and 0.4 milliseconds to evaluate it when it was compiled as a C function. This expression is a function of the extended thrust vector from the previous iteration (u_0) so it only has to be evaluated once for each iteration of the thrust allocation algorithm. The complexity of this expression is therefore not a hindrance against real-time implementation of the thrust allocation algorithm.

The system was implemented in Matlab/Simulink with Bis normalization system per e.g. [25, Section 7.2.5]. The simulated ship starts at $1/5$ of the ship's length away from the setpoint location, and 10 degrees off the setpoint heading. The simulation results are shown in Figures 6.3–6.7. The starting configuration is singular, with all the thrusters pointing towards the starboard. In the first few seconds this leads to the thrusters being driven to saturation, as can be seen in Figure 6.4, while a significant deviation from the commanded generalized force is nevertheless observed (Figure 6.7). This situation illustrates the vulnerability that singular configurations represent – the thruster system may not be physically able to comply with the generalized force order. This problem is most severe in situations in which the direction of the generalized force order may change abruptly.

In steady-state conditions without the singularity avoidance term, it is optimal to have all the rotable thrusters point in the direction of the environmental load. The simulated vessel has only two fixed thrusters. They are located close to each other and they point in the same direction. So for this ship, any configuration in which the rotable thrusters point in the same direction as well (not necessarily the same direction as the fixed thrusters) is singular. However, because of the singularity avoidance term, after a transition – which involves rotation of the azimuth thrusters and positioning of the vessel at the setpoint – the azimuth thrusters converge to 153 and -5 degrees, leading to a slight bias with 22 degrees difference between the azimuth angles and therefore a non-singular configuration.

6.5 Conclusion and future work

A workable thrust allocation algorithm that is a good basis for a practical implementation has been presented and tested in simulation. It is the assertion of the authors that this algorithm can be used on realistic vessels without significant modifications.

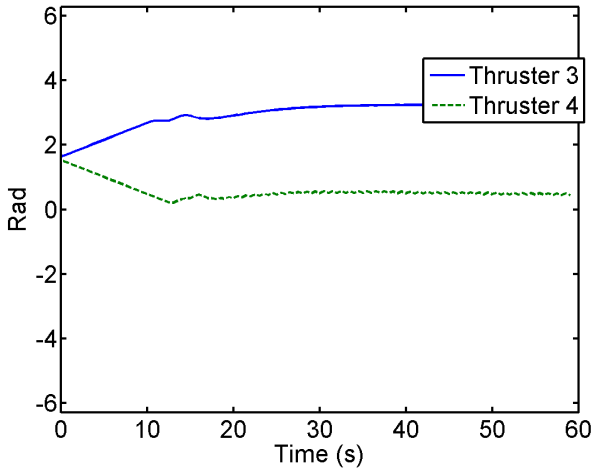

Figure 6.3: Angles of the azimuth thrusters

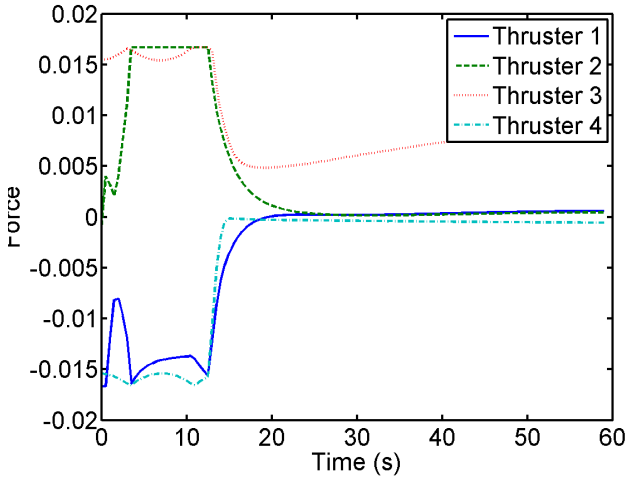

Figure 6.4: Forces from the individual thrusters

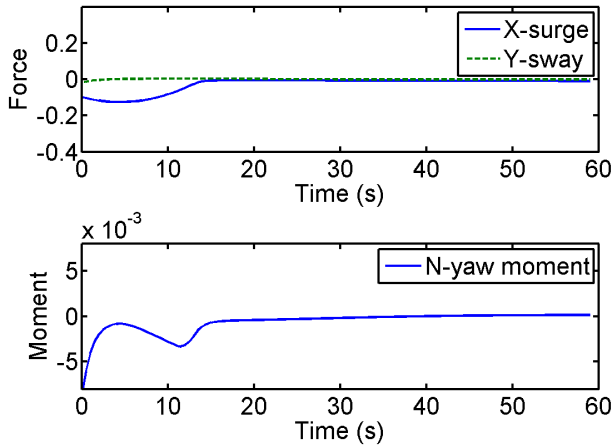

Figure 6.5: Commanded generalized force

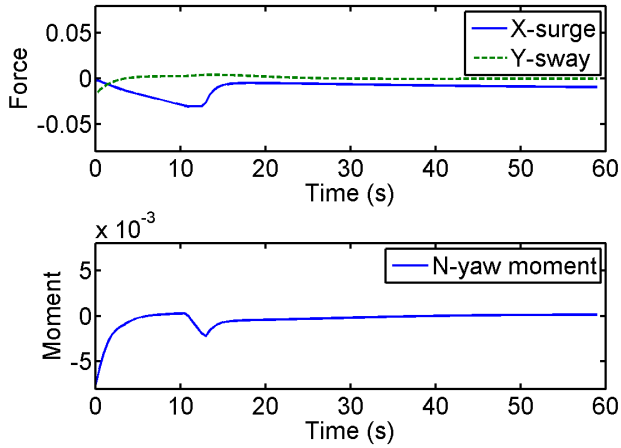

Figure 6.6: Produced resultant generalized force

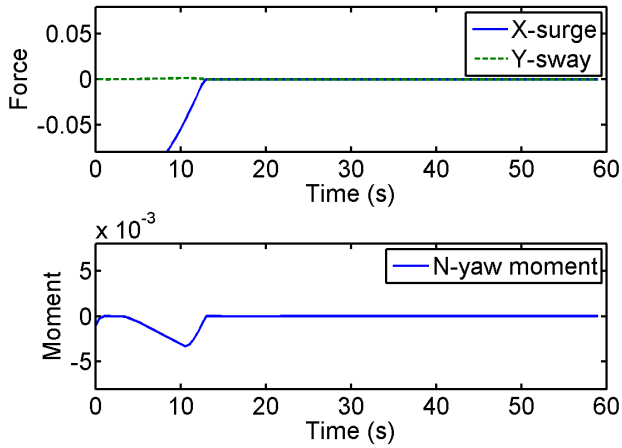

Figure 6.7: The deviation between the produced and the commanded generalized force

Chapter 7

Dynamic positioning with model predictive control

7.1 Introduction

A marine vessel is said to have dynamic positioning (DP) capability if it is able to maintain a predetermined position and heading automatically exclusively by means of thruster force [4]. DP is therefore an alternative, and sometimes a supplement to the more traditional solution of anchoring a ship to the seabed. The advantages of positioning a ship with the thrusters instead of anchoring it include:

- Immediate position acquiring and re-acquiring. A position setpoint change can usually be done with a setpoint change from the operator station, whereas a significant position change for an anchored vessel would require repositioning the anchors.
- Anchors can operate on depths of only up to about 500 meters. No such limitations are present with dynamic positioning.
- No risk of damage to seabed infrastructure and risers, which allows safe and flexible operation in crowded offshore production fields.
- Accurate control of position and heading.

The main disadvantages are that a ship has to be specifically equipped to operate in DP, and that dynamically positioned ships consume more power to stay in position, even though anchored vessels also have to expend energy to continuously adjust the tension in the mooring lines.

DP is usually installed on offshore service vessels, on drill rigs, and now increasingly on production platforms that are intended to operate on locations that are so deep that permanent attachment to the sea floor with e.g. mooring lines is impractical. Several thousand ships worldwide have dynamic positioning installed.

Depending on its function, a DP vessel that fails to keep its position may risk colliding with other vessels, endanger divers, interrupt operations and/or cause damage to equipment such as risers. Vessels that are designed to perform reliably typically have a high degree of redundancy in all critical systems, including power generation, thrusters and the computer system. Classification societies such as DNV

GL and International Maritime Organization (IMO) issue standards that include safety regulations for the DP systems. For example, to be classified as a IMO Class 2, the DP system has to be designed with redundancies in the power distribution system, power generation, thruster system and many others; in particular, the thruster system must continue to be fully capable after failure of any single thruster.

The algorithm that coordinates the thrusters to keep a setpoint position and orientation is called the dynamic positioning algorithm. A commonality for most control algorithms that are available in the literature is that they separate the control task into two parts. First, a high-level motion control algorithm considers the current position and heading of the ship, and determines the total force and moment of force (together called "generalized force", further explained in Appendix A) that needs to be applied on the ship. Somewhat ambiguously, this algorithm is usually called the DP control algorithm. After the generalized force is calculated by the motion control algorithm it is passed as an input to a lower-level thrust allocation algorithm, which determines the directions and magnitudes of the forces that the individual thrusters should produce. The main goal of the thrust allocation algorithm is to ensure that the total generalized force that the thrusters generate matches the commanded output from the high-level motion control algorithm. The output from the thrust allocation algorithm is then sent to the local thruster controllers. The local controllers often have load rate limiting functionality to ensure that the load from the thrusters don't increase so fast that the power plant ends in blackout. A functionality to limit the thruster torque is usually also present.

Achieving the dynamic positioning task may be trivial if the environmental conditions are favorable, positional precision requirements are leisurely and the operator is not too concerned about costs such as fuel and wear-and-tear of the machinery. For the high-level motion controller, one can use three independent PID controllers one for each degree of freedom, and a simplistic thrust allocation algorithm as described in Subsection 7.2.2.

More advanced algorithms aim to have faster position acquiring and recovery, less rapid variation in the thruster commands, handling of variable-direction thrusters, better handling of thruster limitations, etc. Several well-functioning algorithms for the high-level motion control are known, many of them are described in [25, Subsection 12.2]. Also, in [34], the high-level motion control is implemented as an MPC algorithm, resulting in a controller that combines use of leisurely control effort as long as it is sufficient to keep the vessel within a predefined operational area, and more aggressive control effort when dynamic simulations show that the vessel would leave the operational area otherwise; the task of allocating the force order to the individual thrusters is in that implementation left with a classical thrust allocation algorithm. A similar MPC-based high-level motion controller was discussed in [16], although without simulating disturbances or including constraints on the position of the vessel [8], [40], [42].

Thrust allocation remains an active field of research. The most recent trends are towards integration and increased information passing between the thrust allocation and other systems on the ship. In [65], a thrust allocation method that balances how much the thrusters load the different parts of the power plant to reduce the NOx production of the power plant. Using thrust allocation to reduce the load variations on the power plant has been explored in e.g. [56, 78, 79]. Also

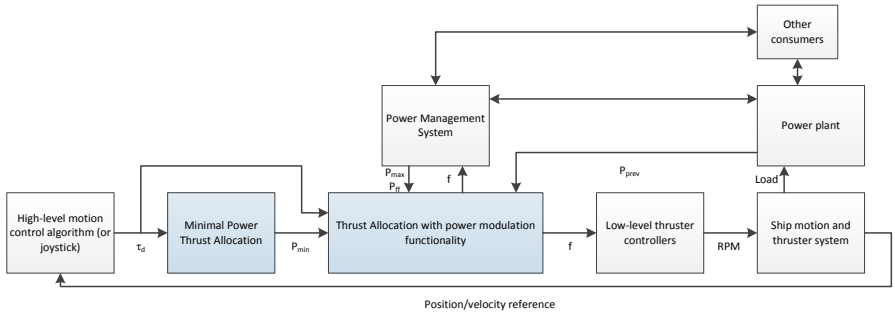

Figure 7.1: The architecture of the feedback loop from the position and velocity reference to the thruster commands for a ship equipped with DP. The classical architecture is to the left, the newly-suggested architecture is to the right.

notably, in [62] the local thruster control was modified to achieve the same purpose, thus bypassing the thrust allocation algorithm. A recent review of the state of the art thrust allocation is available in [39].

The separation into a high-level motion control algorithm and a thrust allocation algorithm has the advantage that it results in a segmentized software architecture. However, since the high-level motion control algorithm does not consider thruster effects such as saturations, asymmetric energy consumption, reconfiguration time (azimuths and rudders), the generalized force command it produces must necessarily be sub-optimal. Industrial implementations usually perform heuristic adaptions to reduce the impact of those suboptimalities, allowing information to pass back from the thrust allocation algorithm to the high-level motion control algorithm. To an extent, this blurs the separation between the algorithms. It usually results in performance that approaches optimal, but at the cost of a large engineering effort and complicated tuning.

A control strategy that simulates the future behavior of the system it controls, and based on the simulation results attempts to find a control output that makes the (simulated) system behave optimally is called "Model Predictive Control", or MPC; the optimal behavior is typically defined as the one that minimizes a specified metric, for example the energy consumption by the actuators, the average distance from the setpoint or a weighed combination thereof. In some cases, the output of the MPC can be calculated with an explicit algebraic expression, but often finding it requires a large number – sometimes millions – of possible scenarios to be evaluated. Introductory texts on MPC are available in e.g. [57, 64]. Continuing expansion of MPC to new applications is made possible by increasingly faster computer hardware, as well as more efficient and user-friendly software design tools [6, 33, 45, 85]. For example, [7, 9, 29, 80] explore control of a diesel-electric power plant with MPC, and MPC has also been used to realize dynamic control allocation [28, 53]. In many of those applications, MPC would earlier be considered to be unimplementable in real time, or too complex to design and maintain.

In light of these developments it is natural to consider controlling a ship by dynamic positioning with a model predictive control algorithm with a sufficiently long horizon, controlling the thrusters directly without a separate thrust allocation algorithm. This architecture is illustrated to the right in Figure 7.1. The expected advantages are:

- More consistent constraint handling. Implementing a high-level motion control algorithm that takes the dynamic thruster capabilities into account is possible with MPC.
- Planning ahead. Even with a reasonably short horizon an MPC can plan ahead maneuvers instead of going towards the goal in the most direct manner possible. Such maneuvers include moving the vessel towards the setpoint along a trajectory that is optimal and coordinated with respect to the saturation limits of the thrusters, as well as their direction and rate of turn where this is applicable. If the MPC is implemented with a sufficiently long horizon, it may be able to escape from local minima, such as situations where a bidirectional thrusters are acting in a direction where they are suboptimal.
- Simpler design and tuning. Since the model predictive control resolves a number of idiosyncrasies that require complex adaptions with the traditional architectures automatically, the engineering effort that is required to design the controller, is also expected to be smaller.

The advantages listed in the first two bullet points result mainly result in reduced power consumption and reduced position deviation in situations with limited thrust and power. The third one result in reduced development cost and faster time-to-market; the time spent configuring the DP system on-site may also be reduced, although it is usually possible to do most of the configuration work off-site with hardware-in-the-loop simulation[41].

The goal of this paper is to explore the advantages and implementability MPC through computer simulation to determine if the technology is viable for implementation.

The mathematical model that is used for forecasting is described in Section 7.2, and the MPC problem is formulated and discussed in Section 7.3. Its implementation as a computer program is discussed in Section 7.4. The proposed MPC controller was tested in simulation, and the results from four simulation scenarios are presented in Section 7.5. A glossary of some of the more important terms can be found in Appendix A.

7.2 Brief introduction to modeling of marine vessels

This section provides a basic explanation of the model that is used to implement the model predictive control in this work.

7.2.1 Geometry and kinematics

The investigation that is presented here deals with a ship that moves on the ocean surface at relatively low velocities. The roll and pitch motions of the vessel are

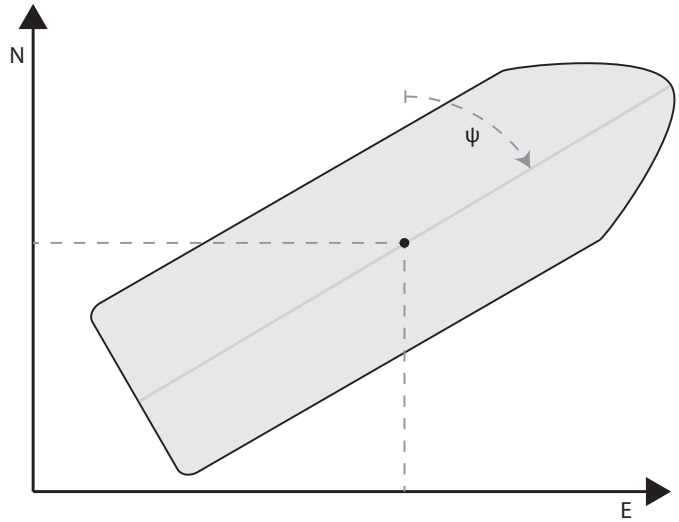

(a) The position of the vessel is defined in the NED coordinate system.

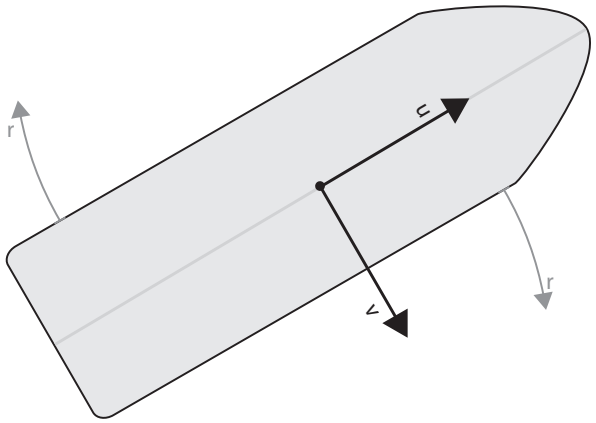

(b) The velocity is defined in the body coordinate system.

Figure 7.2: Coordinate systems.

neither monitored nor compensated. The mathematical model that is used to describe the system can therefore be kept reasonably simple by limiting it to the planar position and orientation of the vessel. A coordinate system is selected with the origin at the DP setpoint, x-axis pointing to North, y-axis pointing to East, and the (unused) z-axis pointing downwards per the right-hand rule. The orientation of the ship in the xy-plane is defined as clockwise rotation with the orientation with the bow pointing to the North as the zero reference.

The velocity of the vessel is usually described in its own frame of reference, in what is called the "body" coordinate system. The forward velocity u in the direction of the bow, sideways velocity v towards the starboard and the clockwise yaw rotation rate r. The abbreviations that are used to describe the position and the velocity of the vessel are presented in Table 7.2 and in Figure 7.2. The relationship between them is purely geometric, and is specified by

$$\dot{\eta} = \underbrace{\begin{bmatrix} \cos(\psi) & \sin(\psi) & 0 \\ -\sin(\psi) & \cos(\psi) & 0 \\ 0 & 0 & 1 \end{bmatrix}}_{P(\psi)} \nu \tag{7.1}$$

Note that $P(\psi)P(\psi)^T = I$.

7.2.2 Dynamics

The forces and torques (taken together they are called "generalized force"[26]) from several physical sources act on the vessel. The resultant effect of those forces is equal to their vector sum; the same applies to the torques as long as they are expressed with the same pivot point. The control force is generated by the thrusters.

Abbreviation	Description
$f \in \mathbb{R}^{Nthrusters}$	The thrust vector describing the forces produced by each thruster that is installed on the ship, with f_i being the force produced by thruster i.
$r_i = \begin{bmatrix} l_{i,x} & l_{i,y} \end{bmatrix}^T$	The location of the thruster device with index i
$\alpha \in \mathbb{R}^{Nthrusters}$	The directions in which the thrusters are pointing, with α_i being the direction of thruster i; $a_i = 0$ means that the thruster i is pointing backward and is generating the force forward unless reversed..
$\tau \in \mathbb{R}^3$	The resultant generalized force produced by all thrusters on the vessel
$T(\alpha) \in \mathbb{R}^{3 \times Nthrusters}$	Thruster effect matrix. The linear operation $T(\alpha)f$ calculates and sums up the general forces produced by the individual thrusters.

Table 7.1: Location and orientation of the thrusters, and the forces they produce on the ship.

Abbreviation	Description
$\eta = \begin{bmatrix} N & E & \psi \end{bmatrix}^T \in \mathbb{R}^3$	Position and orientation of the vessel in an inertial frame of reference, in this case North-East-Down
$\nu = \begin{bmatrix} u & v & r \end{bmatrix}^T \in \mathbb{R}^3$	Velocity of the vessel in its own (body) frame of reference, expressed at the end point of the vector $\begin{bmatrix} N & E \end{bmatrix}^T$

Table 7.2: Abbreviations that are used to describe the position and velocity of the vessel, as per convention from [1] and [25, especially p. 19].

Other forces that act on the ship include hydrodynamic drag, waves and wind. As mentioned above, the velocity and angular rotation speed are expressed in a frame of reference that is bound to the ship. This frame of reference may be rotating, which means that it is not inertial. The equations of motion in a rotating frame of reference normally have to include corrective terms for Coriolis and centripetal pseudo forces. If the rate of yaw rotation is modest however, these terms may reasonably be disregarded, as will be done in this treatment. For low speeds a linearization of the hydrodynamic drag is also reasonable.

Any acceleration of an object moving through a fluid requires that the surrounding fluid is also accelerated to move out of the way of the object. This creates a force on the object that is proportional to acceleration of the object. Mathematically, this effect is equivalent to an increase of the mass of the object [86, p. 567], and it is usually called "added mass" in hydrodynamic modeling. Unlike the physical mass, added mass is not symmetric, and for ships it is typically larger in the lateral direction than in the longitudinal direction. It can be shown that the resulting equations of motions can be represented in vector form as

$$M\dot{\nu} + D\nu = \tau + P^T(\psi)\tau_{env} \tag{7.2}$$

where $M \in \mathbb{R}^{3\times3}$ is the generalized mass matrix and represents the sum of the physical mass and the hydrodynamic added mass. The drag approximation $D\nu$ is conventionally placed on the left side of this equation, changing the signs of the elements of D accordingly.

The thruster forces are represented by τ. The environmental forces that are not included in $M\dot{\nu}$ or $D\nu$ are collected in τ_{env}. Those are the forces due to current, high- and low-frequency components of the wind and wave forces, and the wind. The formulation in (7.2) implies that τ_{env} is expressed in the NED coordinate system, which is of course a matter of convenience.

Counteracting those forces doesn't always require measuring them. The current force and the low-frequency components of the wave forces can be handled by the integral action in the DP control algorithm; it will also to some extent compensate for the actual thruster forces being different from what is modeled (ref. Subsection 7.2.2). Typically, it is not necessary to compensate for the high-frequency components of the wave forces, since they are essentially rock the boat back and forth. Those motions are usually discarded by a wave filter (ref Appendix A) before the

position measurement is sent to the DP system. The wind forces are usually estimated with wind sensors; theoretically, this can be done fairly accurately, but the practitioners often encount complications due to the difficult geometry of typical ships and local variations in the wind speed.

Resultant thruster force calculations

A thruster that is located at r_i relative to the origin of a common coordinate system, generating force f_i at an angle α_i clockwise from the forward direction (ref Table 7.1) will generate a generalized force

$$\tau_i = \begin{bmatrix} \cos(\alpha_i) \\ \sin(\alpha_i) \\ -l_{yi}\cos(\alpha_i) + l_{xi}\sin(\alpha_i) \end{bmatrix} f_i \tag{7.3}$$

The resultant generalized force from all the thrusters can be represented as

$$\tau = T(\alpha) f \tag{7.4}$$

where the columns of $T(\alpha) \in \mathbb{R}^{3\times Nthrusters}$ are of the form (7.3). A very simple thrust allocation algorithm can be implemented by Moore-Penrose pseudo-inverting $T(\alpha)$, calculating the force commands f per

$$f = \underbrace{\left(T(\alpha)T^T(\alpha)\right)^{-1} T^T(\alpha)}_{T^+(\alpha)} \tau \tag{7.5}$$

This algorithm does not consider thruster saturations or azimuth changes, so the algorithms in practical use are normally more advanced[39].

Relationship between generated force, RPM, and power consumption of the thrusters

Dimensional analysis of a propeller in free water (i.e. far from a ship hull or other obstructions and disturbances) combined with a few other hydrodynamical assumptions lead to a model where both the thrust and the torque produced by a propeller which is stationary in water are proportional to the square of the speed of rotation of the propeller [77, p. 145].

The power that is required to keep the propeller at a constant speed of rotation is the torque times the speed of rotation, which means that it is reasonable to assume that the power required to drive a propeller is proportional to the force it produces to the power of 3/2. This approximation is used in many cases, such as [39, 78, 79], while in the following we use quadratic force penalties instead of minimizing power consumption.

In this work, the actual force that is produced by the thrusters is assumed to be the controlled variable. This assumption implies that the local thruster controllers can accept a force setpoint [59].

7.3 MPC formulation

The following continuous-time numerical optimization formulation summarizes the discussion in the previous section, and is proposed as a basis for the model predictive control of the dynamical system:

$$J^* = \min_{f^+, f^-, \dot{\alpha}} \int_0^{T_e} \Big\{ \left\| f^+ \right\|^2_{Q_{f+}} + \left\| f^- \right\|^2_{Q_{f-}} + \left\| \dot{\alpha} \right\|^2_{Q_\alpha} + \\ + \left\| \nu \right\|^2_{Q_\nu} + \left\| \eta \right\|^2_{Q_\eta} + \left\| \int_0^{T_e} \eta dt \right\|^2_{Q_{\int \eta}} \Big\} dt \\ + \text{similar terminal costs} \tag{7.6}$$

subject to

$$T(\alpha) f^+ - T(\alpha) f^- = \tau \tag{7.7}$$

$$0 \leq \begin{bmatrix} f^+, & f^- \end{bmatrix}^T \leq \begin{bmatrix} \bar{f}, & \underline{f} \end{bmatrix}^T \tag{7.8}$$

$$|\dot{\alpha}| \leq \dot{\bar{\alpha}} \tag{7.9}$$

$$M\dot{\nu} + D\nu = \tau - P(\psi)^T \tau_{env} \tag{7.10}$$

$$P(\psi)\nu = \dot{\eta} \tag{7.11}$$

$$\text{Initial conditions on } \eta, \nu, \alpha \tag{7.12}$$

$$\tau(T_e) = \tau_{env}(T_e) \tag{7.13}$$

Implementation of this problem as a computer algorithm is explained in Section 7.4. The thruster system constraint (7.7) is based on (7.4), but it is separated into a positive and a negative term to accomodate assymmetric thrusters. Asymmetric thrusters are designed for maximal efficiency in one direction, and are less efficient when running in reverse. The cost associated with running them in reverse is for this reason higher, and usually the maximal attainable thrust is lower.

The rate of change of the vector of azimuth angles for the variable-angle thrusters α is limited in (7.9) because some thrusters such as azumuth thrusters and rudderes cannot change their direction very quickly. The maximum rate of rotation varies, but is typically on the scale of 30 seconds for a 360 degree turn.

With traditional thrust allocation algorithms, a slack term is often necessary in (7.7) to make sure that the allocation problem is feasible even if a thrust command cannot be achieved. In this case, this term is not necessary, since τ represents the actual generalized force on the vessel, and not a setpoint command as with the traditional thrust algorithms.

The constraint (7.8) limits the force produced by the individual thrusters. Not all thrusters can produce force in negative direction, and some thrusters can produce more force in positive direction than in negative, so the values of $\overline{f}$ and $\underline{f}$ have to be set accordingly.

The constraints (7.10)–(7.11) are the dynamic and kinematic constraints of the ship, and are a vector form formulation of the Newtonian laws of motion for the system as discussed in Section 7.2. Environmental generalized force τ_{env} represents

the resultant of the various environmental forces such as wind, currents, waves, moorings, anchors, risers, cables (cable lay), pipes (pipe lay), hoses (offloading), sea ice, etc. Typically, the high-frequency component of the wave forces are filtered out of the model. The value of τ_{env} at the initial time can be estimated with a combination of direct measurment with e.g. wind sensors and model-based observers; the latter is mathematically equivalent to the integral action in a traditional PID controller. The future values of τ_{env} can of course not be known, which is one of the factors that limit the forecasting power of the model. This will be further discussed in Subsection 7.3.2.

The terminal costs represent how good the system state is at the end of the horizon. They can also be seen as a representation of the costs that will be incurred after the optimization horizon. The only terminal costs that were found to be necessary in the tested models are the cost associated with the the generalized position η and the cost associated with its integral. Without the terminal constraint (7.13), the optimizer will decide to turn off the thrusters at the end of the optimization horizon simply to save the fuel costs, capitalizing on the fact that the resulting drift-off lags after the thrusters turn off, which fall after the end of the intergration interval of (7.6).

The DP setpoint is set to the origin of the NED coordinate system without loss of generality.

7.3.1 Turning the thrusters around

A complication with the standard control architecture for dynamic positioning is that the thrust allocation problem is often non-convex. In practice, this means that a thruster may end up stuck in a direction where it either has to produce thrust in reverse of its optimal direction ($f^- > 0$), or, in case of unidirectional thrusters, a direction where it cannot produce any thrust that can be useful. A standard solution to this is having an exogenous algorithm evaluate the situation, and turn the thrusters around if this is considered beneficial. Other sources of non-singularity are forbidden sectors and the use of rudders [39, 42].

An MPC formulation with a horizon that is as long as the turn-around time for the thrusters could automatically consider if the thrusters should be turned or not. Care should be taken that either numerical solver can reliably find non-local minima, or, as in case with the test implementation in Section 7.4, that the numerical solver is provided with an approximate direction for where to look by means of an appropriate warm-start trajectory.

The transition of the thrusters incurs a short-term cost, and unless the horizon is significantly longer than the turn-around time, the majority of the benifit of turning the thrusters is seen in the (reduction of the) terminal costs. Care should therefore be taken during tuning to ensure that the terminal costs correctly reflect the long-term advantage of having a thruster point in the right direction.

7.3.2 Modeling simplifications and predictability

The MPC solver simulates the expected behavior of the vessel and calculates the thruster commands that result in a behavior of the ship that is optimal based on

specified criteria. In general, the quality of MPC increases with the length of the prediction horizon. However, the stochastic nature of the marine environment limits the predictive power of any possible mathematical model. The predictive power is certainly not improved by the approximations that are made during the model design in Section 7.2. The constraint (7.10) requires an estimate of the environmental forces τ_{env} until the end of the simulation horizon T_e; this estimate naturally degrades with increased length of T_e. It is therefore unreasonable to expect that the forecasting made by the model predictive control is a close approximation of the actual behavior of the ship.

Extending the prediction horizon T_e beyond a few seconds is therefore not necessarily better than other heuristic adaptions.

7.4 Implementation

In this section, the implementation of the continuous-time MPC formulation (7.6)–(7.13) as a computer program will be discussed.

The MPC problem formulation includes the continuous-time constraints (7.9)–(7.11) that describe the physical laws of the system. If the state variables α, ν and η and the control outputs f^+, f^- and $\dot{\alpha}$ satisfy those constraints, then they represent a possible trajectory of the system – in this case a possible scenario for the movement of the vessel. The constraint (7.12) ensures that this trajectory is in fact a possible future trajectory of the vessel by matching the initial values of α, ν and η to the current state of the physical system.

Every possible future trajectory has a cost associated with it which is described by (7.6). There are costs associated with the use of thruster force, rotating the thrusters, and with position and velocity deviations from the setpoint. *A global solution of this problem is a possible trajectory for the states and control outputs that minimizes (7.6).* Because of computational limitations, this cost is only evaluated for a limited time, until T_e.

The continuous-time formulation has to be discretized to be solved on a digital computer. In a discrete-time representation, the continuous-time trajectories of variables such as position of the ship and thruster forces are represented by a (finite) number of discrete samples; the continuous-time constraints should then be replaced with a finite number of equality constraints between the samples. For example, with a prediction horizon of 45 seconds and discretization interval of 0.5 seconds, there will be 90 discrete variables representing each (schalar) continuous variable. By doing this for each state and input, it is possible to represent (7.6)–(7.13) as a – typically very large – numerical optimization problem; several algorithms are available to solve such problems, both open-source and commercial.

Software packages that are capable of handling discrete- or continuous-time MPC formulations also exist. Typically, they will also automatically hand off the resulting discrete-time numerical optimization problem to a solver. The package that was selected for this project is called BLOM, which stands for Berkeley Library for Optimization Modeling. It is desgined to assist in rapid implemention of model predictive control by providing a graphical interface to allow users to create optimization problems using Simulink. Using such package allows significant time

Unit	Normalization variable	Numerical value
Length/Position	L	76.20 m
Force	Mg	$4.507 \cdot 10^7$ kg $\cdot$ m/s^2
Moment	MgL	$3.4342 \cdot 10^9$ kg $\cdot$ m $\cdot$ m/s^2

Table 7.3: Relevant bis normalization constants [25, table 7.2].

Figure 7.3: Thruster layout of the simulated vessel, with two tunnel thrusters near the bow two rotable azimuth thrusters at the stern. The thruster numbers are shown.

savings compared to tranforming the model into a numerical optimization problem, and graphical design usually means faster and less error-prone implementation implementation.

BLOM has a capability to handle discretization automatically, but in this implementation the model was discretized "by hand" with Forward Euler discretization scheme.

7.5 Simulation results

The proposed thrust allocation algorithm was tested in simulation, on a model of SV Northern Clipper, featured in [24]. It is 76.20 m long, with a mass of $4.591 \cdot 10^6$ kg. It has four thrusters, with two tunnel thrusters near the bow and two azimuth thrusters at the stern. This configuration is illustrated in Figure 7.3. The maximal force for each thruster was set to $1/60$ of the ship's dry weight. The turnaround time for the thrusters was set to relatively slow 60 seconds, and the prediction horizon T_e in the MPC formulation was set to 45 seconds in all simulations except the last one, where it was set to 10 seconds to demonstrate the effects of a short prediction horizon. All the thrusters are bi-directional; the tunnel thrusters in the bow are symmetric, while the azimuth thrusters use twice as much power to produce force in reverse compared to their normal direction. It was implemented in discrete-time in BLOM, using a forward Euler discretization with 0.5 seconds discretization interval.

The environmental forces were set to be a constant wind in the direction towards North. All numerical values were transfered to per-unit in bis system per Table 7.3. The performance of the algorithm is compared to a baseline algorithm with a standard architecture with a separate DP control algorithm and a TA algorithm;

it is based on elements from several available publications on the topic, and it is described in detail in Chapter 6.

Four simulations are reported. The first two simulations start off 0.2 ship lengths in surge from the setpoint, and no deviation in either sway or yaw. In some cases this results in motion of the vessel being mostly limited to one dimension, which makes it easier to distinguish the various patterns in the movement of the ship. The third and the fourth simulation starts with the ship having a 10 deg deviation in heading, in addition to the deviation in surge, resulting in a more complex scenario.

First scenario

The first simulation is a deliberate worst-case scenario for the classical controller. Both azimuth thrusters point towards the starboard, resulting in a singular thruster configuration. At the start, there is no way for the thruster system to create force in the longituidal direction where it is needed. The results are shown in Figures 7.4–7.7. The classical motion control immediately drives the thrusters to saturation, forcing them to act against one another without producing much force in total. The MPC-based controller does not command the thrusters to use significant forces until they have had the time to turn so that they can produce significant force in the direction where it is needed. In fact, the MPC controller *also turns the ship* to allow some use of the the bow thrusters, which would otherwise remain perpendicular to the direction where force is needed and therefore almost useless. The maximal deviation is 0.41 rad. Such behavior is desirable in many situations while in others it is essential to maintain the heading of the ship. In the second and the third configurations, the cost associated with deviation in yaw is set to be much larger, so the resulting wandering in yaw is much smaller.

As can be seen in Figure 7.5, the MPC formulation leaves the system with both the azimuth thrusters pointing in the right direction against the environment, while in the classical formulation only one thruster, number 3, does that. In the latter situation it is optimal to use thruster 3 to produce most of the force that is required to hold the ship against the wind, while the other thrusters are only used to keep the ship from turning in yaw, which is needed because thruster 3 is slightly off-center. The thruster force asymptotically approaches 0.009 bis (it does not have quite enough time to fully converge within the time frame that is included in the figure), while with MPC the two thrusters converge to producing about 0.005 bis each. As mentioned in Subsection 7.2.2, the power consumption can reasonably be approximated to be proportional to the produced force to the power of $3/2$, so the power consumption for thruster 3 is approximately $\left(\frac{0.009}{0.005}\right)^{3/2}/2 = 1.21$ times greater than the power consumed by the two thrusters controlled by the MPC algorithm. The total force produced by the thruster system is in both cases very close to the environmental force.

Second scenario

The second simulation scenario was set up so that a thruster turnaround was advantageous assuming that the environmental forces remain constant, specifically by initially pointing the azimuth thrusters in the same direction as the environ-

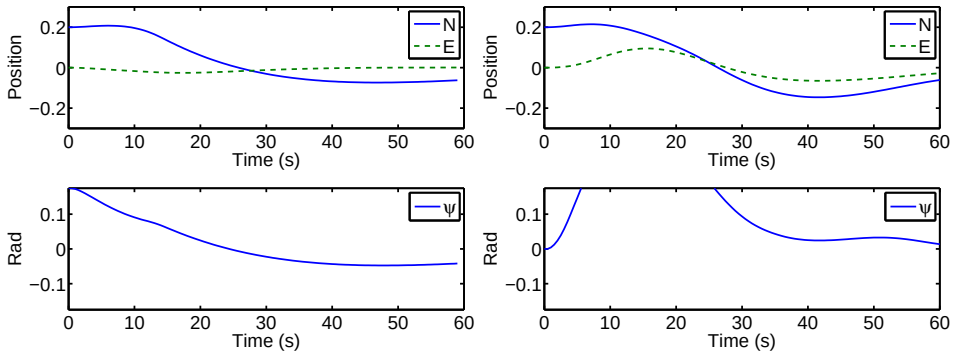

(a) Baseline (b) MPC

Figure 7.4: *First scenario:* position of the vessel.

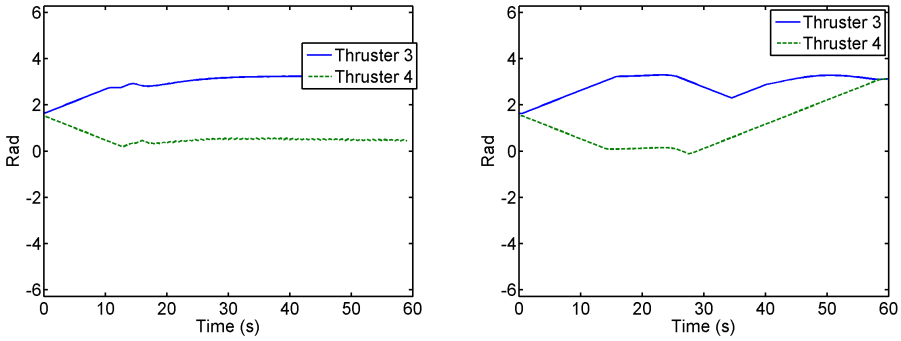

(a) Baseline (b) MPC

Figure 7.5: *First scenario:* azimuth thruster angles.

mental force. The baseline controller gets locked in negative direction, while the MPC-based one successfully turns around the thrusters, as can be seen in Figures 7.8–7.10. Unlike in the first simulation, the heading remains close to constant in this case because of increased penalty for heading deviation.

Third scenario

The third scenario is presented in Figures 7.11–7.14. It is more realistic, starting with the thrusters pointing towards the center line of the ship, exactly as illustrated in Figure 7.3. The resulting configuration is well-actuated, but, again, the azimuth thrusters point in a direction where they have to act in reverse to counteract the wind force. The MPC controller responds by first aligning the azimuth thrusters towards the center line to bring the vessel close to the setpoint as fast as possible, and when it is well underway about 10 seconds into the simulation,

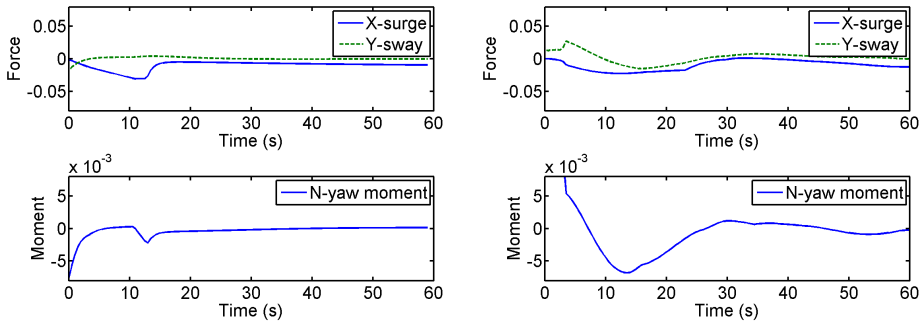

(a) Baseline (b) MPC

Figure 7.6: *First scenario:* total forces.

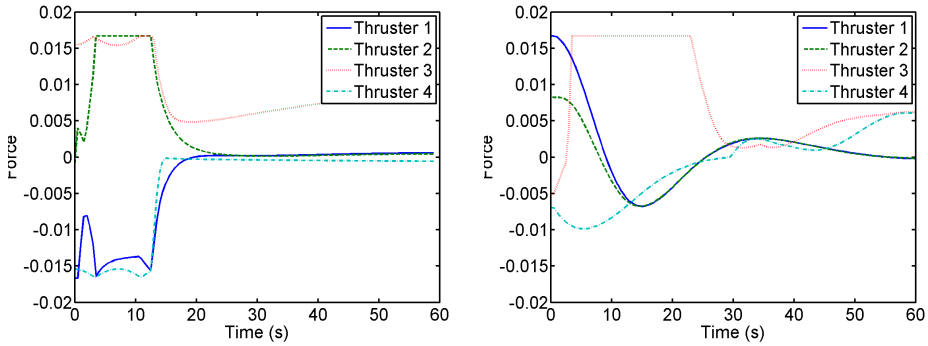

(a) Baseline (b) MPC

Figure 7.7: *First scenario:* thruster forces.

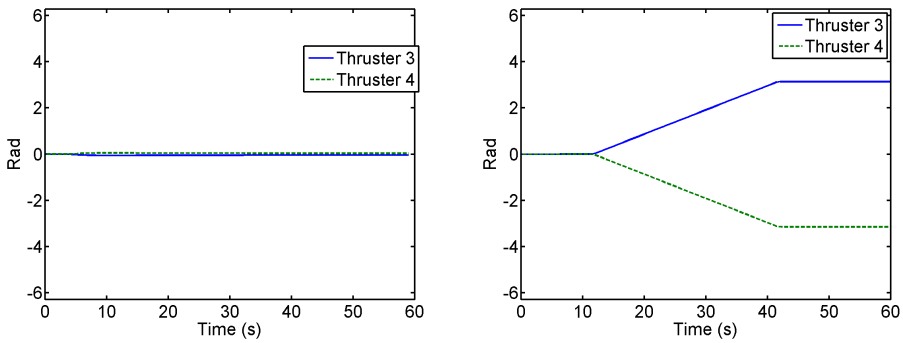

(a) Baseline (b) MPC

Figure 7.8: *Second scenario:* angles of the azimuth thrusters.

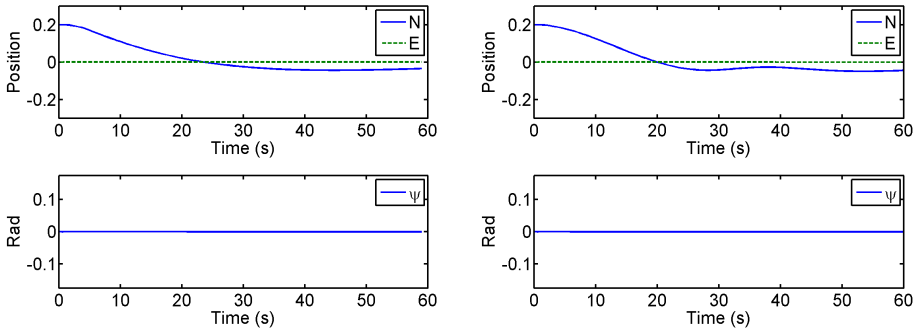

(a) Baseline (b) MPC

Figure 7.9: *Second scenario:* position of the ship.

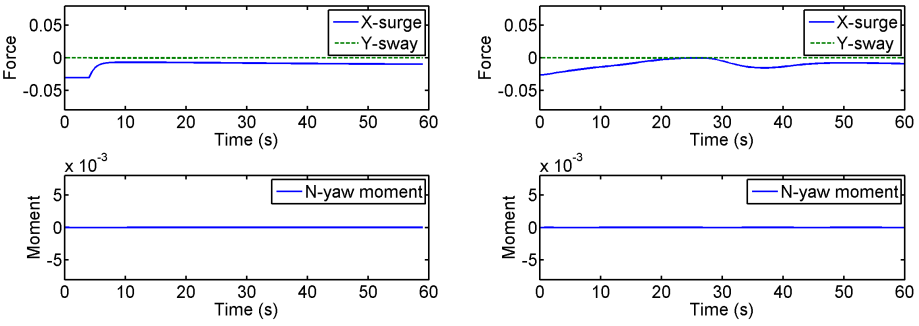

(a) Baseline (b) MPC

Figure 7.10: *Second scenario:* resultant force in the ship.

it starts the procedure of turning the azimuth thrusters around – a procedure it carefully coordinates with the position and velocity of the ship. The result is that at the end of the simulation the thrusters point in the right direction – with the classical controller they continue working in reverse, which requires usually requires much higher power consumption (twice of that in the forward direction with the parameters chosen for this simulation).

Fourth scenario

The fourth simulation is illustrated in Figures 7.15–7.18. Its starting configuration is similar to the fourth scenario, but the prediction horizon of the MPC controller was reduced to 10 seconds. With this prediction length, the MPC controller does not consider turning around the thrusters, since no advantages of doing that are seen within that period. The thrusters angles are not commanded to do significant

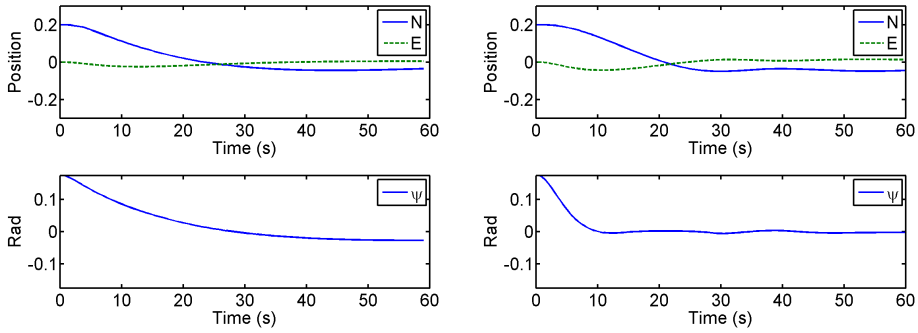

(a) Baseline (b) MPC

Figure 7.11: *Third scenario:* position of the vessel.

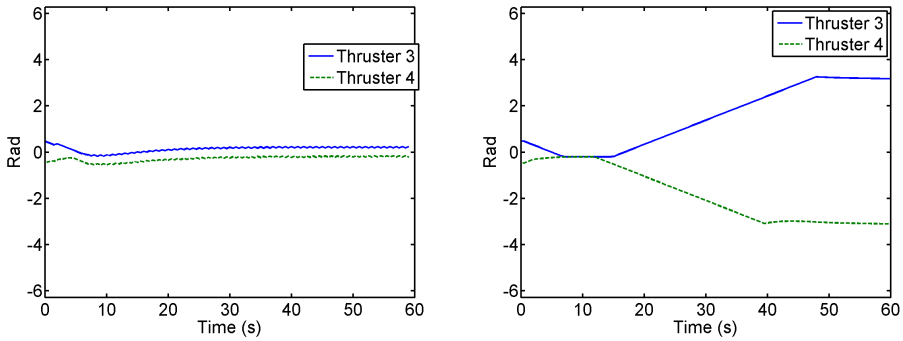

(a) Baseline (b) MPC

Figure 7.12: *Third scenario:* azimuth thruster angles.

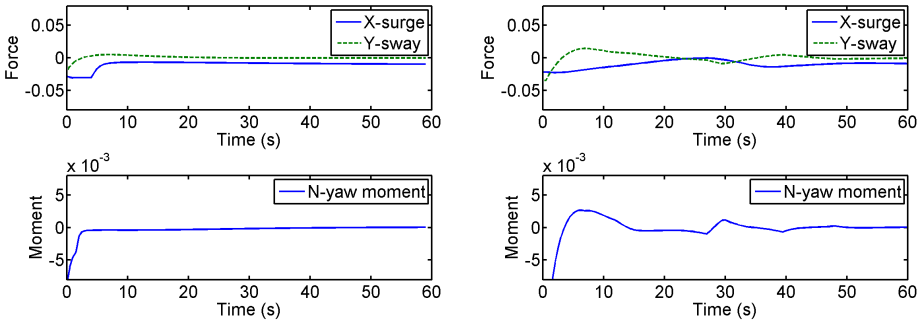

(a) Baseline (b) MPC

Figure 7.13: *Third scenario:* thruster forces.

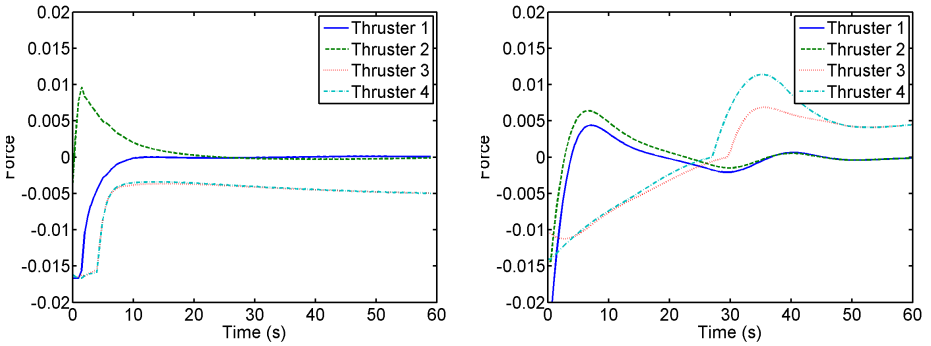

(a) Baseline (b) MPC

Figure 7.14: *Third scenario:* thruster forces.

excursions; as can be seen in Figure 7.16 they tend to remain close to zero. When the transients settle, the forces from from the azimuth thrusters (thruster 3 and thruster 4) converge to a negative value, i.e. they run in reverse – despite the fact that it is twice as expensive as having their propellers spin in the direction they were designed for.

The execution time on a laptop computer in this scenario is appoximately 2.7 seconds per iteration with cold start in the beginning of the simulation, and 0.2 seconds for the subsequent iterations which receive a reasonable initial trajectory guess; this is about five time faster than with the previous scenarios. This suggests that this algorithm could feasibly be run in real-time on modern hardware.

7.6 Conclusion and future work

Implementing dynamical positioning with MPC appears to offer significant advantages compared to the current state-of-the-art. The MPC implementation is able to distribute force generation over a period of time and plan the motion of the vessel according to changes in configuration of the rotable thrusters; overall this results in less biasing (ref Appendix A, "Thruster Biasing"). Having large-scale model predictive control in real-time loops has its own challenges, mainly due to reliability and timely calculation of the results. Additionally, azimuth turning has to be implemented *ad hoc*, as with conventional thrust allocation. An MPC controller with a long enough horizon could theoretically dispose of those problems.

Convergence of nonlinear MPC is an active research area, and real-time guarantees on a complex model are difficult to make. A practical real-time implementation should have a classical DP implementation running as a safety fallback, in case the MPC solver fails to deliver a solution in time. Since the fallback algorithm is highly independent from the primary algorithm, the resulting architecture is in principle significantly more reliable than running a classical algorithm alone [14]. An MPC controller implementation with a shorter horizon should be investigated for possi-

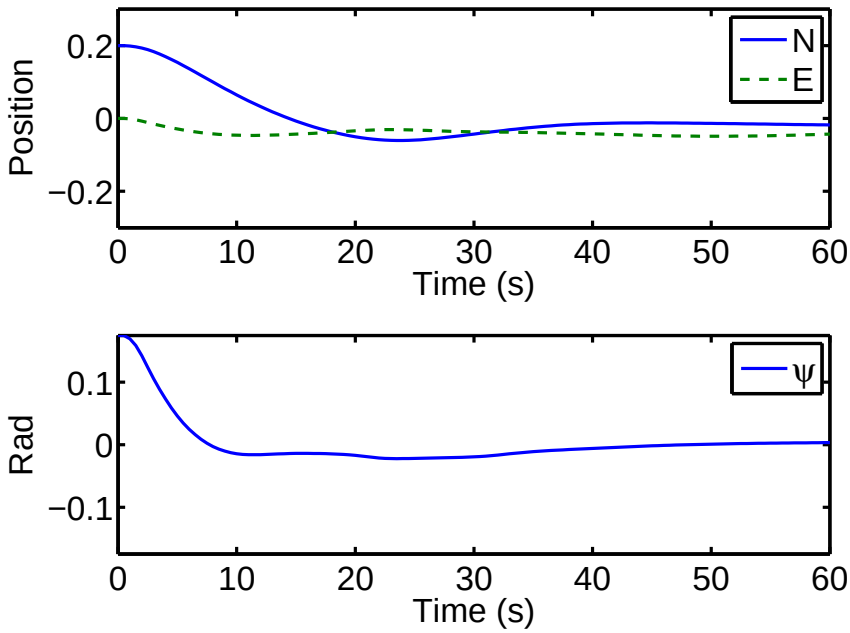

Figure 7.15: *Fourth scenario:* position of the vessel

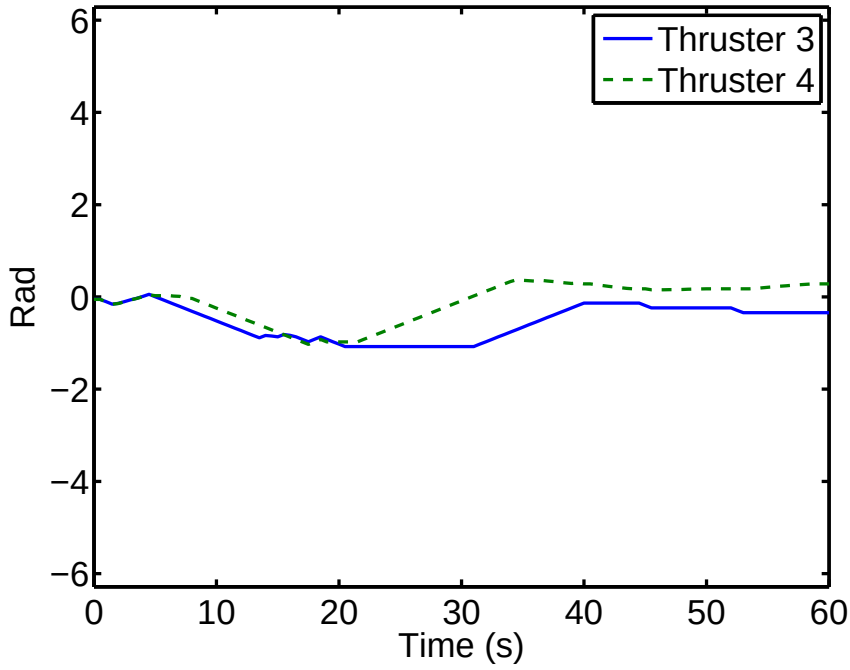

Figure 7.16: *Fourth scenario:* azimuth thruster angles.

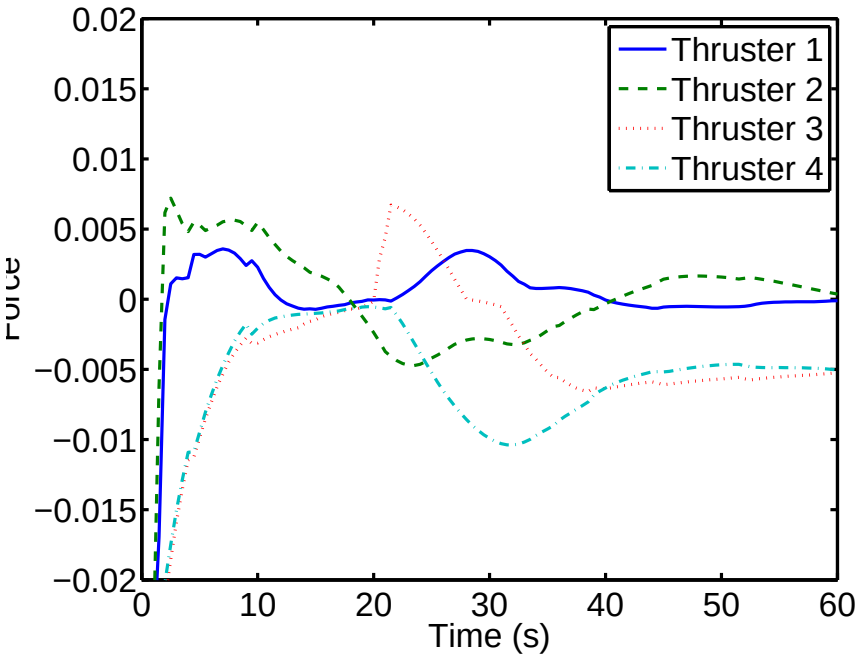

Figure 7.17: *Fourth scenario:* thruster forces.

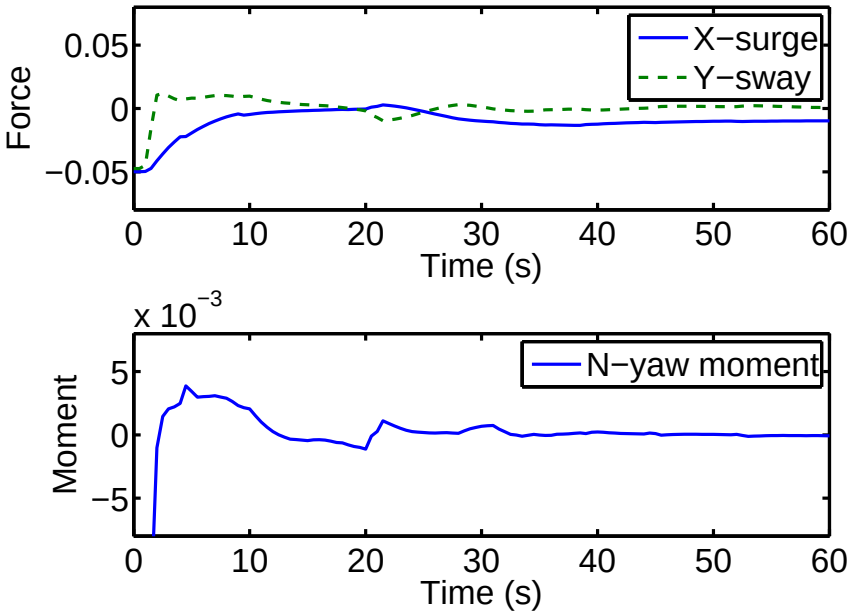

Figure 7.18: *Fourth scenario:* total forces.

bility to run it real-time on current hardware.

Chapter 8

Concluding remarks

This thesis explores the topic of control of ships with diesel-electric propulsion, operating in dynamic positioning. This technology is in a reasonably mature state, and current research is directed towards making improvements in terms operational parameters such as fuel efficiency, lifetime of the equipment, ability to operate safely in more adverse environmental conditions and safety in general. Another important goal – even if it is less apparent to the final user – is to reduce the amount of work the practitioners spend to implement the control system algorithms and to adapt them to individual vessel deliveries.

The main enabler for the improvements that are proposed in this thesis is that the advances in computer hardware and algorithms make it possible to implement algorithms that could not have been considered with earlier technologies. Whereas before the control system had to be separated into several algorithms with limited communication between them, those advances make it possible to implement a more wholistic approach, with either more information exchange between the controllers or merging of several hereto independent controllers.

Additionally, the control decisions can be made by projecting the future behavior of the controlled system using the mathematical model of the relevant systems on the ship, and making the decision that ensures that the future behavior is close to the best one possible with regards to the operational parameters that were mentioned above. Under most practical circumstances this requires numerical simulation of many possible trajectories of the controlled system, trying many possible values for the control input, a technique called Model Predictive Control, or MPC. This task typically requires a lot of computing power, and the control engineer often had to contend him- or herself to ensuring that the ship maintains its position with mainly heuristic concern for the operational parameters.

Chapters 2 and 3 each describe a thrust allocation algorithm that dynamically controls the power consumption in the thrusters without spending significantly more power overall. To achieve that, slight variations in the position of the vessel (about 20 cm) are allowed. This ability is used to compensate for the variations in the power consumption from other consumers on the ship, reducing the overall load variations. Mathematically, this is equivalent to using the hull of the vessel as a store of potential energy in the field of the environmental forces – energy can

be stored in the hull by moving it against the environmental forces and it can be released by allowing the vessel to move with the environmental forces. The control over power consumption can be taken advantage in two ways:

- less load variations mean that the frequency variations on the grid can be reduced, allowing a larger margin to blackout due to underfequency and more reliable synchronization of additional generators, or
- the governors could exploit the reduced load variations by reducing the variations in the fuel injection rate, thus extending the lifetime on the power plant, as well reducing emissions and sooting; in addition, the power plant as a whole may be able to manage with fewer connected generators due to lower peak loads.

The principal difference between the algorithms in Chapter 2 and Chapter 3 is that the latter algorithm is more efficient, but more complex.

Chapter 4 verifies the feasibility and capability of this thrust allocation algorithm modification from a theoretical perspective.

When the diesel engine controllers (which are usually called governors) receive information about the load on the power plant as soon as it changes, the governors get the opportunity to act proactively, and greatly limit the impact of the load variations on the bus frequency. Similarly, if it is known that a load increase is temporary, a governor with a properly implemented feed-forward functionality will not respond to this increase as dramatically as it would for a passing load increase, thus extending the life time of the engine it controls. A controller with this functionality implemented with model predictive control is described in Chapter 5.

The literature on thrust allocation algorithms that is currently available usually focuses on solving only a few of the many facets of the thrust allocation problem at a time. Chapter 6 describes a thrust allocation algorithm that combines and integrates the elements from the earlier contributions, thus providing an implementation with singularity avoidance functionality that is able to control both azimuth thrusters and ruddered propellers. It does not attempt to improve performance relative to the existing literature, however a practitioner may save time and effort by using the algorithm presented there as a starting point for his or her implementation.

In Chapter 7, MPC is used to control the individual thrusters directly based on the position and velocity reference. It is thus capable to plan ahead the use of thrusters, and coordinate those with the motion of the ship itself. Dynamic positioning implemented with MPC appears to be allowing significant advantages compared to traditional implementations where DP control algorithm and thrust allocation are separate. The MPC implementation is able to distribute force generation over a period of time and plan the motion of the vessel according to changes in configuration of the rotable thrusters; overall this results in less biasing (ref Appendix A, “Thruster Biasing”) and faster position re-acquiring. When the DP system is operating at the limit of its capability, those improvements could mean recovering from a sudden change in the environmental force where a traditional DP algorithm would not be able to prevent a drift-off outside the acceptable margins from the DP set point.

Combining the control architecture that is proposed in Chapter 7 with a traditional control architecture in a redundant configuration will decrease the probability of a software failure because those two architectures are largely independent from one another.

Appendices

Appendix A

Glossary

Dynamic Positioning System, DP

An automatic system that maintains position of a ship or vessel using its thrusters, in presence of disturbances such as wind, waves and current. In the context of control algorithm design, the DP is an algorithm which assesses the position of the vessel based on various instruments, calculates how far it is from a desired position setpoint selected by the operator, and based on that decides the thruster force needed to get to the desired position.

Thrust allocation algorithm, TA

An algorithm that takes as input an order for the total force and moment that the thrusters should enact upon a ship, and calculates what forces the individual thrusters should produce so that resultant force and moment on the ship becomes as ordered. A more general concept of *control allocation* is applicable to any fully- or overactuated vehicle [39].

Generalized force

A generalization of the Newtonian force concept for systems that are described in generalized coordinates[26]. In the context of 3DOF surface ship modeling, generalized force is a three-dimensional vector consisting of the two-dimensional force vector and the torque acting on a chosen pivot point.

Thruster

Any unit capable of producing controlled thrust on the vessel. For some thrusters, the direction in which they produce thrust can be controlled, while others can only produce thrust in a fixed direction. The main types of thrusters used for dynamic positioning are:

- **Tunnel thrusters.** Typically located at the bow of the ship, tunnel thrusters consist of a "tunnel" through the hull of this ship, through which a propeller can push water, typically in either direction.

- **Azimuth thrusters** have their propellers mounted on a rotable assembly. This allows the azimuth thrusters to change their direction freely, with turn-around times on the scale of one minute. On may ships, the azimuth thrusters are not allowed to push water in certain directions, such as against other thrusters or at other critical machinery. This type of thruster is typically located at the aft of the ship, or beneath the columns of semi-submersible rigs.
- **Ruddered or unruddered propellers** are classical propellers, typically located at the aft of the ship and pointing backwards. They are often powered mechanically through a drive shaft. A rudder is most effective when a propeller pushes water pass its surface, which is typically behind the propeller. Rudders are therefore often installed behind propellers to allow generating a sideways force at the location of the rudder, which normally also creates a yaw moment on the ship.

Thruster biasing

Deliberately increasing the power consumption in the thrusters without changing the total produced force and moment on the ship, effectively forcing the thrusters to push against one another.

For a given azimuth and rudder angle vector α, the combined force vector and angular momentum produced by the thrusters is

$$\tau = B(\alpha)f \tag{A.1}$$

and is a linear combination of the forces f generated by the individual thrusters. If there are four or more thrusters on board the ship, then the matrix $B(\alpha)$ is guaranteed to have a non-trivial null space F_0. Additionally, if f^* is a strict global minimizer of the power consumption for a given τ, then for any $f_0 \in F_0 \backslash \mathbf{0}$ the power consumption for $f^* + f_0$ will be higher than for f^*, with the resultant generalized force remaining the same. Therefore, biasing can always be achieved as long as there are at least four non-saturated thrusters available for the purpose. Fewer than four thrusters are sufficient for configurations in which the columns of the matrix $B(\alpha)$ are not independent.

Wave filter

Waves characteristically induce a cyclic high-frequency "back-and-forth" motion on ships. Compensating for the wave-induced motions would demand large power expenditure and increased wear-and-tear. For this reason, the cyclic wave-induced motions of the vessel are usually allowed to run their course, without interference from the dynamic positioning system. This is implemented by passing the position reference through a wave filter algorithm, which calculates what the position of the vessel would have been without the cyclic wave-induced motions[25].

Appendix B

Row and column vector volume

Theorem 1: For a matrix $A \in \mathbb{R}^{N\times M}$ with $N > M$, the volume of the M-dimensional parallelepiped that is spanned by the column vectors of A is given by

$$\begin{aligned} VolP(A) &= \sqrt{det\,(A^T A)} \\ &= \prod_{i=1}^{M} S_{ii} \end{aligned} \tag{B.1}$$

where S_{ii} is the i-th singular value of A.

Proof. By singular volume decomposition, $A = USV^T$; the rows of the matrix $H = SV^T \in \mathbb{R}^{N\times M}$ consist of the M columns of V, multiplied by the respective elements of S, with the remaining $N - M$ rows of H being zero. The columns of V are orthonormal, so the volume of the parallelepiped that is spanned by the first M rows of H is $\mathcal{V} = S_{11}S_{22}\dots S_{MM}$. Defining $H' \in \mathbb{R}^{M\times M}$ as the matrix consisting of those first M rows, notice that since H' is square, $VolP(H') = det(H')$. The volume that is spanned by the column vectors of H' is therefore also $\mathcal{V}$. The column vectors of H are identical to H', so its volume is also $\mathcal{V}$. Pre-multiplying H with the orthogonal matrix S does not affect lengths or relative angles of the column vectors of M, and the volume of the parallelepiped must also stay the same. Therefore $VolP(A) = \mathcal{V}$.

Examining (B.1),

$$\begin{aligned} \sqrt{det\,(A^T A)} &= \sqrt{det(VS^T U^T \cdot USV^T)} \\ &= \sqrt{det(V)det(S^T S)det(V^T)} \\ &= S_{11}S_{22}\dots S_{MM} = \mathcal{V} \end{aligned} \tag{B.2}$$

Therefore, $VolP(A) = \sqrt{det\,(A^T A)}$.

□

Corollary 1: For a matrix $A \in \mathbb{R}^{N\times M}$ with $N < M$, the volume $VolP(A)$ of the N-dimensional parallelepiped that is spanned by the row vectors of A is given by

$$VolP(A) = \sqrt{det\left(AA^T\right)} \tag{B.3}$$

Proof. Let $A' = A^T$. Per Theorem 1, $VolP(A) = VolP(A') = \sqrt{det(A'A'^T)} = \sqrt{det(A^T A)}$.

□

References

[1] Nomenclature for treating the motion of a submerged body through a fluid. Technical report, The Society of Naval Architects and Marine Engineers, Technical and Research Committee, 1950.

[2] Experimental drilling in deep water. Technical report, National Research Council (U.S.). AMSOC Committee, 1959.

[3] Guidelines for vessels with dynamic positioning systems. Technical Report MSC/circ. 645, International Maritime Organization (IMO), 1994.

[4] Rules for classification of ships. Technical Report Part 6 Chapter 7, Dynamic Positioning Systems, DNV GL, July 2013. URL https://exchange.dnv.com/publishing/RulesShip/2011-01/ts607.pdf.

[5] U. Aharoni. Visualization of the coriolis and centrifugal forces, 2007. URL http://youtu.be/49JwbrXcPjc.

[6] D. Ariens, B. Houska, H. Ferreau, and F. Logist. Acado: Toolkit for automatic control and dynamic optimization. http://www.acadotoolkit.org.

[7] T. I. Bø and T. A. Johansen. Scenario based fault tolerant model predictive control for diesel-electric marine power plant. In *Proc. MTS/IEEE OCEANS*, 2013.

[8] S. P. Berge and T. I. Fossen. Robust control allocation of overactuated ships; experiments with a model ship. In *in Preprints IFAC Conference on Maneuvering and Control of Marine Craft*, 1997.

[9] T. I. Bø. Dynamic model predictive control for load sharing in electric power plants for ships. Master's thesis, Norwegian University of Science and Technology, Department of Marine Technology, 2012.

[10] T. I. Bø, T. A. Johansen, and E. Mathiesen. Unit commitment of generator sets during dynamic positioning operation based on consequence simulation. In *9th IFAC Conference on Control Applications in Marine Systems, Osaka, Japan*, 2013.

[11] I. Boldea. *Synchronous Generators*. CRC Press, November 2005. ISBN 084935725X.

[12] D. Breu and C. L. A. Francescutto. *Parametric Resonance in Dynamical Systems*, chapter Ship Model for Parametric Roll Incorporating the Effects of Time-Varying Speed, page Chapter 9. Springer, 2012.

[13] D. A. Breu, L. Feng, and T. I. Fossen. Optimal speed and heading control for stabilization of parametric oscillations in ships. In T. I. Fossen and H. Nijmeijer, editors, *Parametric Resonance in Dynamical Systems*, chapter 11. Springer, 2012.

[14] A. Burns and A. J. Wellings. *Real-Time Systems and Programming Languages:*. Addison Wesley, 3rd edition, 2001.

[15] J. Chauvin, G. Corde, and N. Petit. Transient control of a diesel engine airpath. In *Proc. American Control Conf.*, pages 4394–4400, 2007. doi: 10.1109/ACC.2007.4282942.

[16] H. Chen, L. Wan, F. Wang, and G. Zhang. Model predictive controller design for the dynamic positioning system of a semi-submersible platform. *Journal of Marine Science and Application*, 11(3):361–367, 2012. ISSN 1671-9433. doi: 10.1007/s11804-012-1144-z.

[17] J. A. Cook, J. W. Grizzle, and J. Sun. *The Control Handbook*, chapter Engine Control, pages 1261–1273. CRC Press-Times Mirror Books, 1996.

[18] M. S. R. Costa and G. B. Machado. Analyzing petrobras DP incidents. In *MTS Dynamic Positioning Conference*, Houston, 2006.

[19] A. K. Ådnanes. Maritime electrical installations and diesel electric propulsion. Technical report, ABB AS, 2003.

[20] DNV. Dynamic positioning system - enhanced reliability DYNPOS-ER. Technical Report Rules for classification of ships, Part 6, Chapter 26, 2010.

[21] P. Eckert and S. Rakowski. *Combustion Engines Development*, chapter Pollutant Formation. Springer-Verlag, 2012.

[22] O. M. Faltinsen. *Hydrodynamics of High-Speed Marine Vehicles*. Cambridge University Press, 2006.

[23] H. Fay. *Dynamic Positioning Systems*. Editions Technip, 1990.

[24] T. I. Fossen. *Marine Control Systems*. Tapir Trykkeri, 2002.

[25] T. I. Fossen. *Handbook of Marine Craft Hydrodynamics and Motion Control*. John Wiley & Sons, Ltd, April 2011.

[26] H. Goldstein, C. P. Poole, and J. L. Safko. *Classical Mechanics*. Addison Wesley, June 2001. ISBN 0321188977.

[27] L. Guzzella and C. H. Onder. *Introduction to Modeling and Control of Internal Combustion Engine Systems*. Springer-Verlag, Berlin, Heidelberg, 2010. ISBN 9783642107757.

[28] M. Hanger, T. A. Johansen, G. K. Mykland, and A. Skullestad. Dynamic model predictive control allocation using CVXGEN. In *9th IEEE International Conference on Control and Automation (ICCA'11), Santiago, Chile*, 2011.

[29] J. F. Hansen. *Modelling and Control of Marine Power Systems*. PhD thesis, NTNU, Trondheim, Norway, 2000.

[30] V. Hassani, A. J. Sørensen, and A. M. Pascoal. Robust dynamic positioning of offshore vessels using mixed-μ synthesis part I: A control system design methodology. In *IFAC Workshop on Automatic Control in Offshore Oil and Gas Production*, 2012.

[31] C. Holden. *Modelling and Control of Parametric Roll Resonance*. PhD thesis, NTNU, June 2011.

[32] D. Holmes. *Principles of Physical Geology*. Van Nostrand Reinhold, 1978.

[33] B. Houska, H. J. Ferreau, and M. Diehl. An auto-generated real-time iteration algorithm for nonlinear MPC in the microsecond range. *Automatica*, 47(10):2279 – 2285, 2011. ISSN 0005-1098. doi: http://dx.doi.org/10.1016/j.automatica.2011.08.020.

[34] O. G. Hvamb. A new concept for fuel tight DP control. In *Proc. Dynamic Positioning Conference*, Houston, Texas, September 2001. Marine Technology Society.

[35] In notes and comments. Mohole trials yield samples of deep-water sediments. *New Scientist*, 227:730, March 1961.

[36] N. A. Jenssen. Improved DP performance in deep water operations through advanced reference system processing and situation assessment. In *Proc. Dynamic Positioning Conference*. Marine Technology Society, 1997.

[37] N. A. Jenssen and B. Realfsen. Power optimal thruster allocation. In *Proc. Dynamic Positioning Conference, Houston*, 2006.

[38] J. Jiang. Optimal gain scheduling controller for a diesel engine. *Control Systems, IEEE*, 14(4):42–48, 1994. ISSN 1066-033X. doi: 10.1109/37.295969.

[39] T. A. Johansen and T. I. Fossen. Control allocation - a survey. *Automatica*, 49 (5):1087 – 1103, 2013. ISSN 0005-1098. doi: 10.1016/j.automatica.2013.01.035.

[40] T. A. Johansen, T. I. Fossen, and S. P. Berge. Constrained nonlinear control allocation with singularity avoidance using sequential quadratic programming. *IEEE Trans. Control Systems Technology*, 12:211–216, 2004.

[41] T. A. Johansen, A. J. Sørensen, O. J. Nordahl, O. Mo, and T. I. Fossen. Experiences from hardware-in-the-loop (HIL) testing of dynamic positioning and power management systems. In *OSV Singapore*, 2007.

[42] T. A. Johansen, T. P. Fuglseth, P. Tøndel, and T. I. Fossen. Optimal constrained control allocation in marine surface vessels with rudders. *Control Engineering Practice*, 16(4):457 – 464, 2008. ISSN 0967-0661. doi: 10.1016/j.conengprac.2007.01.012.

[43] T. A. Johansen, T. I. Bø, E. Mathiesen, A. Veksler, and A. Sørensen. Dynamic positioning system as dynamic energy storage on diesel-electric ships. *IEEE Transactions on Power Systems*, 2014. (in press).

[44] P. Johnstone. *The sea-craft of prehistory.* Routledge, 1988. ISBN 978-0-415-02635-2.

[45] D. K. M. Kufoalor, S. Richter, L. Imsland, T. A. Johansen, M. Morari, and G. O. Eikrem. Embedded Model Predictive Control on a PLC Using a Primal-Dual First-Order Method for a Subsea Separation Process. In *Mediterranean Conference on Control and Automation*, Palermo, IT, June 2014.

[46] P. Lakshminarayanan and Y. V. Aghav. *Modeling Diesel Combustion.* Springer, 2009.

[47] S.-H. Lee, J.-S. Yim, J.-H. Lee, and S.-K. Sul. Design of speed control loop of a variable speed diesel engine generator by electric governor. In *Industry Applications Society Annual Meeting, 2008. IAS '08. IEEE*, pages 1–5, 2008. doi: 10.1109/08IAS.2008.202.

[48] Y. Levron and D. Shmilovitz. Power systems' optimal peak-shaving applying secondary storage. *Electric Power Systems Research*, 89(0):80 – 84, 2012. ISSN 0378-7796.

[49] Y. Levron, J. Guerrero, and Y. Beck. Optimal power flow in microgrids with energy storage. *IEEE Transactions on Power Systems*, 28(3):3226–3234, 2013.

[50] M. Lewander, A. Widd, B. Johansson, and P. Tunestal. Steady state fuel consumption optimization through feedback control of estimated cylinder individual efficiency. In *American Control Conference (ACC), 2012*, pages 4210–4214, 2012.

[51] T. Lin, E. Tseng, and F. Borrelli. Modeling driver behavior during complex maneuvers. In *American Control Conference*, 2013.

[52] M. Lindgren and P.-A. Hansson. Effects of transient conditions on exhaust emissions from two non-road diesel engines. *Biosystems Engineering*, 87(1):57 – 66, 2004. ISSN 1537-5110. doi: 10.1016/j.biosystemseng.2003.10.001.

[53] Y. Luo, A. Serrani, S. Yurkovich, D. B. Doman, and M. W. Oppenheimer. Model predictive dynamic control allocation with actuator dynamics. In *Proc. American Control Conference, Boston*, pages 1695–1700, 2004.

[54] P. Maciel, A. Koop, and G. Vaz. Modelling thruster-hull interaction with CFD. In *32nd International Conference on Ocean, Offshore and Arctic Engineering, Nantes, France.*, June 2013.

[55] *TCA - The Benchmark*. MAN Diesel & Turbo, 86224 Augsburg, Germany, 2013.

[56] E. Mathiesen, B. Realfsen, and M. Breivik. Methods for reducing frequency and voltage variations on dp vessels. In *Proc. Dynamic Positioning Conference*, October 2012.

[57] D. Mayne, J. Rawlings, C. Rao, and P. Scokaert. Constrained model predictive control: Stability and optimality. *Automatica*, 36(6):789 – 814, 2000. ISSN 0005-1098. doi: http://dx.doi.org/10.1016/S0005-1098(99)00214-9.

[58] W. NIerenberg and M. Peterson. Deep sea drilling project technical report no. 3. Technical report, Scripps Institution of Oceanography, UCSD, december 1971. URL http://www.deepseadrilling.org/trepts/TRNOTE_03.PDF.

[59] L. Pivano, T. A. Johansen, and Ø. N. Smogeli. A four-quadrant thrust estimation scheme for marine propellers: Theory and experiments. *Control Systems Technology, IEEE Transactions on*, 17(1):215–226, Jan 2009. ISSN 1063-6536. doi: 10.1109/TCST.2008.922602.

[60] D. Radan. *Integrated Control of Marine Electrical Power Systems*. PhD thesis, NTNU, 2008.

[61] D. Radan, T. A. Johansen, A. J. Sørensen, and A. K. Ådnanes. Optimization of load dependent start tables in marine power management systems with blackout prevention. *WSEAS Trans. Circuits and Systems*, 4, 2005.

[62] D. Radan, A. J. Sørensen, A. K. Ådnanes, and T. A. Johansen. Reducing power load fluctuations on ships using power redistribution control. *SNAME Journal of Marine Technology*, 45:162–174, 2008.

[63] C. D. Rakopoulos and E. G. Giakoumis. *Diesel Engine Transient Operation*. Springer, 2009.

[64] J. B. Rawlings. Tutorial overview of model predictive control. *Control Systems, IEEE*, 20(3):38–52, 2000.

[65] B. Realfsen. Reducing NOx emission in DP2 and DP3 operations. In *Proc. Dynamic Positioning Conference*, 2009.

[66] M. Rindarøy and T. A. Johansen. Fuel optimal thrust allocation in dynamic positioning. In *9th IFAC Conference on Control Applications in Marine Systems*, Osaka, Japan, 2013.

[67] S. Roy, O. Malik, and G. Hope. Adaptive control of speed and equivalence ratio dynamics of a diesel driven power-plant. *IEEE Transactions on Energy Conversion*, 8(1):13 –19, mar 1993. ISSN 0885-8969. doi: 10.1109/60.207400.

[68] E. Ruth. *Propulsion control and thrust allocation on marine vessels*. PhD thesis, NTNU, 2008.

[69] S. Savoy. Ensco 7500 power management system design, functionality and testing. In *Proc. Dynamic Positioning Conference*, 2002.

[70] X. Shi, Y. Wei, J. Ning, M. Fu, and D. Zhao. Optimizing adaptive thrust allocation based on group biasing method for ship dynamic positioning. In *Proceeding of the IEEE International Conference on Automation and Logistics, Chongqing, China*, 2011.

[71] R. Skjetne. Modeling a diesel-generator power plant. Lecture notes in course TMR4290, 2011, NTNU, October 2011.

[72] A. J. Sørensen. A survey of dynamic positioning control systems. *Annual Reviews in Control*, 35:123–136, 2011.

[73] O. J. Sørdalen. Optimal thrust allocation for marine vessels. *Control Engineering Practice*, 5(9):1223 – 1231, 1997. ISSN 0967-0661. doi: http://dx.doi.org/10.1016/S0967-0661(97)84361-4.

[74] G. Theotokatos. Ship propulsion plant transient response investigation using a mean value engine model. *International Journal Of Energy*, 2(4):66–74, 2008. ISSN 1998-4316.

[75] G. Theotokatos. A comparative study on mean value modelling of two-stroke marine diesel engine. In *Proceedings of the 2nd International Conference on Maritime and Naval Science and Engineering*, pages 107–112. World Scientific and Engineering Academy and Society, 2009. ISBN 978-960-474-120-5.

[76] K. Torsethaugen. A two peak wave spectrum model. In *Proc. 12th Int. Conf. Offshore Mechanics and Arctic Technolog*, volume 2, pages 175–180, 1993.

[77] J. D. van Manen and P. van Oossanen. Propulsion. In E. V. Lewis, editor, *Principles of Naval Architecture*, chapter VI. The Society of Naval Architects and Marine Engineers, 1988.

[78] A. Veksler, T. A. Johansen, and R. Skjetne. Thrust allocation with power management functionality on dynamically positioned vessels. In *Proc. American Control Conf.*, 2012.

[79] A. Veksler, T. A. Johansen, and R. Skjetne. Transient power control in dynamic positioning-governor feedforward and dynamic thrust allocation. In *9th IFAC Conference on Manoeuvring and Control of Marine Craft*, 2012.

[80] A. Veksler, T. A. Johansen, E. Mathiesen, and R. Skjetne. Governor principle for increased safety and economy on vessels with diesel-electric propulsion. In *Proc. European Control Conf.*, Zürich, Switzerland, 2013. European Control Association.

[81] A. Veksler, T. A. Johansen, F. Borrelli, and B. Realfsen. Cartesian thrust allocation algorithm with variable direction thrusters, turn rate limits and singularity avoidance. In *IEEE Multi-conference on Systems and Control*, Antibes Juan-les-Pins, France, October 2014.

[82] A. Veksler, T. A. Johansen, F. Borrelli, and B. Realfsen. Dynamic positioning with model predictive control. *IEEE Transactions on Control Systems Technology*, 2014. submitted for review.

[83] A. Veksler, T. A. Johansen, R. Skjetne, and E. Mathiesen. Thrust allocation with dynamic power modulation for diesel-electric ships. *Transactions on Control Systems Technology*, 2014. submitted for review.

[84] A. Veksler, T. A. Johansen, R. Skjetne, and E. Mathiesen. Reducing power transients in diesel-electric dynamically positioned ships using re-positioning. In *The 40th Annual Conference of the IEEE Industrial Electronics Society*, Dallas, TX, USA, 2014.

[85] Y. Wang and S. Boyd. Fast model predictive control using online optimization. *Control Systems Technology, IEEE Transactions on*, 18(2):267–278, March 2010. ISSN 1063-6536. doi: 10.1109/TCST.2009.2017934.

[86] F. M. White. *Fluid Mech.* McGraw-Hill, 2003.

[87] *Governing Fundamentals and Power Management.* Woodward, 2620 edition, 2004.

[88] H. Xi and J. Sun. Feedback stabilization of high-speed planing vessels by a controllable transom flap. *Oceanic Engineering, IEEE Journal of*, 31(2): 421–431, April 2006. ISSN 0364-9059. doi: 10.1109/JOE.2006.875097.

[89] N. Xiros. *Robust Control of Diesel Ship Propulsion.* Springer-Verlag, 2002. ISBN 1852335432.

[90] B. Zahedi and L. Norum. Modeling and simulation of all-electric ships with low-voltage DC hybrid power systems. *IEEE Transactions on Power Electronics*, 28(10):4525–4537, 2013.